Interface of Cosmology and Magnetic Fields with High Energy Cosmic Rays: News from the Pierre Auger Experiment

1. Observations
2. Anisotropies and Mass Composition
3. Tests of Lorentz Symmetry
4. Cosmic Rays and Cosmic Magnetic Fields
5. Primordial Magnetic Fields

DFG Deutsche Forschungsgemeinschaft

PROJEKTTRÄGER FÜR DAS Bundesministerium für Bildung und Forschung

Günter Sigl
II. Institut theoretische Physik, Universität Hamburg

Universität Hamburg
DER FORSCHUNG | DER LEHRE | DER BILDUNG

The All Particle Cosmic Ray Spectrum

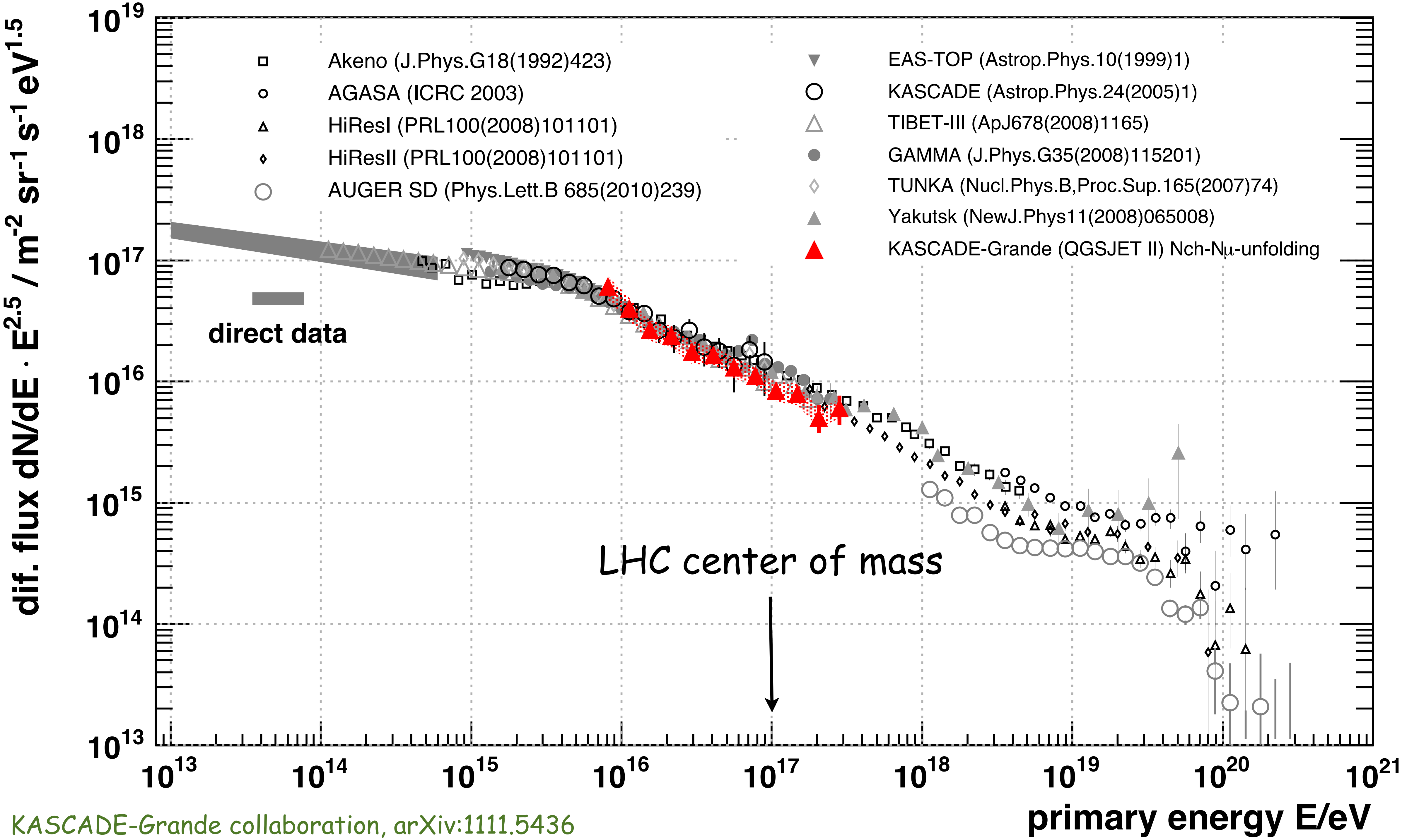

KASCADE-Grande collaboration, arXiv:1111.5436

Pierre Auger Spectra

Auger exposure = 31645 km^2 sr yr
up to December 2012

Pierre Auger Collaboration, PRL 101, 061101 (2008)
and Phys.Lett.B 685 (2010) 239
and ICRC 2013, arXiv:1307.5059, higlight talk Letessier-Selvon

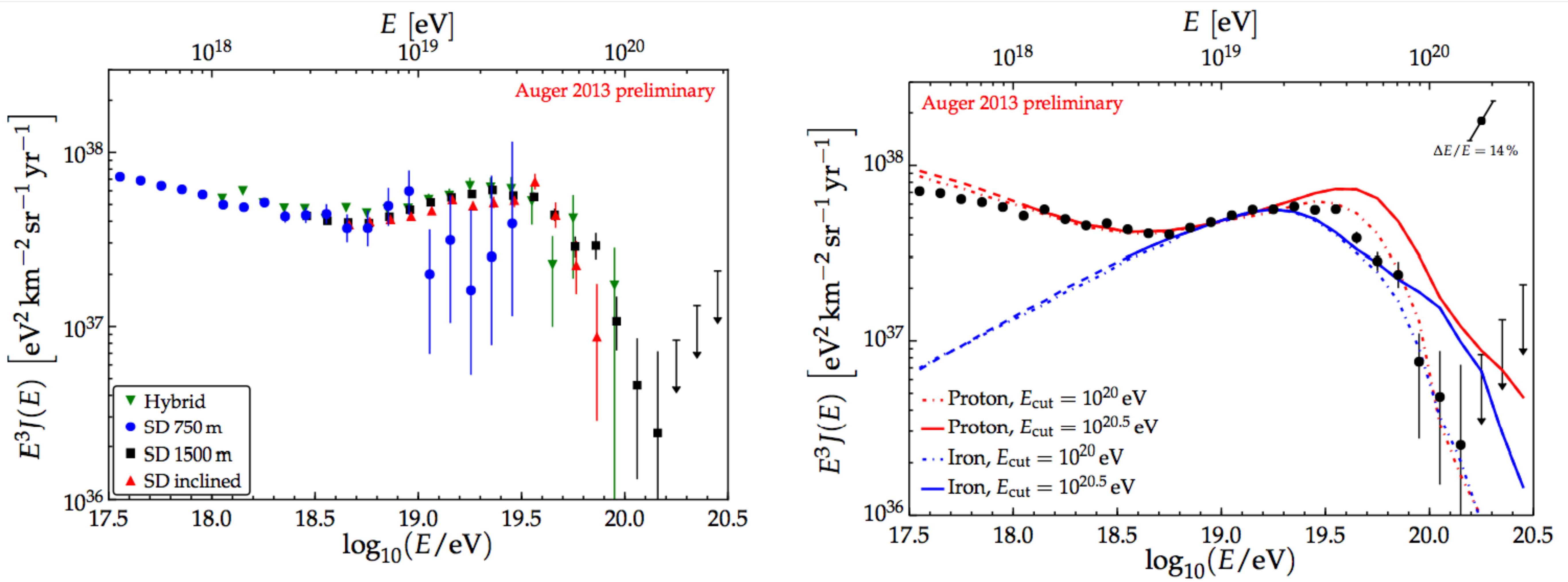

Atmospheric Showers and their Detection

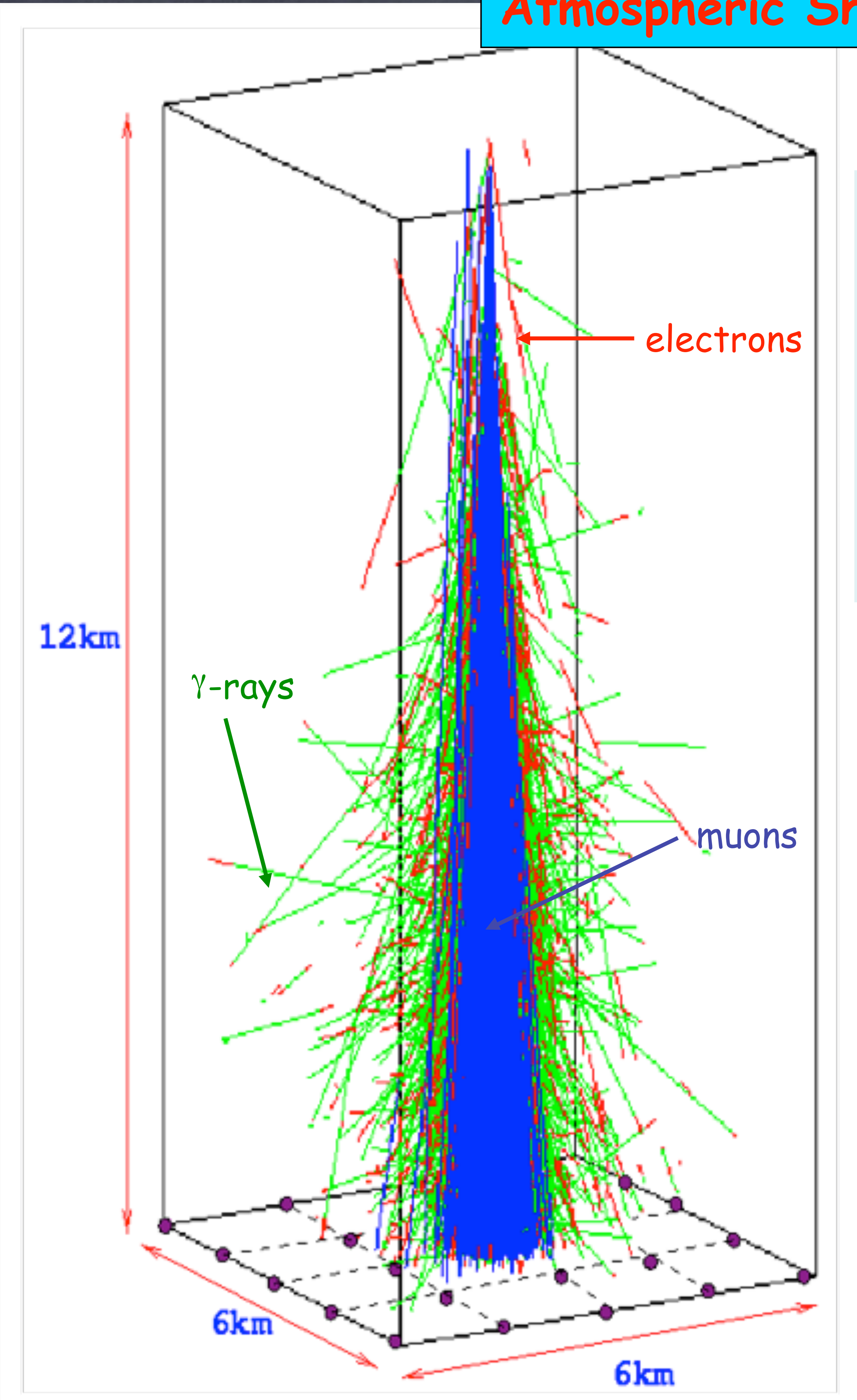

Fly's Eye technique measures fluorescence emission

The shower maximum is given by

$$X_{max} \sim X_0 + X_1 \log E_p$$

where X_0 depends on primary type for given energy E_p

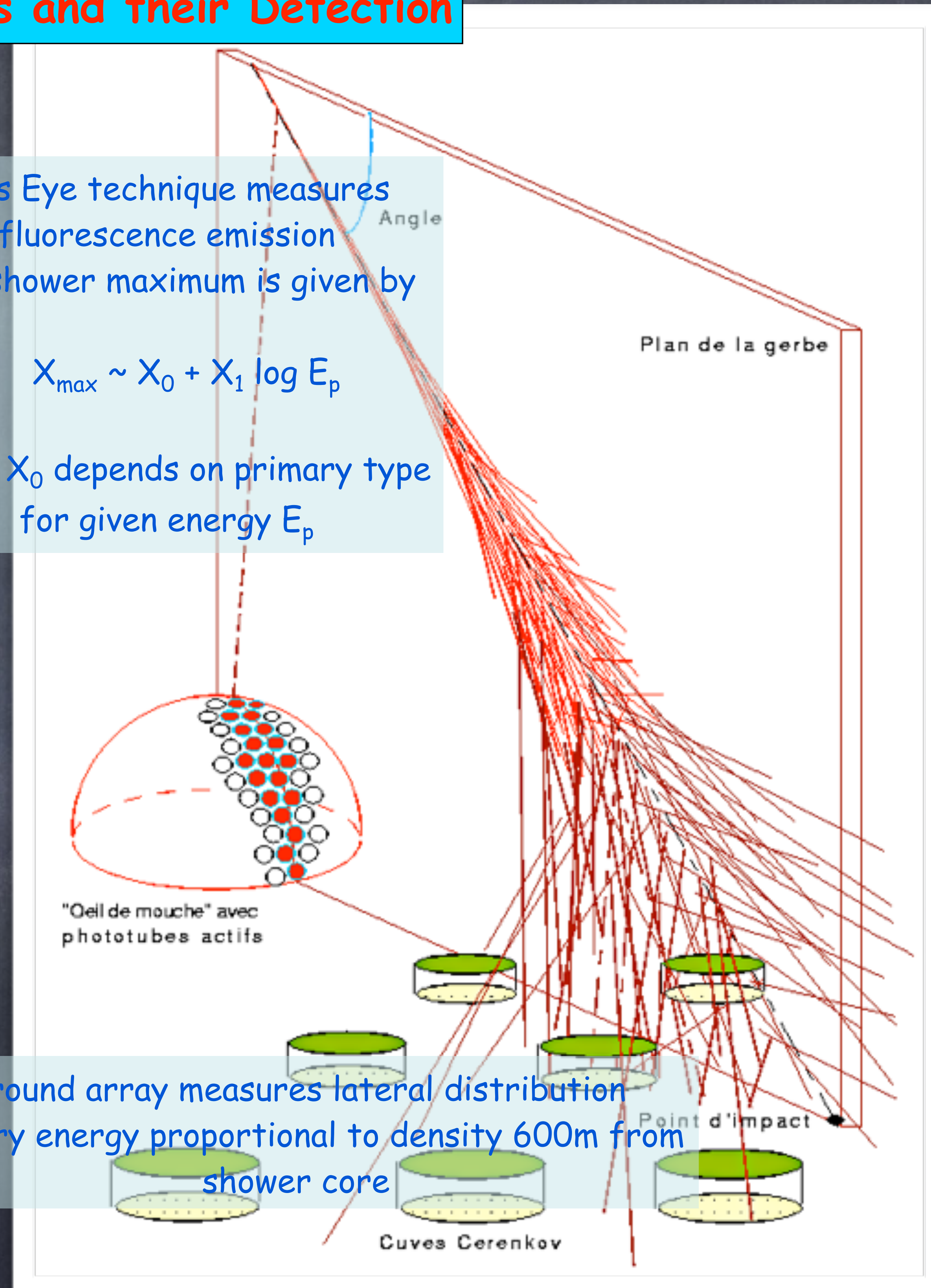

Ground array measures lateral distribution

Primary energy proportional to density 600m from shower core

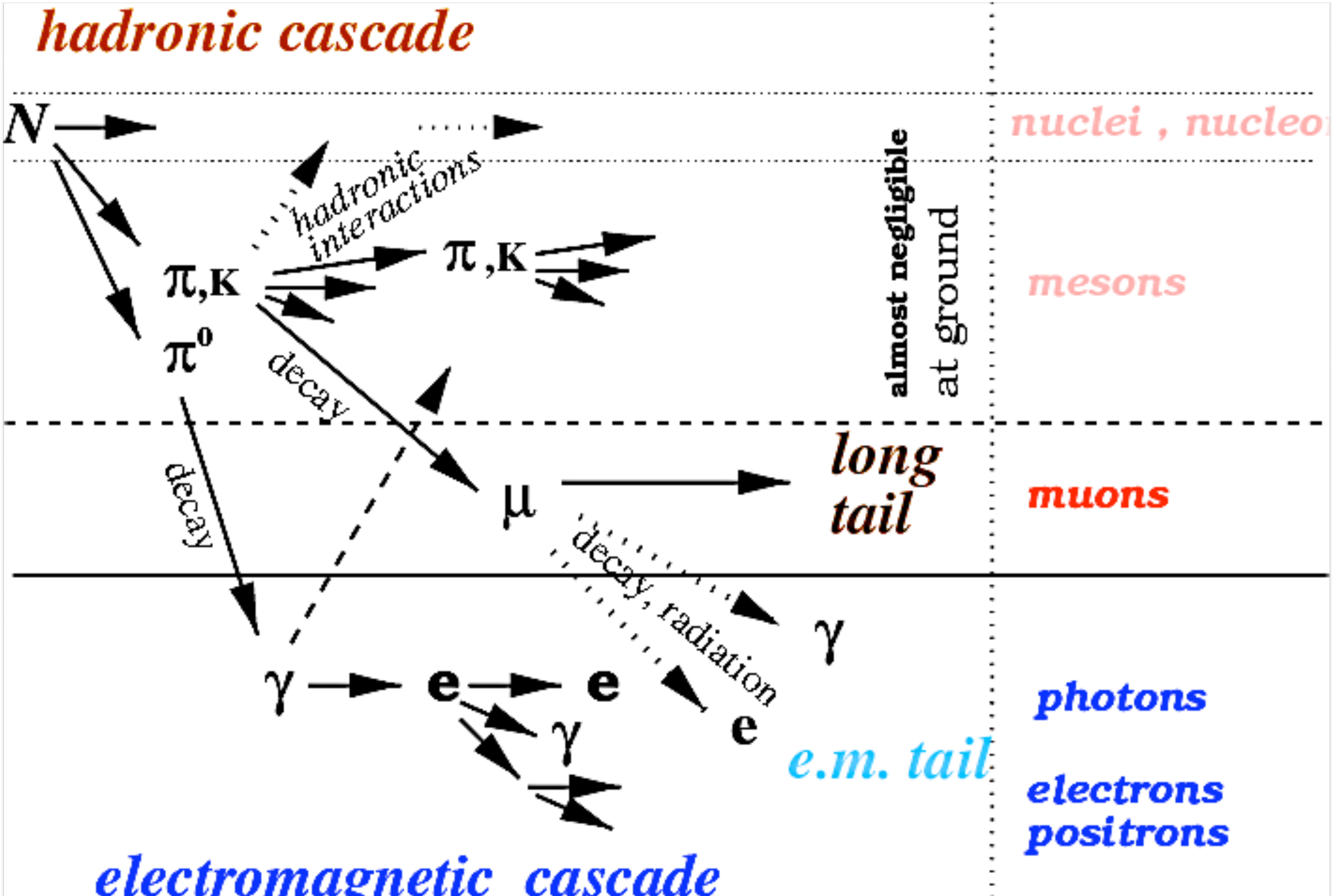
hadronic cascade
N
nuclei , nucleo
hadronic interactions
π,K
π ,K
π⁰
almost negligible
at ground
mesons
decay
decay
μ
long tail
muons
decay, radiation
γ
γ
e
e
γ
e
e.m. tail
photons
electrons
positrons
electromagnetic cascade

Cosmic ray versus neutrino induced air showers

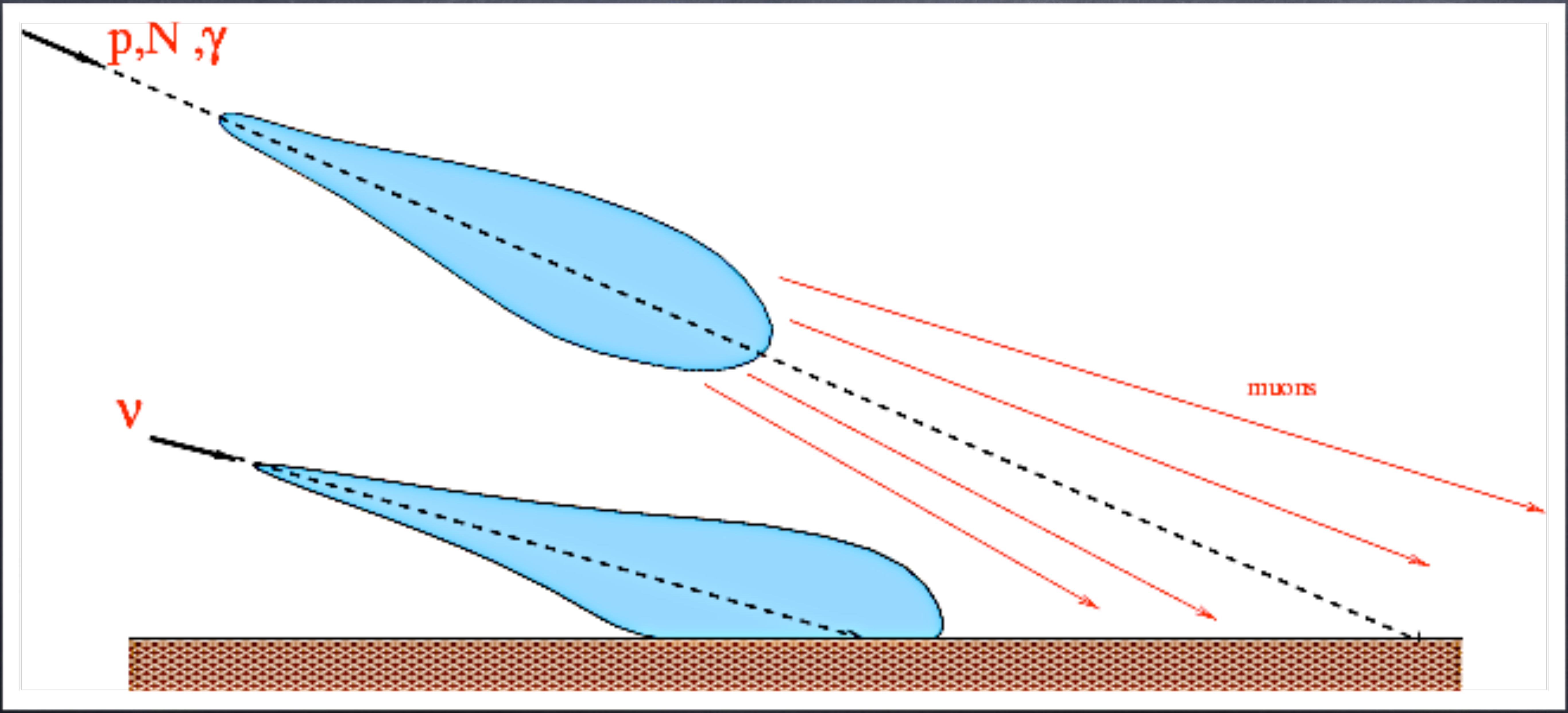

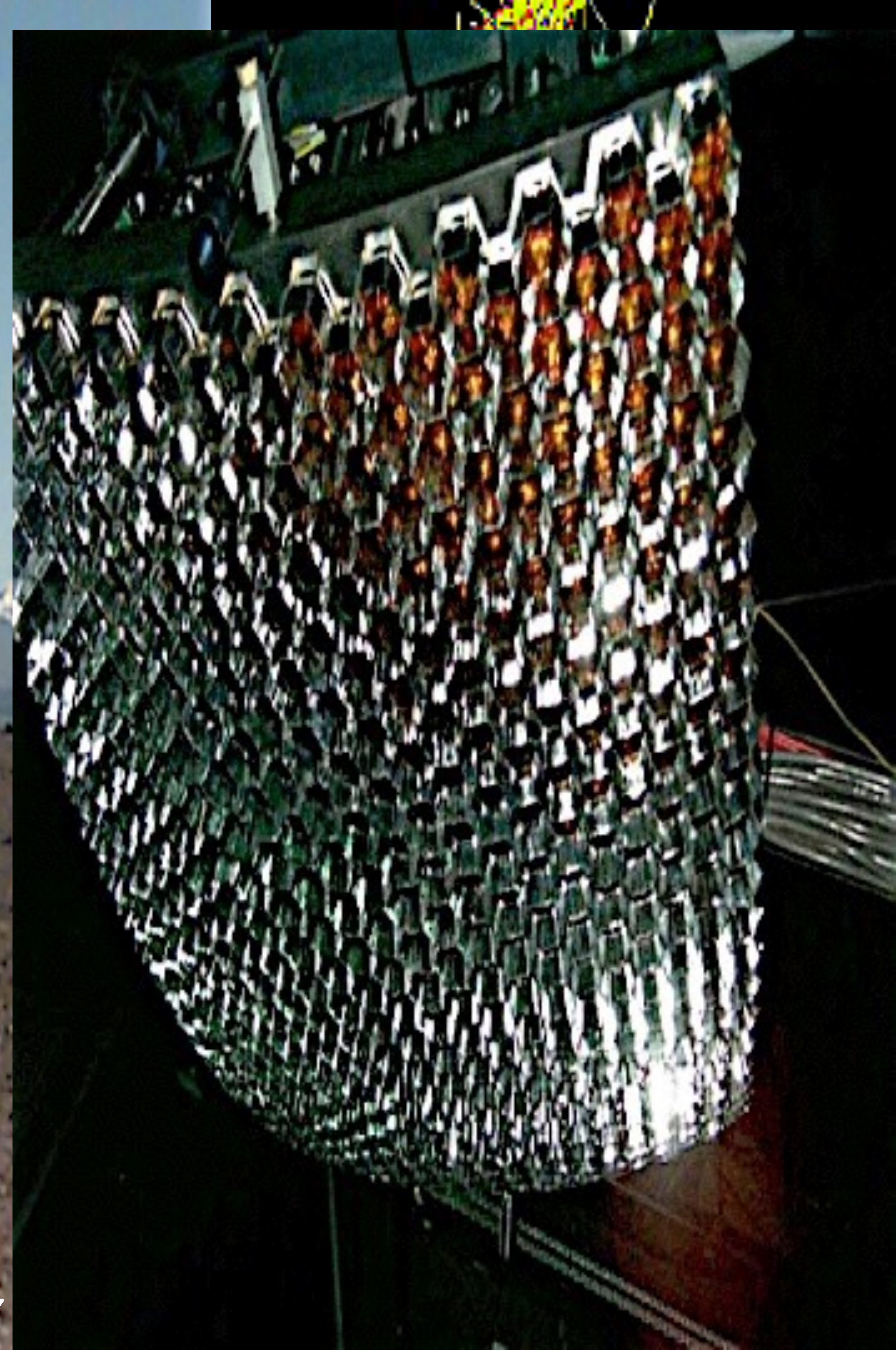

Southern Auger Site

Pampa Amarilla, Province of Mendoza
3000 km², 875 g/cm², 1400 m
Lat.: 35.5° south

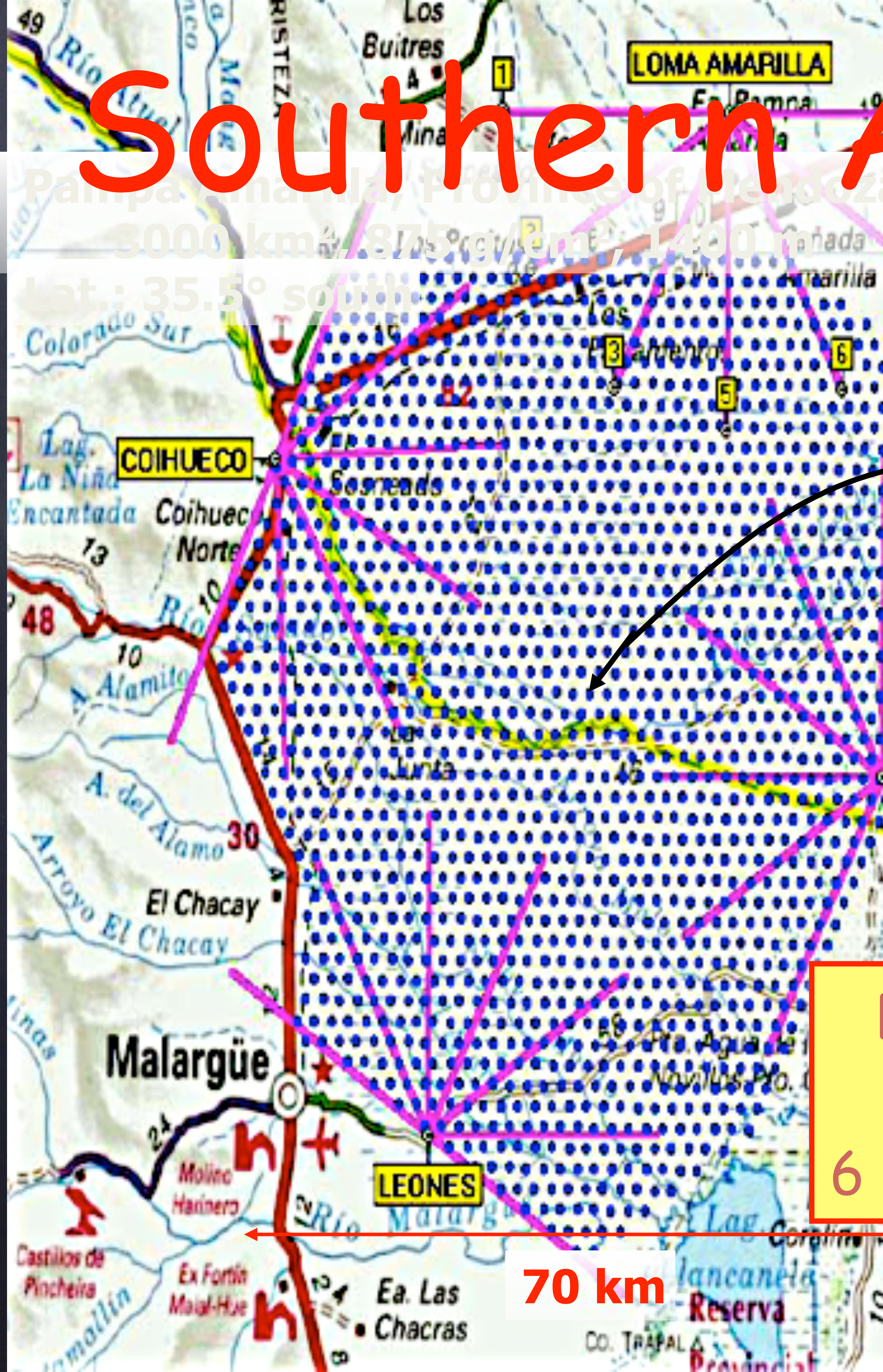

Surface Array (SD):
1600 Water Tanks
1.5 km spacing
3000 km^2

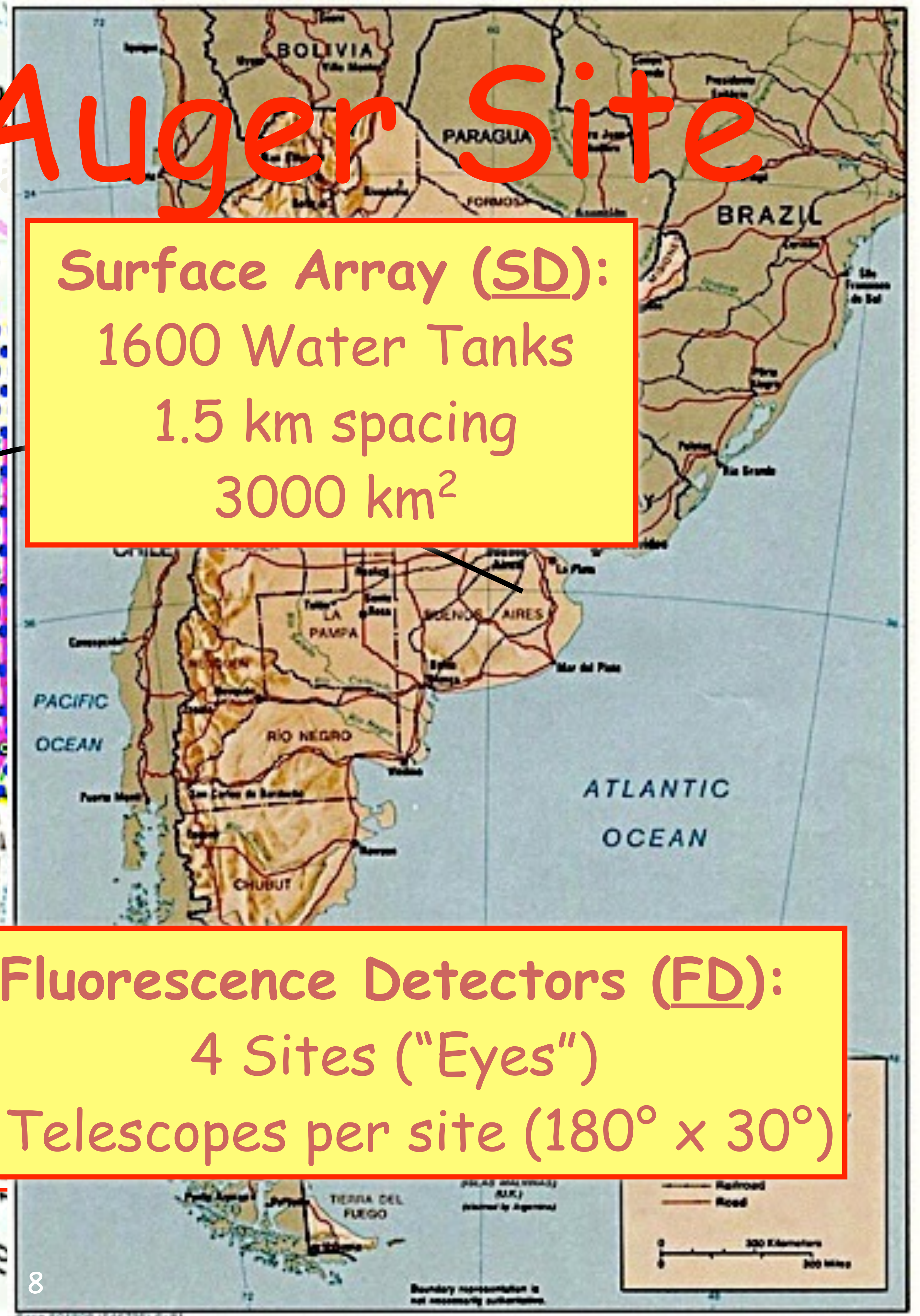

Fluorescence Detectors (FD):
4 Sites ("Eyes")
6 Telescopes per site (180° x 30°)

The Ultra-High Energy Cosmic Ray Mystery consists of (at least) Four Interrelated Challenges

1.) electromagnetically or strongly interacting particles above 10^{20} eV loose energy within less than about 50 Mpc.

2.) in most conventional scenarios exceptionally powerful acceleration sources within that distance are needed.

3.) The observed distribution does not yet reveal unambiguously the sources, although there are hints of correlations with local large scale structure

4.) The observed mass composition may become heavy toward highest energies, but no completely clear picture yet between experiments and air shower models

The Greisen-Zatsepin-Kuzmin (GZK) effect

Nucleons can produce pions on the cosmic microwave background

$$E_{\rm th} = \frac{2m_N m_\pi + m_\pi^2}{4\varepsilon} \simeq 4 \times 10^{19}\,{\rm eV}$$

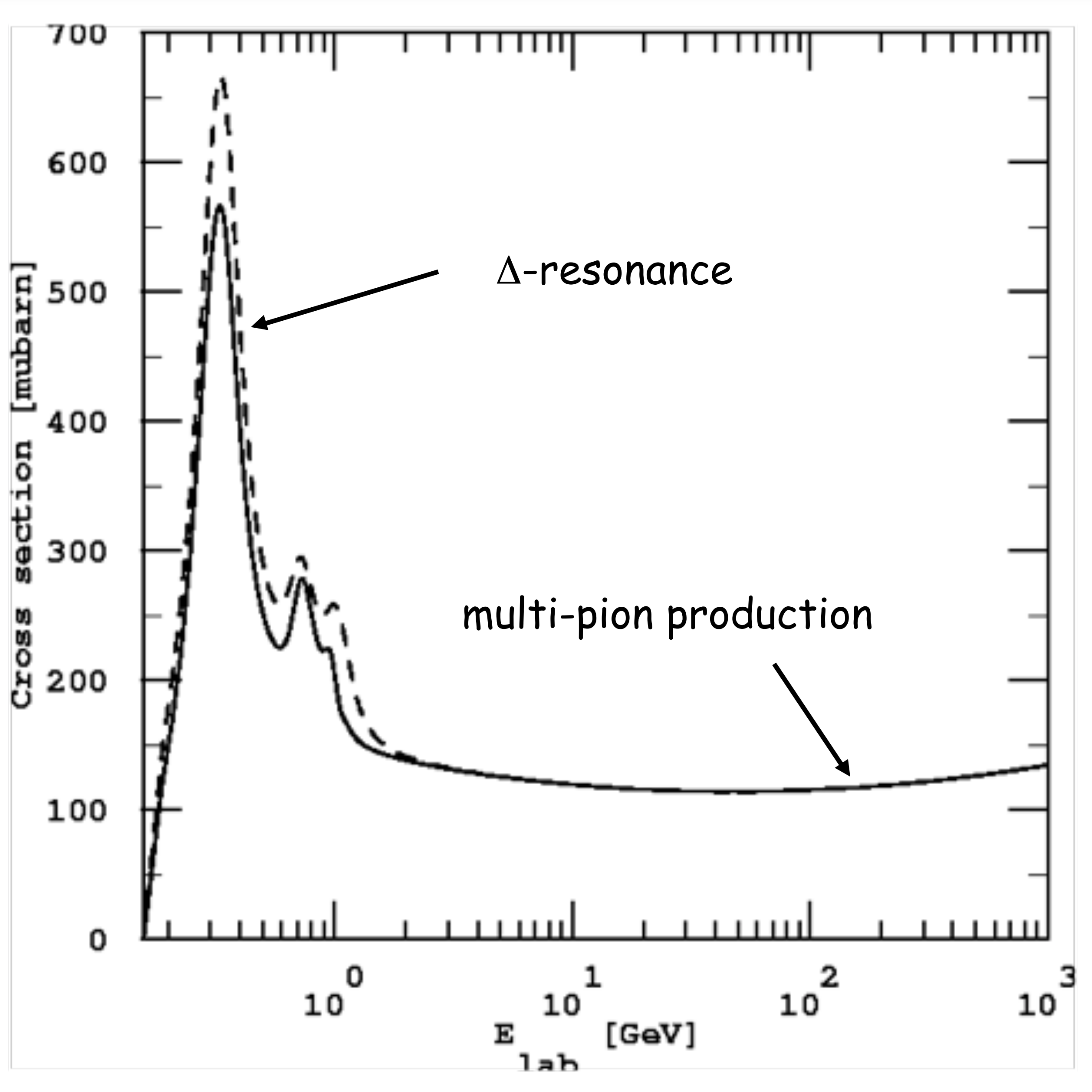

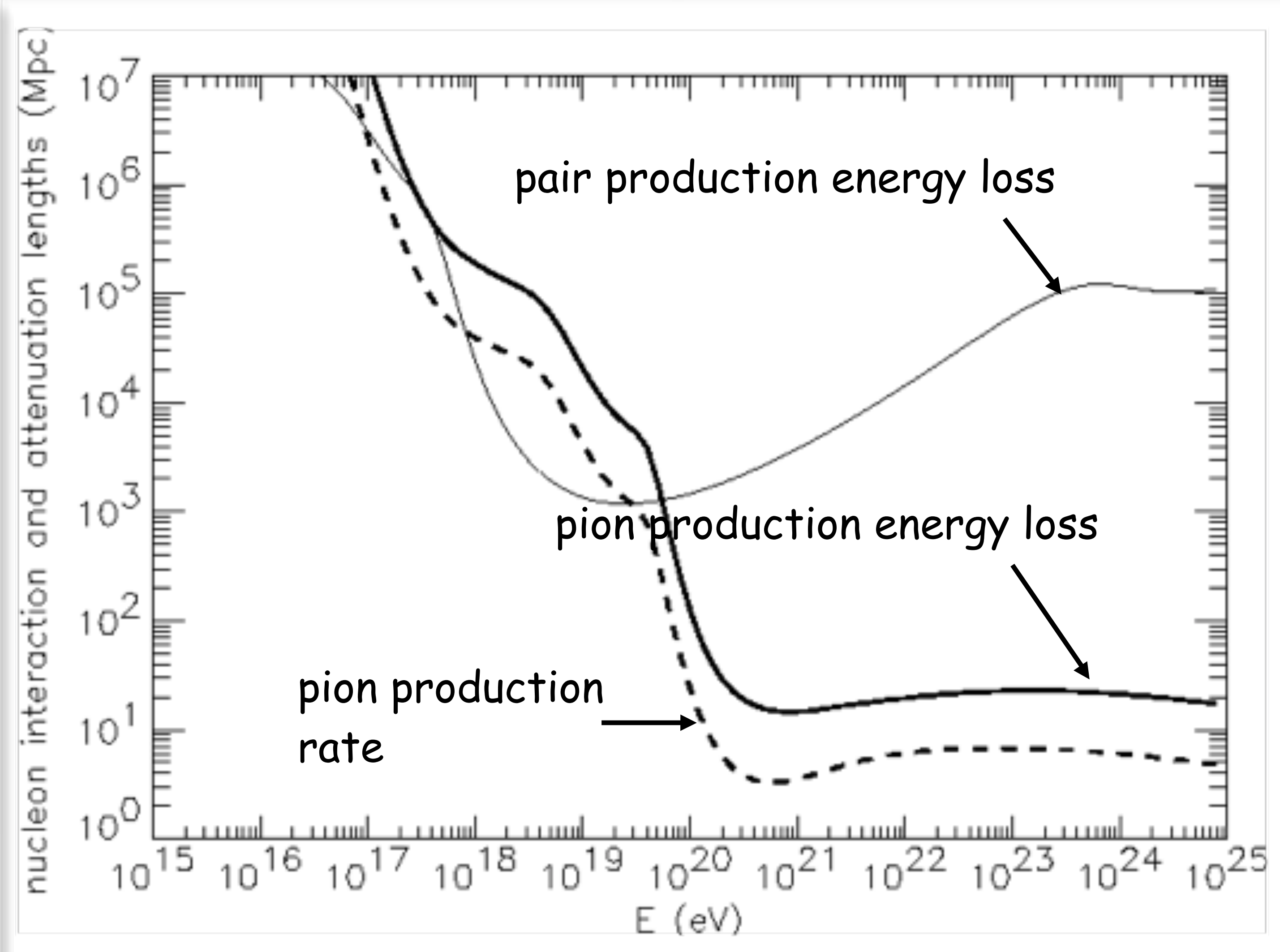

sources must be in cosmological backyard
Only Lorentz symmetry breaking at $\Gamma > 10^{11}$ could avoid this conclusion.

Length scales for relevant processes of a typical heavy nucleus

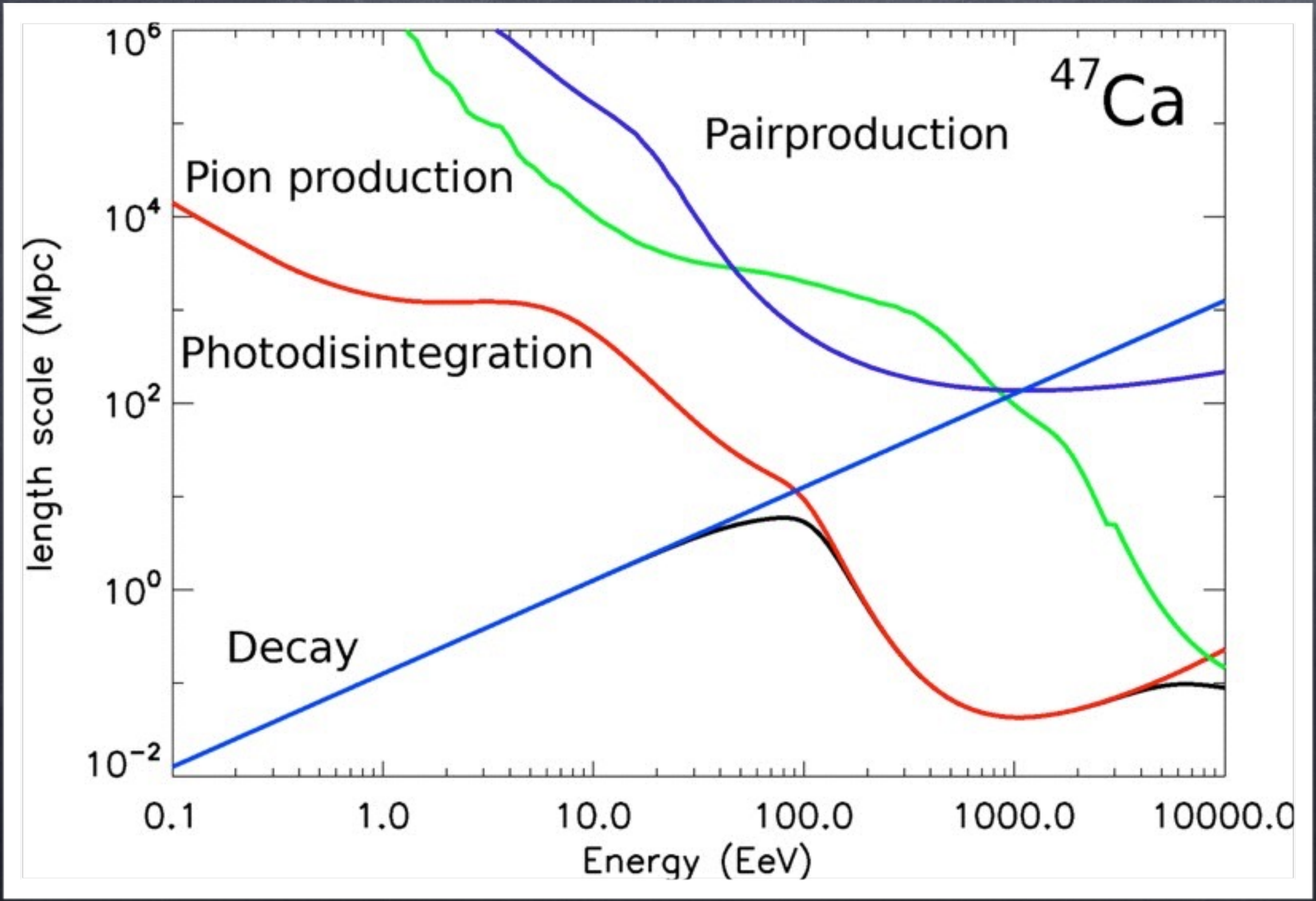

Interaction Horizons

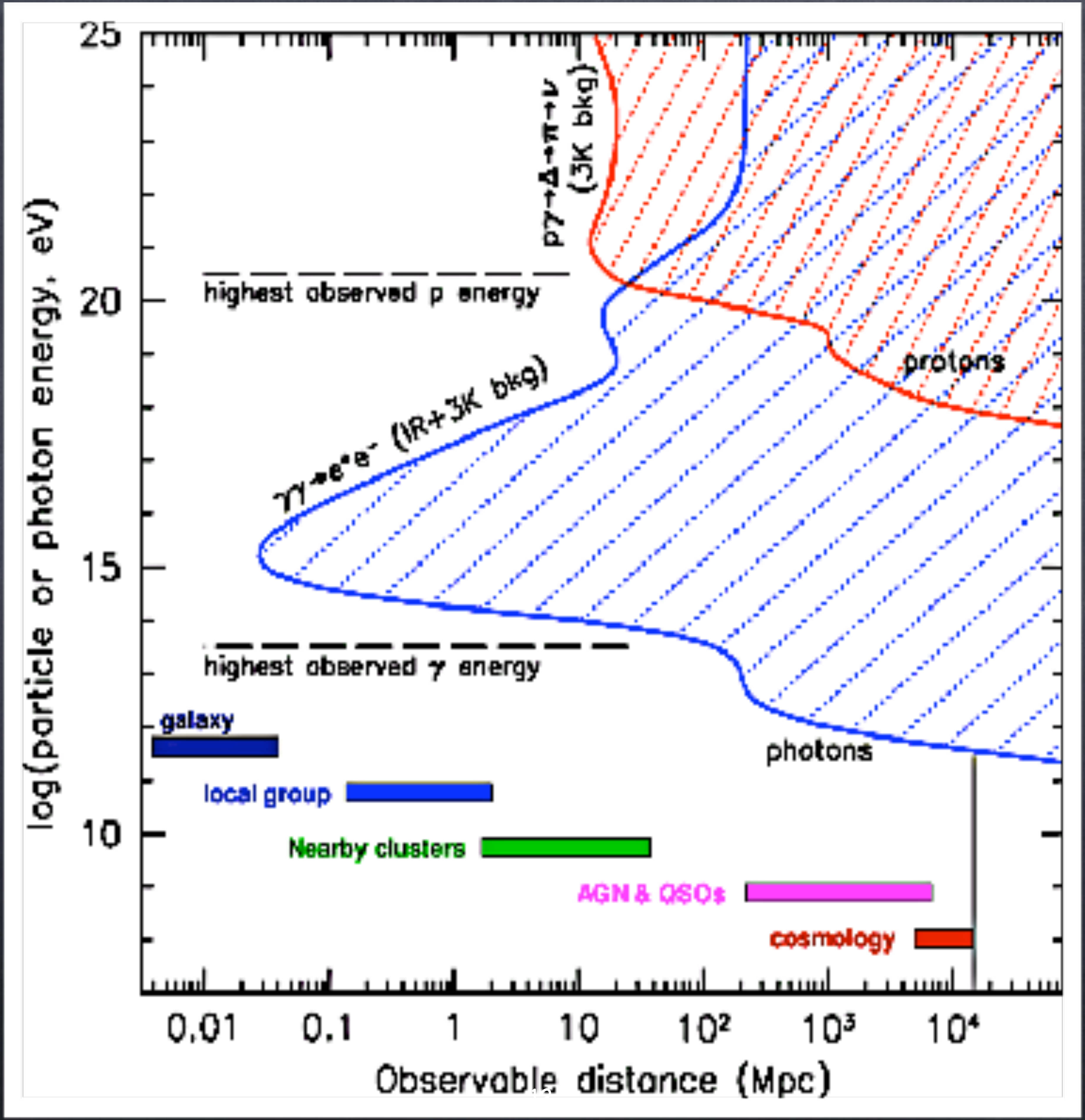

1^{st} Order Fermi Shock Acceleration

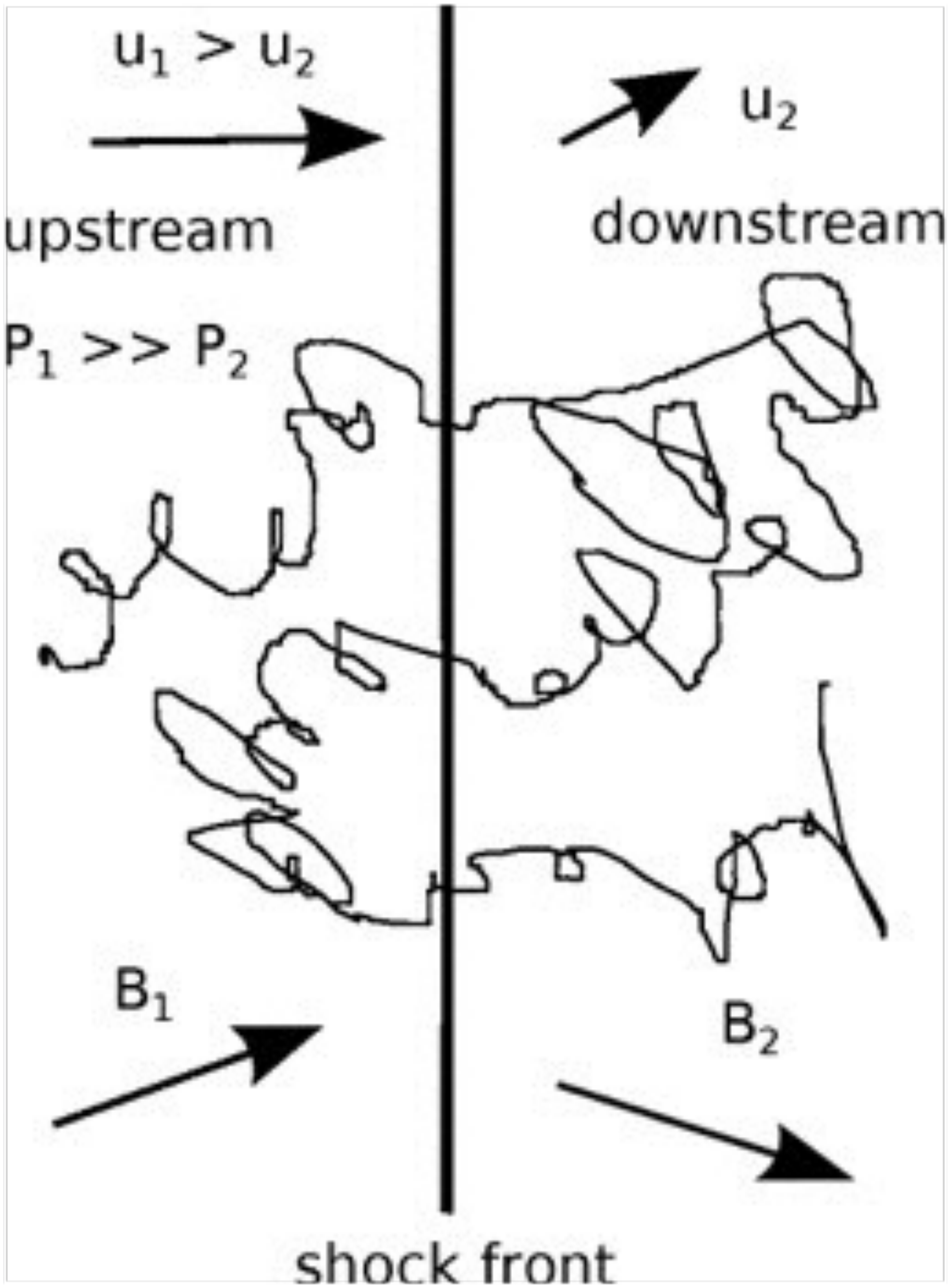

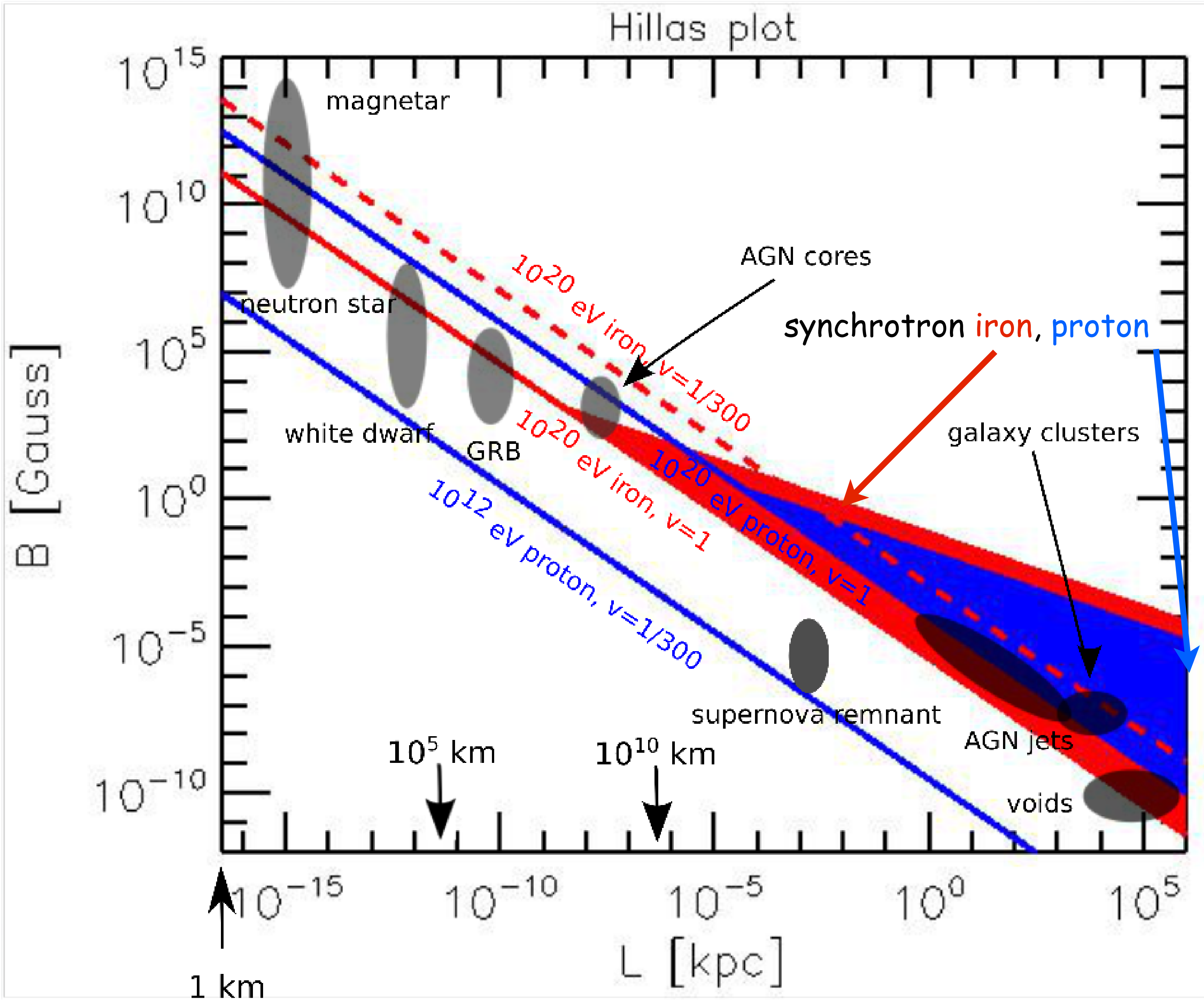

Fractional energy gain per shock crossing ~ $u_1 - u_2$ on a time scale r_L/u_2 .

Together with downstream losses this leads to a spectrum E^{-q} with $q > 2$ typically.
Confinement, gyroradius < shock size, and energy loss times define maximal energy

Some general Requirements for Sources

Accelerating particles of charge eZ to energy E_{max} requires induction $\varepsilon > E_{max}/eZ$. With $Z_0 \sim 100\Omega$ the vacuum impedance, this requires dissipation of minimum power of

$$L_{\rm min} \sim \frac{\epsilon^2}{Z_0} \simeq 10^{45}\, Z^{-2} \left(\frac{E_{\rm max}}{10^{20}\,{\rm eV}}\right)^2 \,{\rm erg\,s^{-1}}$$

This „Poynting" luminosity can also be obtained from $L_{min} \sim (BR)^2$ where BR is given by the „Hillas criterium":

$$BR > 3 \times 10^{17}\,\Gamma^{-1} \left(\frac{E_{\rm max}/Z}{10^{20}\,{\rm eV}}\right) {\rm Gauss\,cm}$$

where Γ is a possible beaming factor.
If most of this goes into electromagnetic channel, only AGNs and maybe gamma-ray bursts could be consistent with this.

A possible acceleration site associated with shocks in hot spots of active galaxies

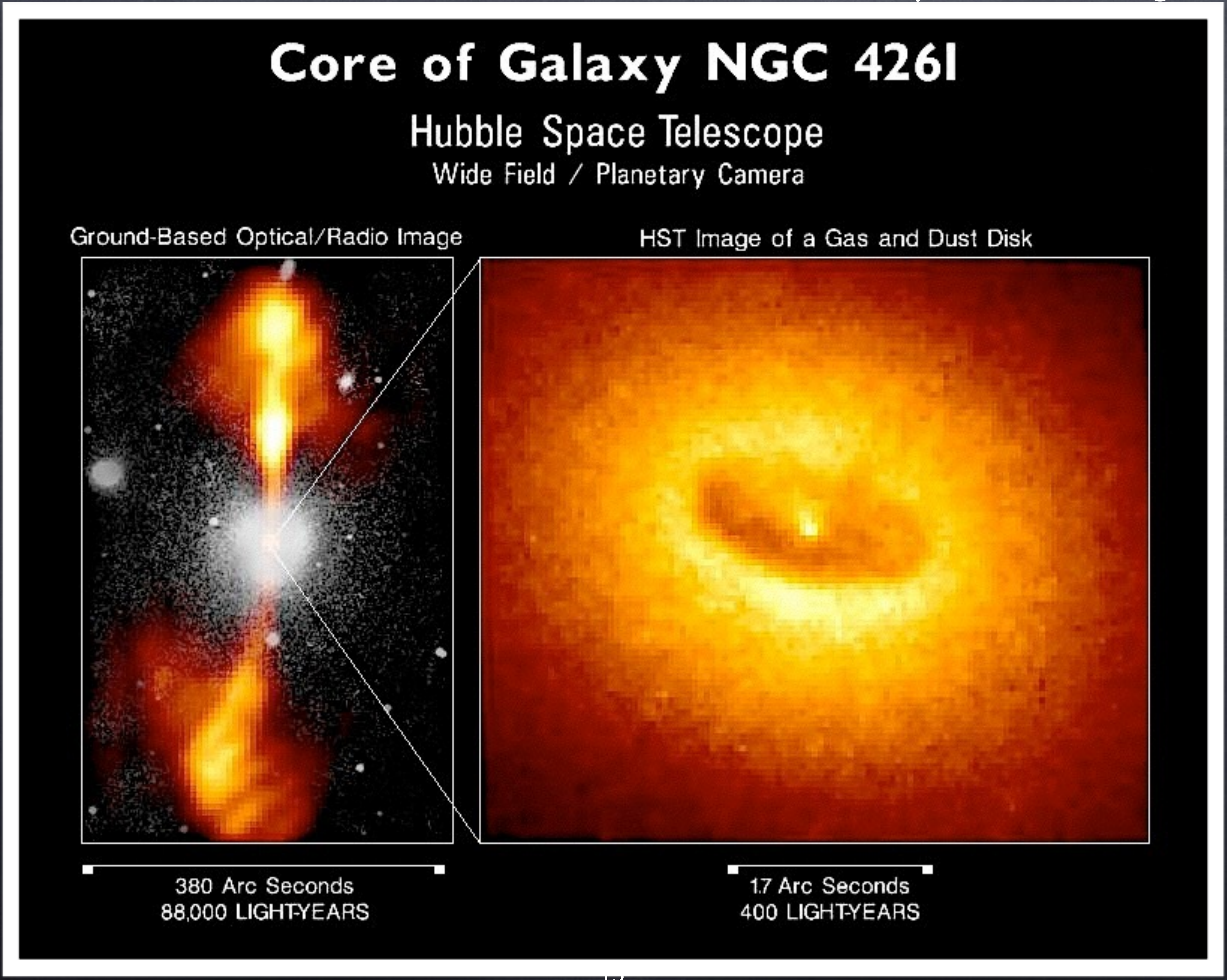

Or Cygnus A

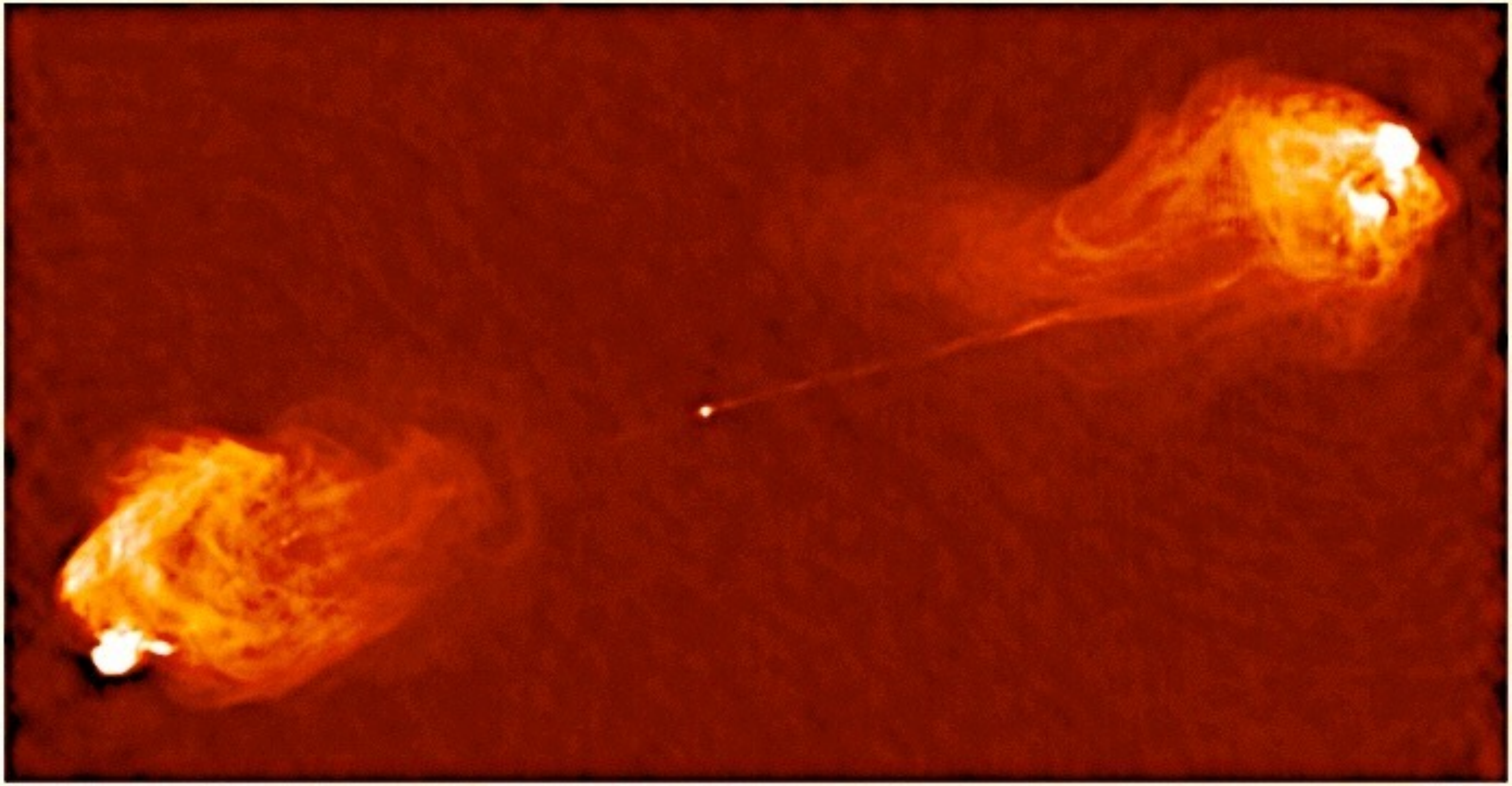

Status of Large Scale UHECR Anisotropy

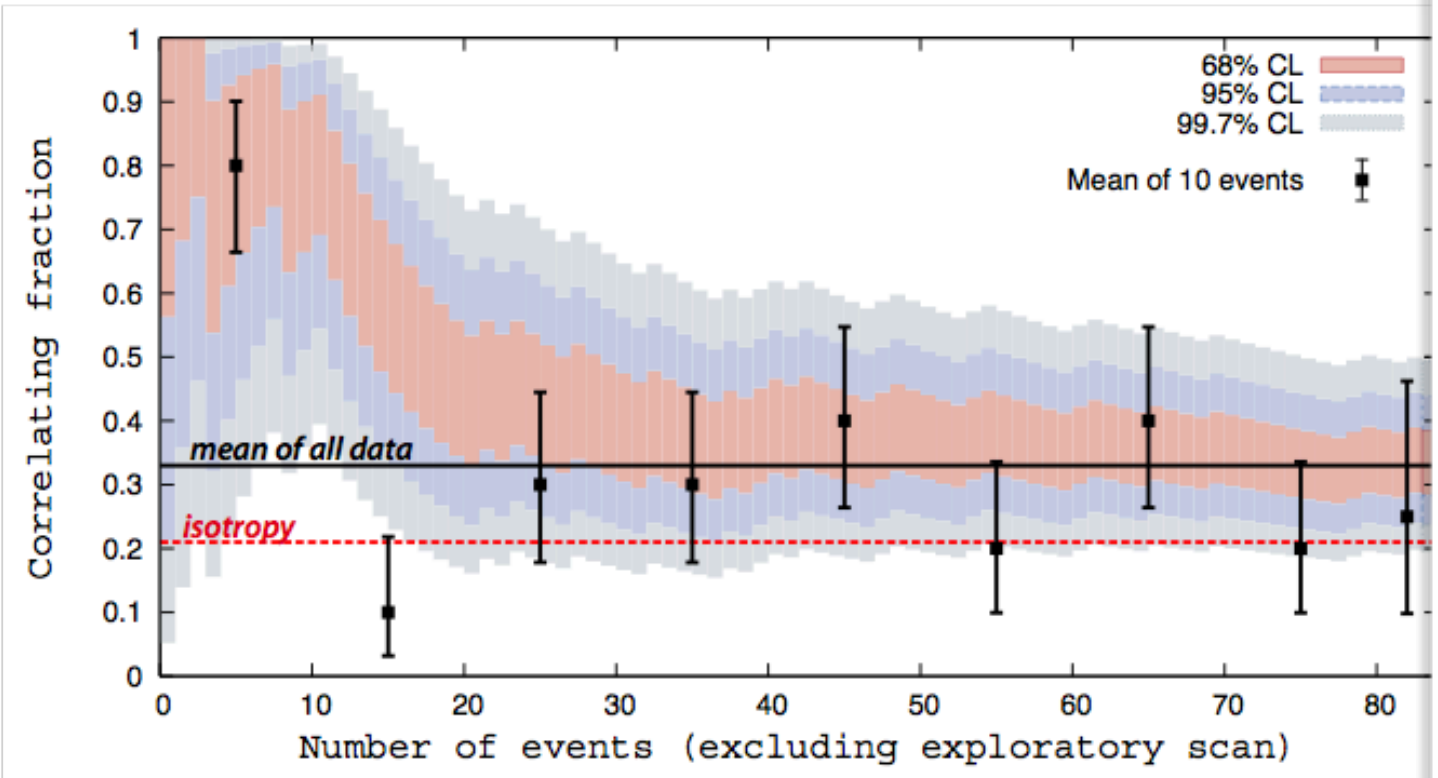

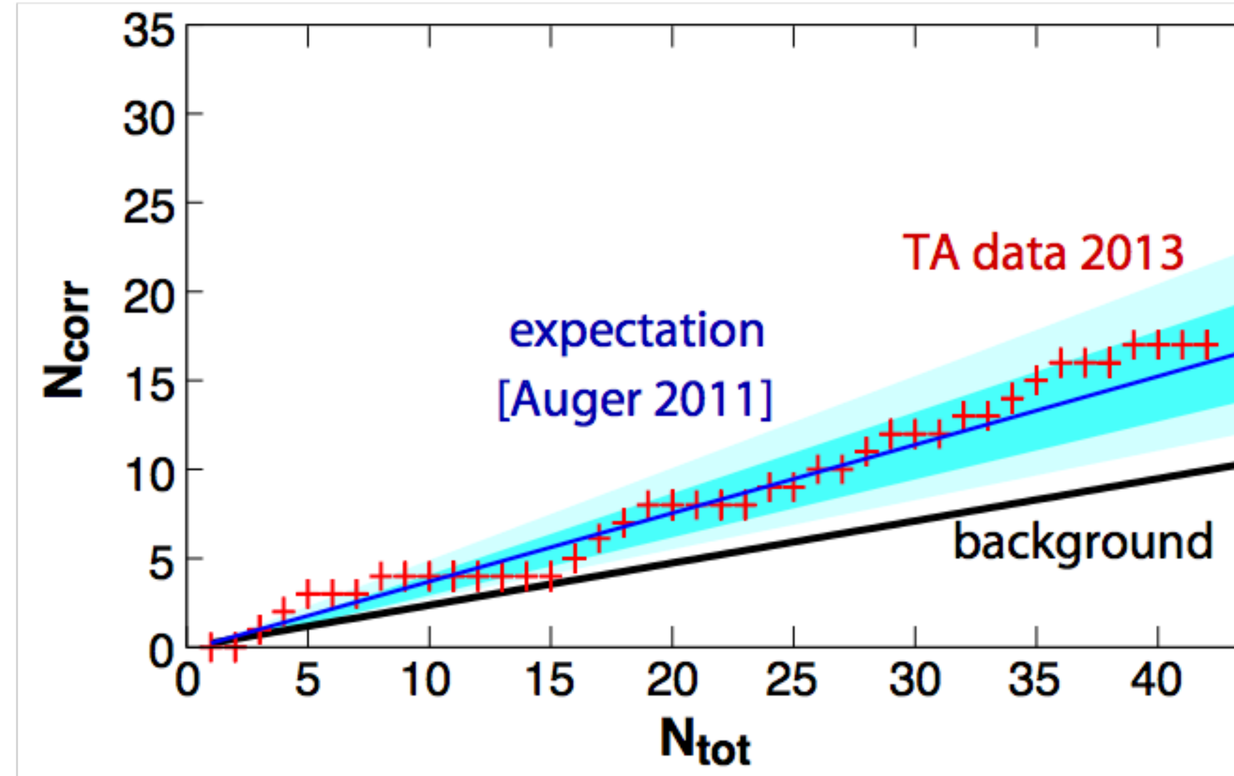

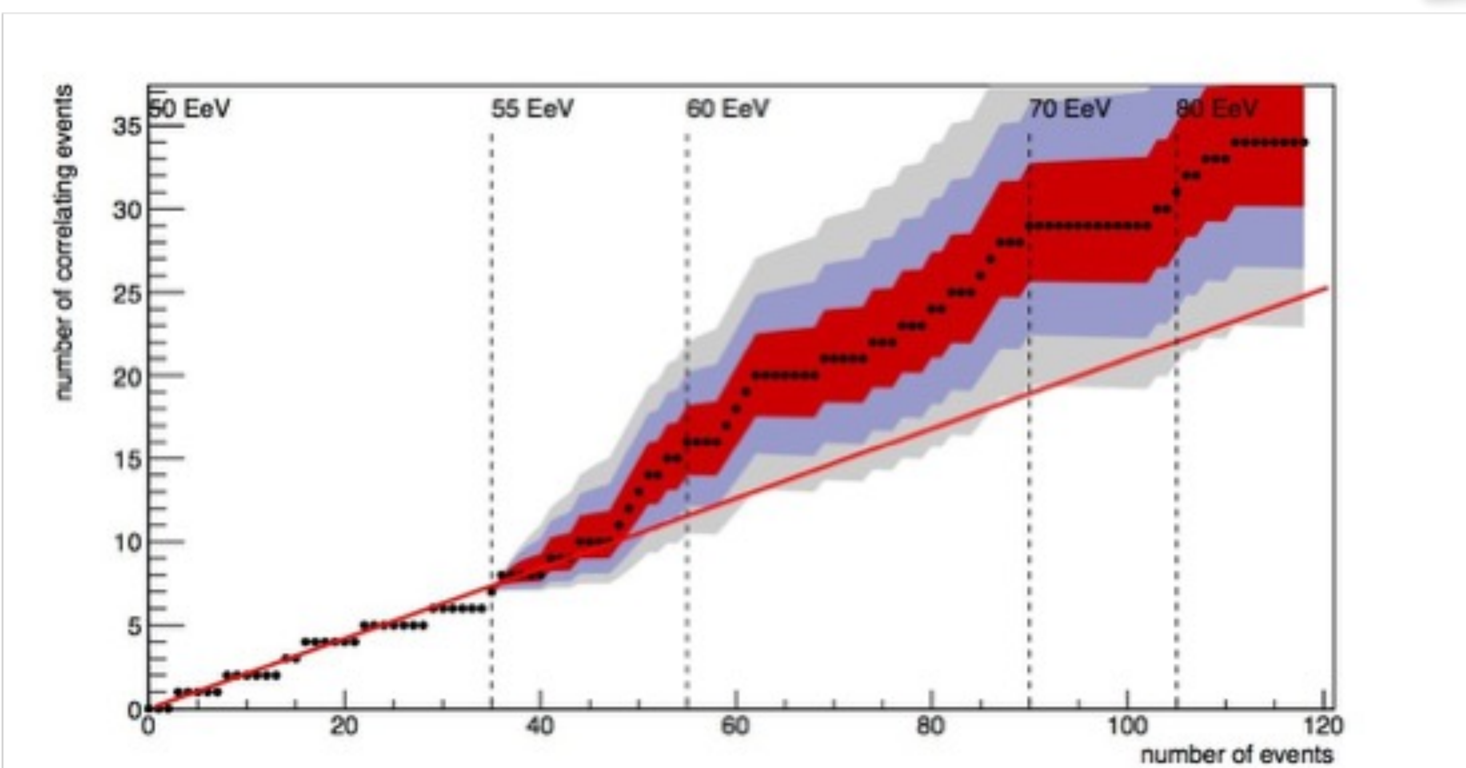

Kampert and Tinyakov,arXiv:1405.0575

All Sky View from Pierre Auger and Telescope Array

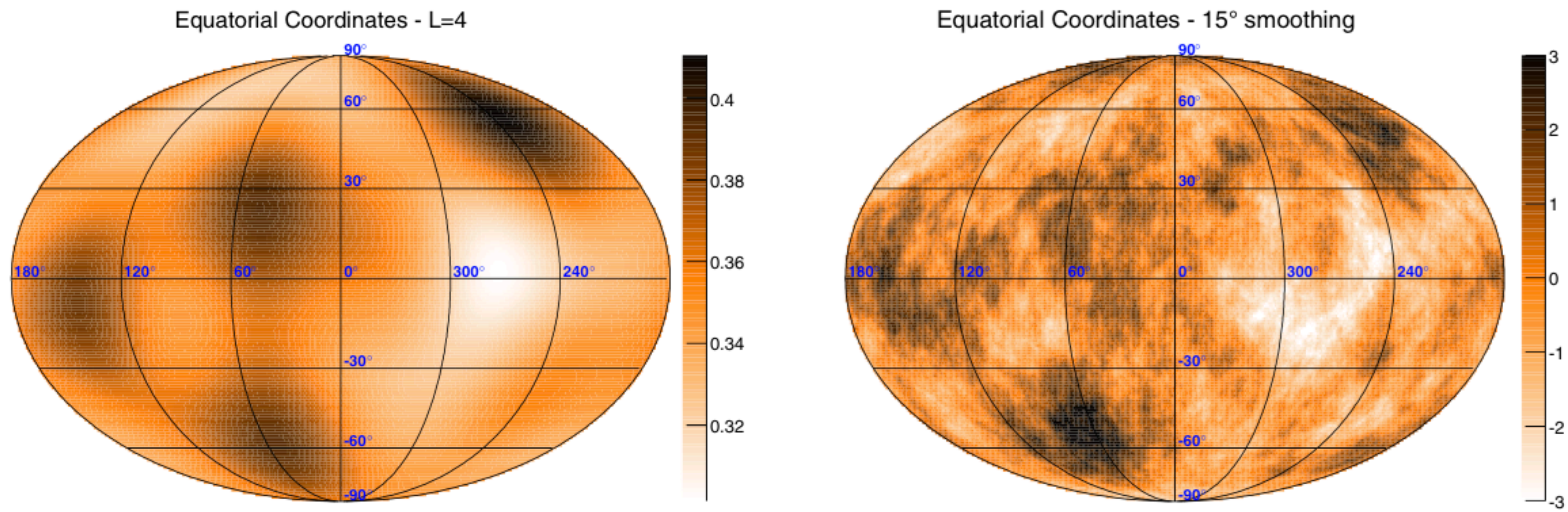

Figure 9. Left: flux sky map in km^{-2} yr^{-1} sr^{-1} units, using a multipolar expansion up to $\ell = 4$. Right: significance sky map smoothed out at a 15° angular scale.
(A color version of this figure is available in the online journal.)

Pierre Auger and Telescope Collaborations, ApJ 794 (2014) 172 [arXiv:1409.3128]

Li-Ma significances: Pierre Auger Collaboration arXiv:1411.6111]

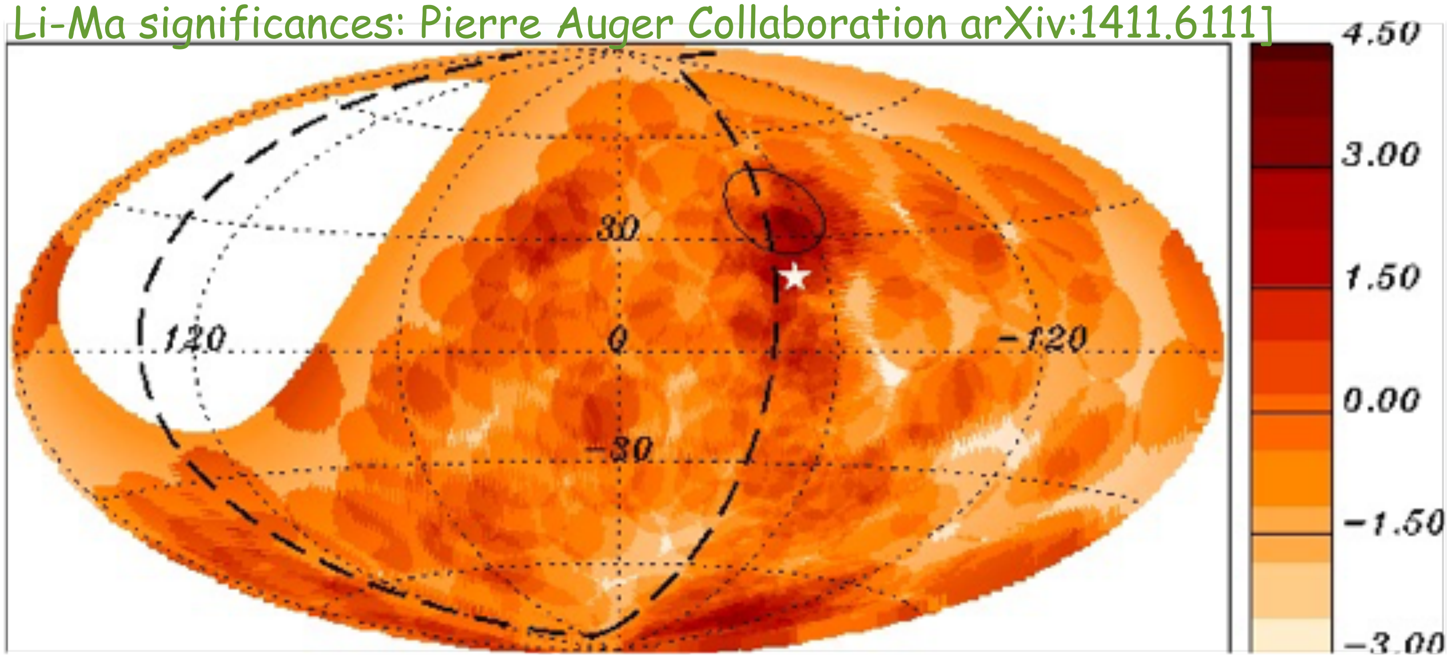

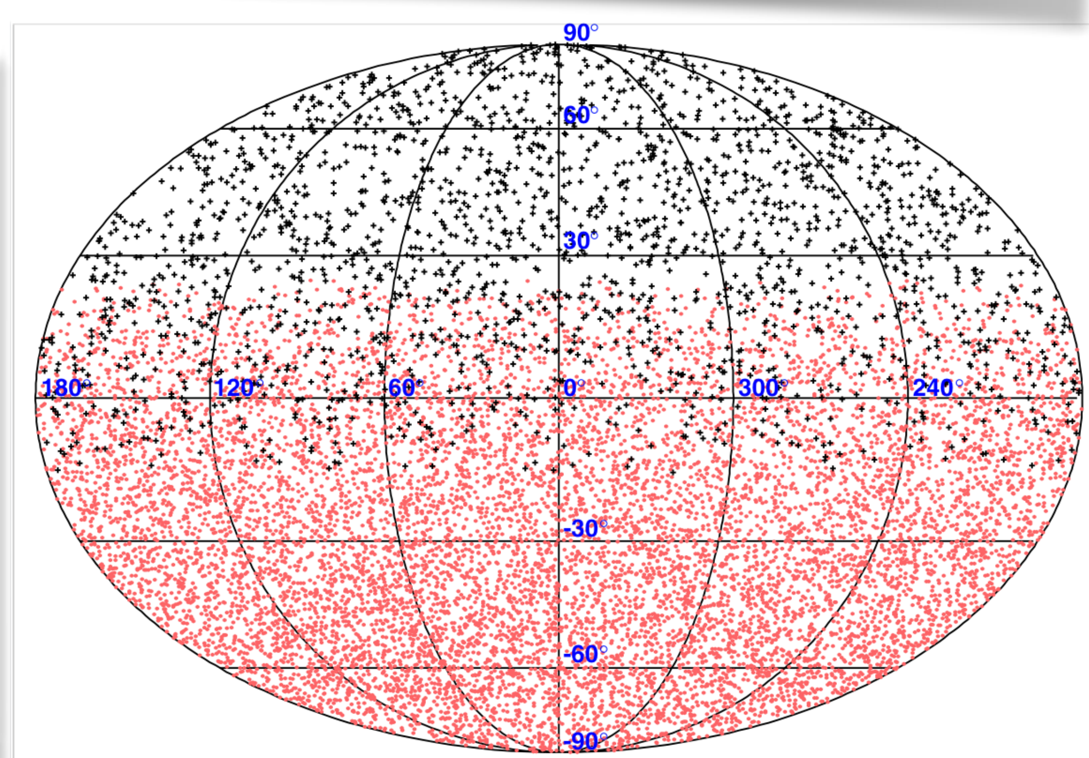

Mass Composition

Depth of shower maximum X_{max} and its distribution contain information on primary mass composition

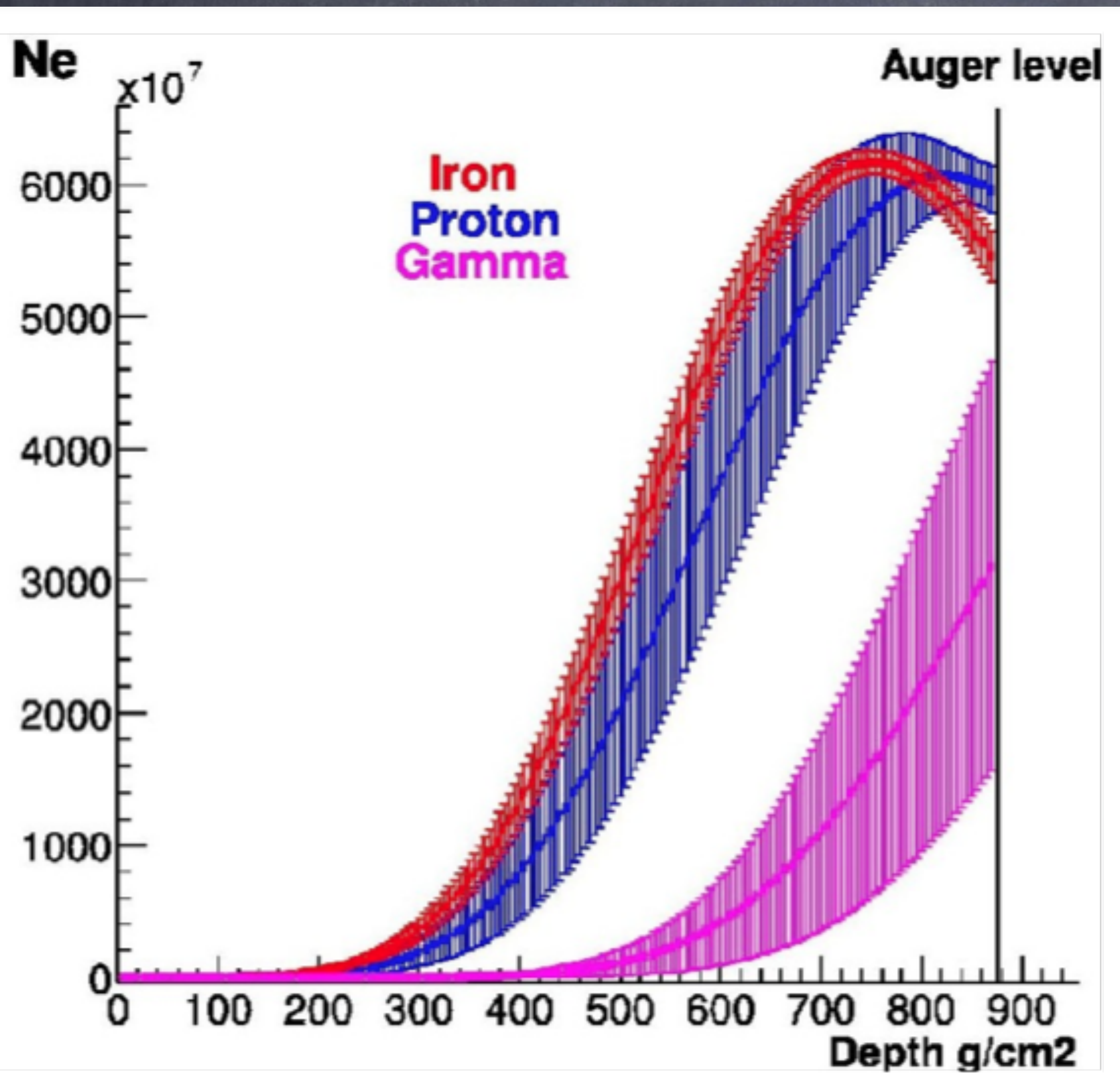

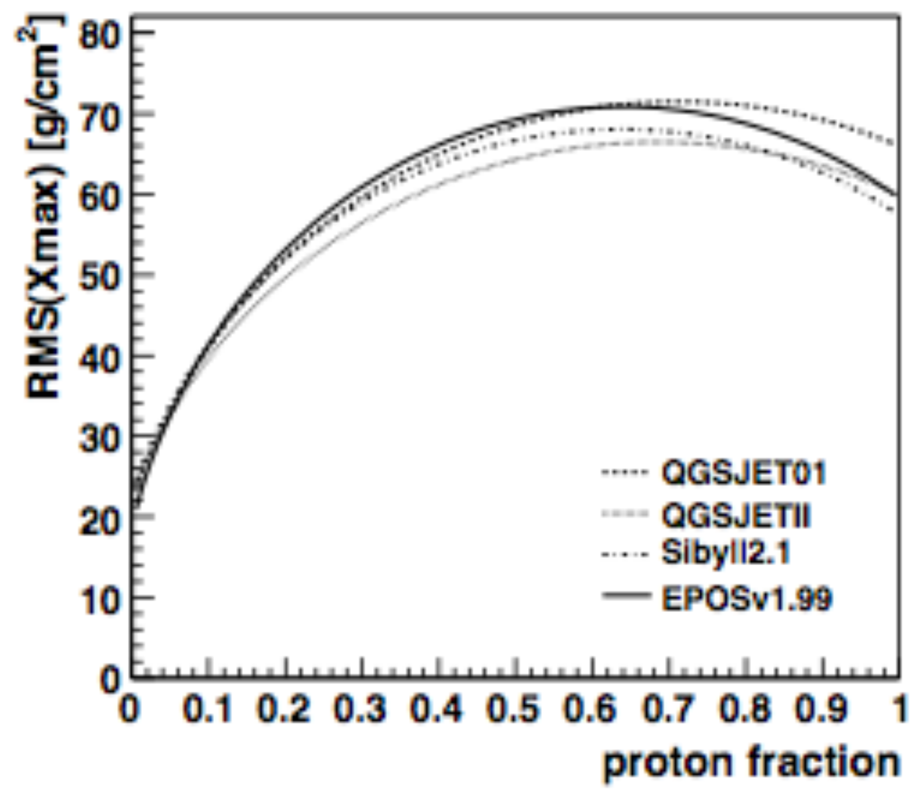

FIGURE 1. RMS(X_{max}) from different hadronic interaction models [23] and a two-component p/Fe composition model ($E = 10^{18}$ eV).

Pierre Auger data suggest a heavier composition toward highest energies:

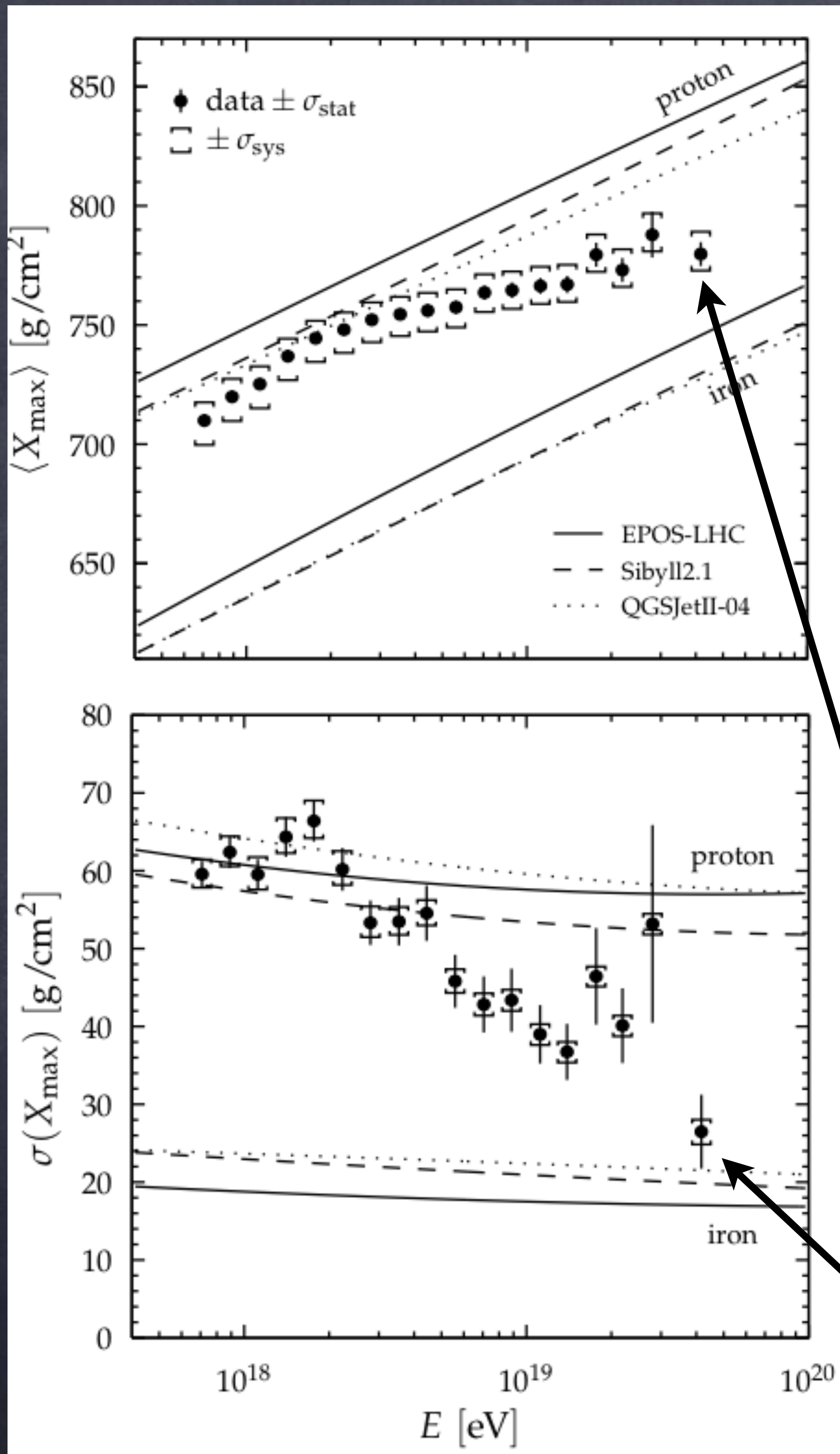

Pierre Auger Collaboration, arXiv:1409.4809

but not confirmed on the northern hemisphere by HiRes and Telescope Array which are consistent with protons

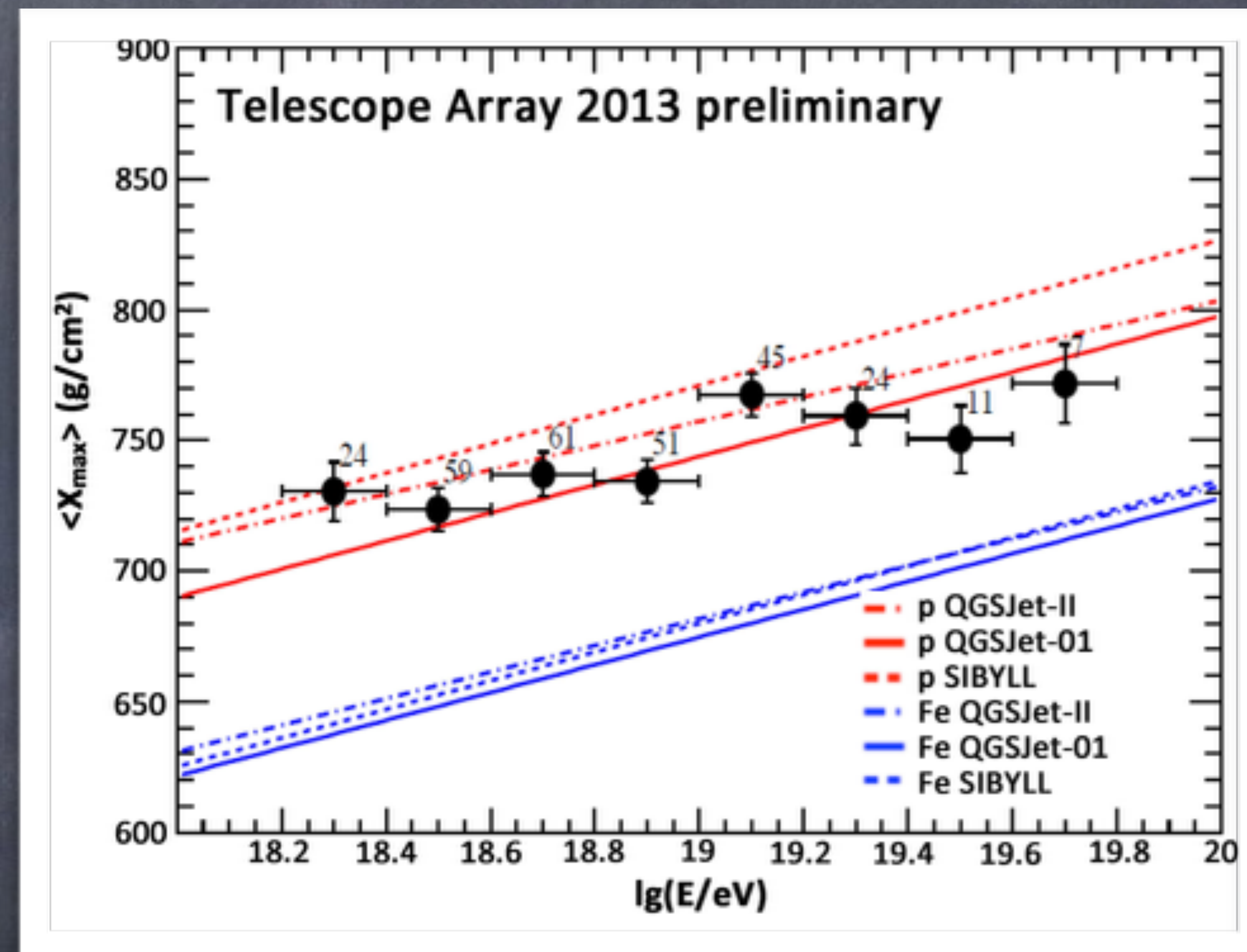

potential tension with air shower simulations and some hadronic interaction models because a mixed composition would predict larger RMS(X_{max})

combined measurement of X_{max} and its fluctuation $\sigma(X_{max})$ can be translated to distribution of atomic mass A **within a given hadronic interaction model**

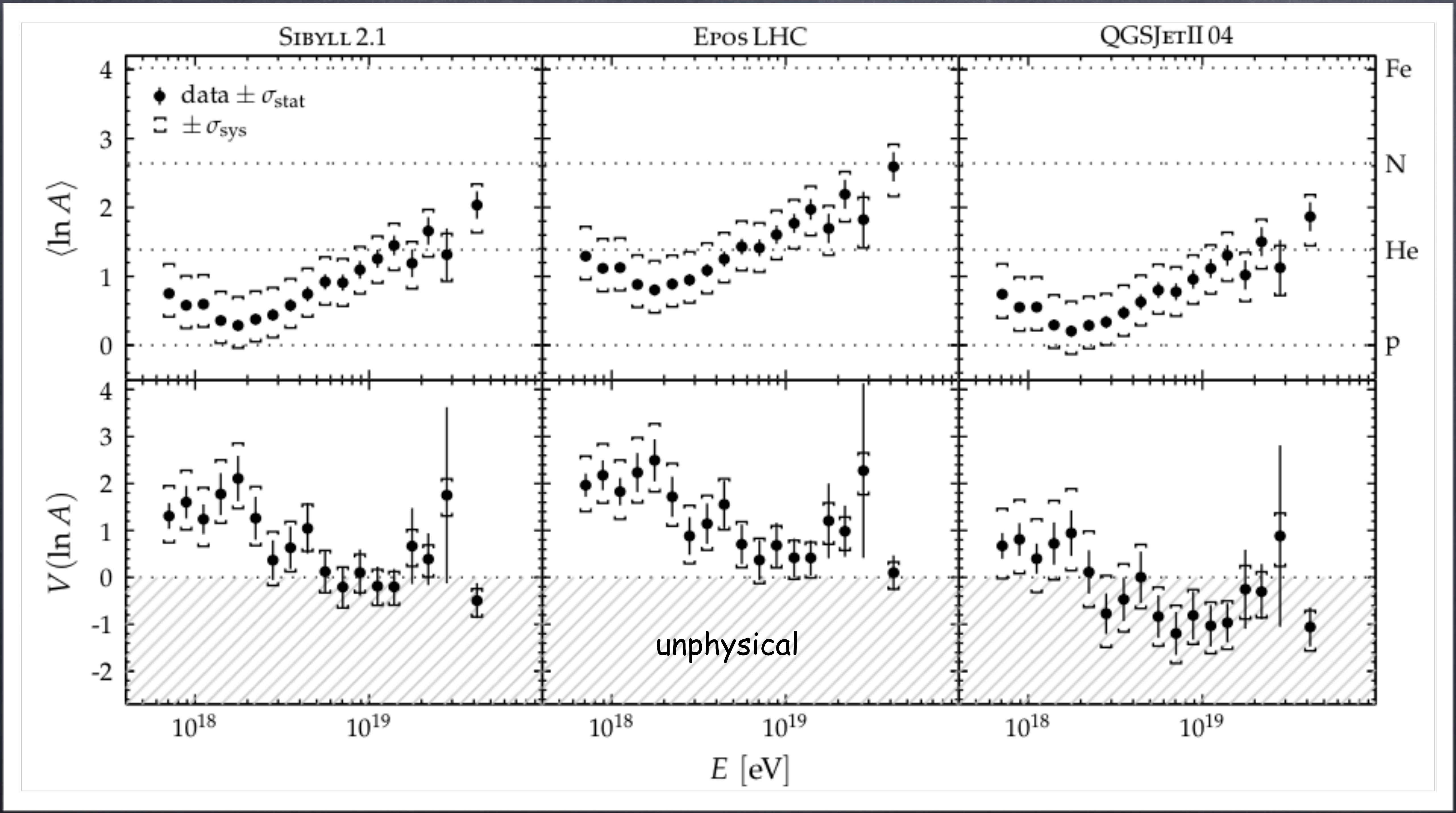

Pierre Auger Collaboration, arXiv:1409.4809

would imply that fluctuations predicted by a pure composition already higher than observed

Muon number measured at 1000 m from shower core a factor ~2 higher than predicted

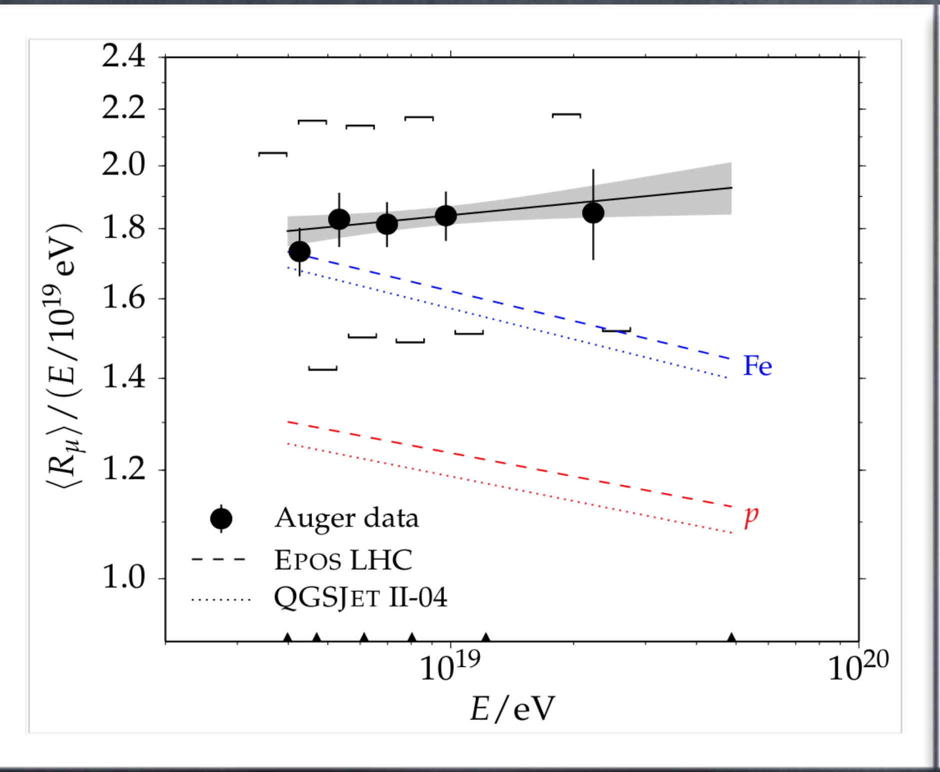

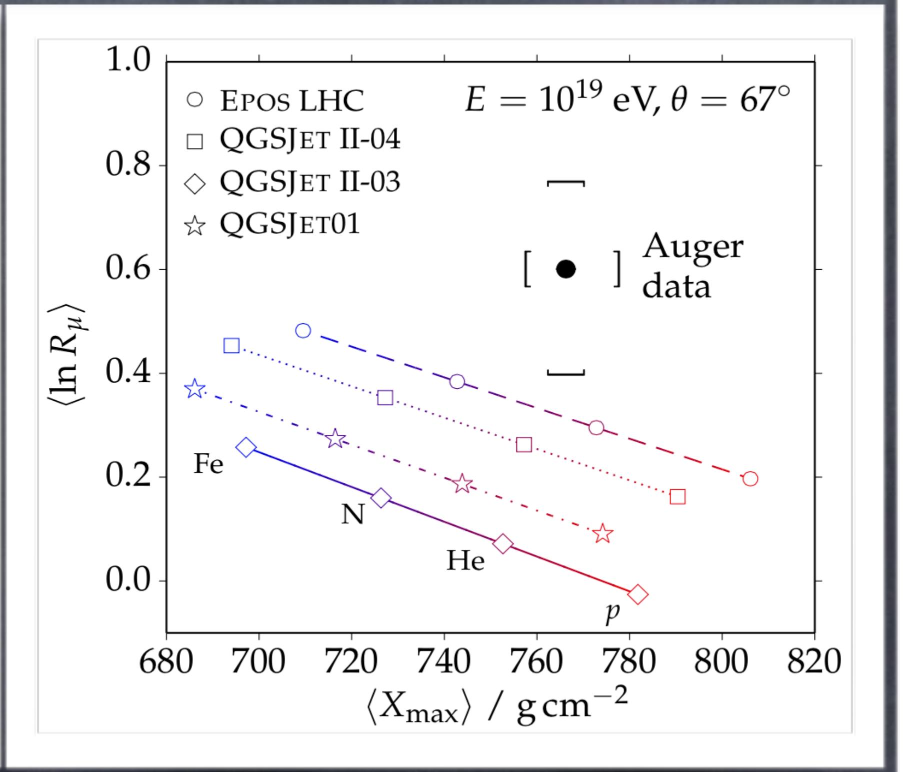

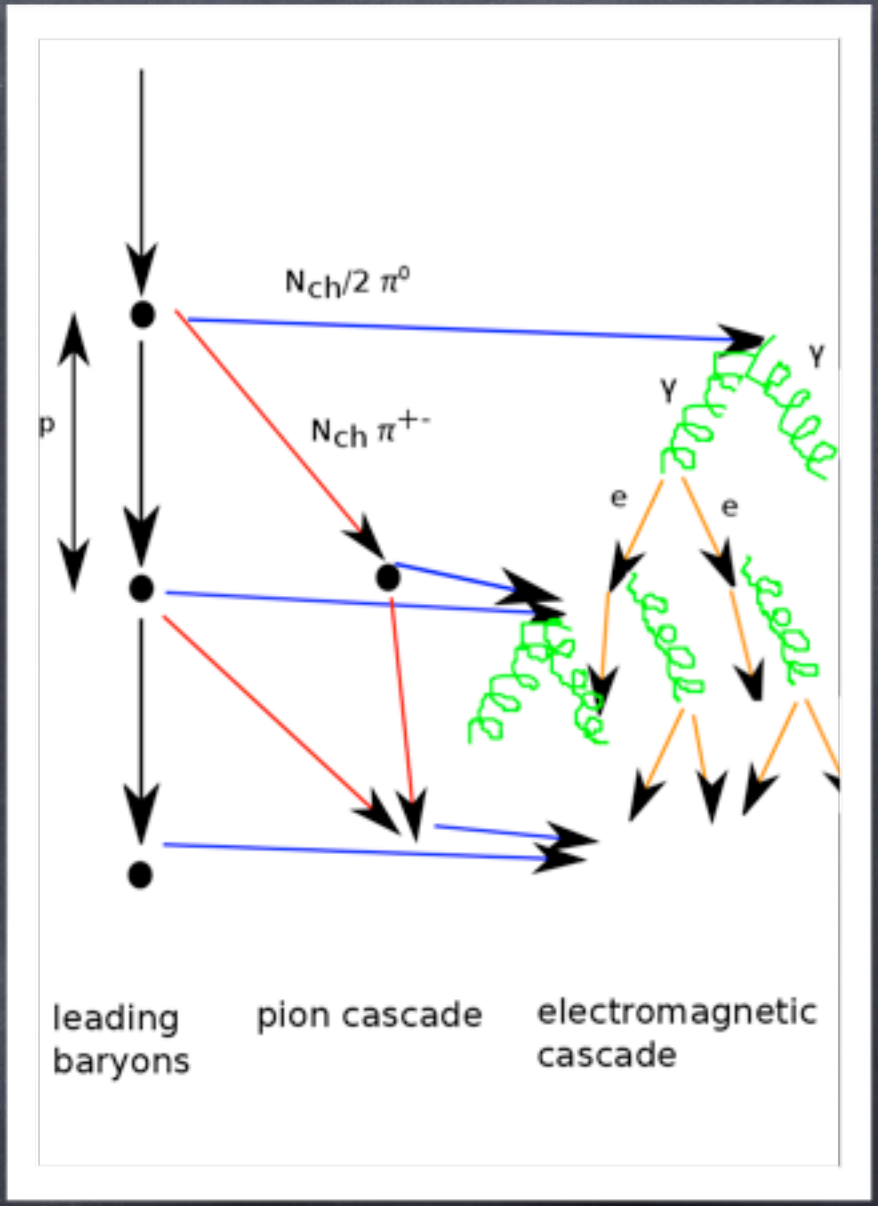

Pierre Auger Collaboration, arXiv:1408.1421

The muon number scales as

$$N_\mu \propto E_{\mathrm{had}} \propto (1 - f_{\pi^0})^N \ ,$$

with the fraction going into the electromagnetic channel $f_{\pi^0} \simeq \frac{1}{3}$ and the number of generations N strongly constrained by X_{max}. Larger N_μ thus requires smaller f_{π^0} !

The global picture for the mass composition

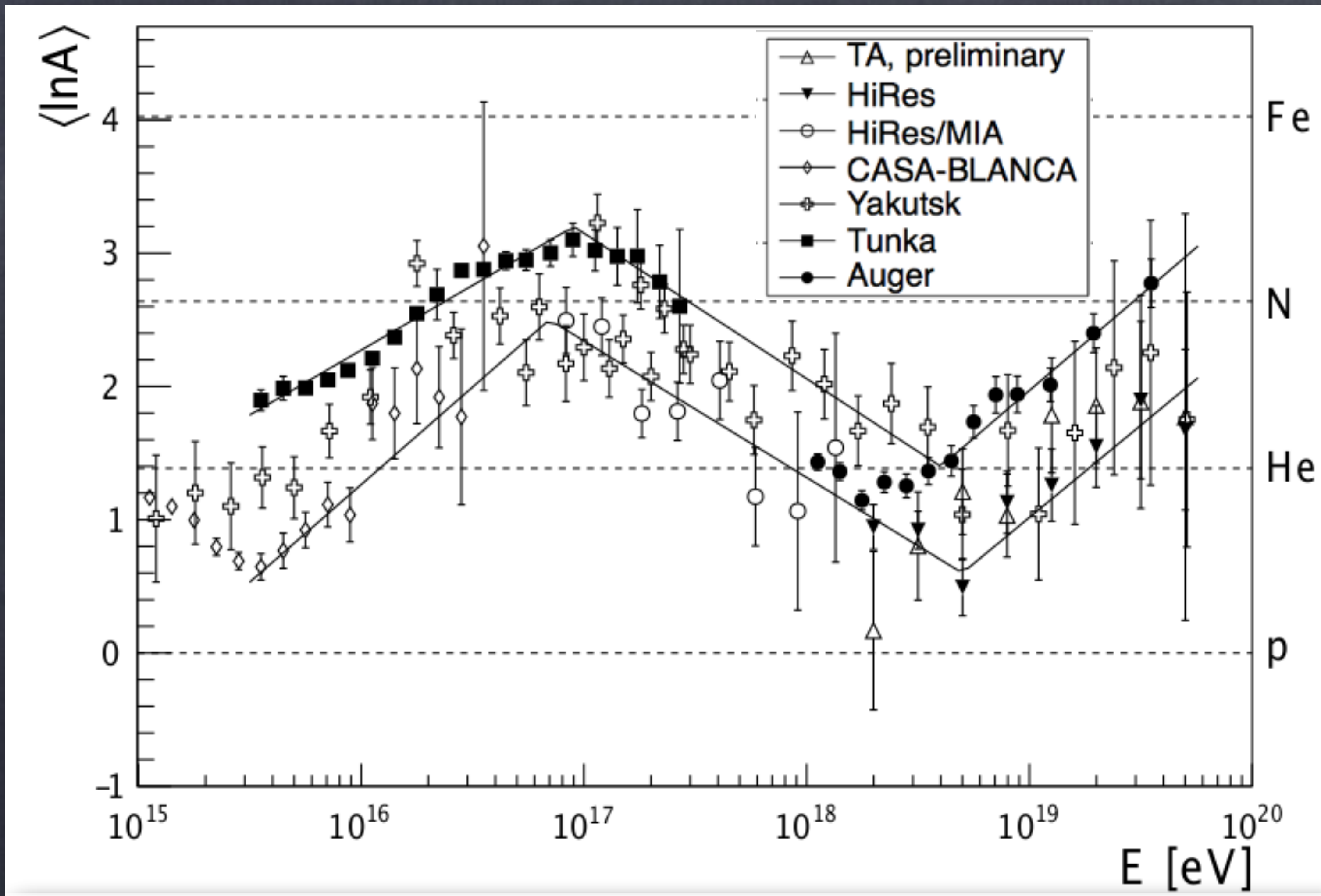

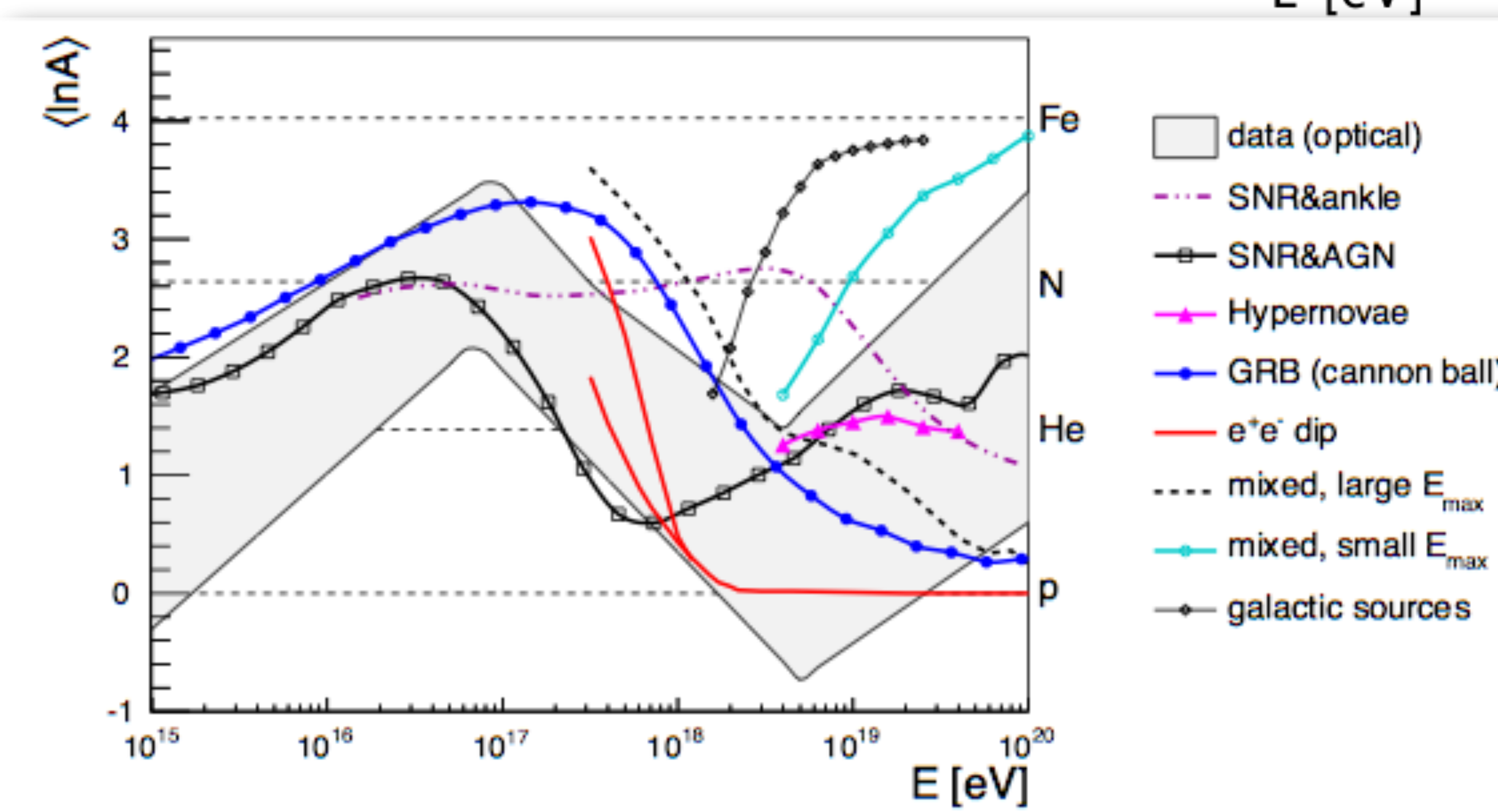

K.-H.Kampert and M.Unger, Astropart.Phys. 35 (2012) 660

Indications of “Peters cycles” for galactic and extragalactic sources whose maximal energies are proportional to the charge Z and extend up to ~ 10^{17} and 10^{20} eV, respectively

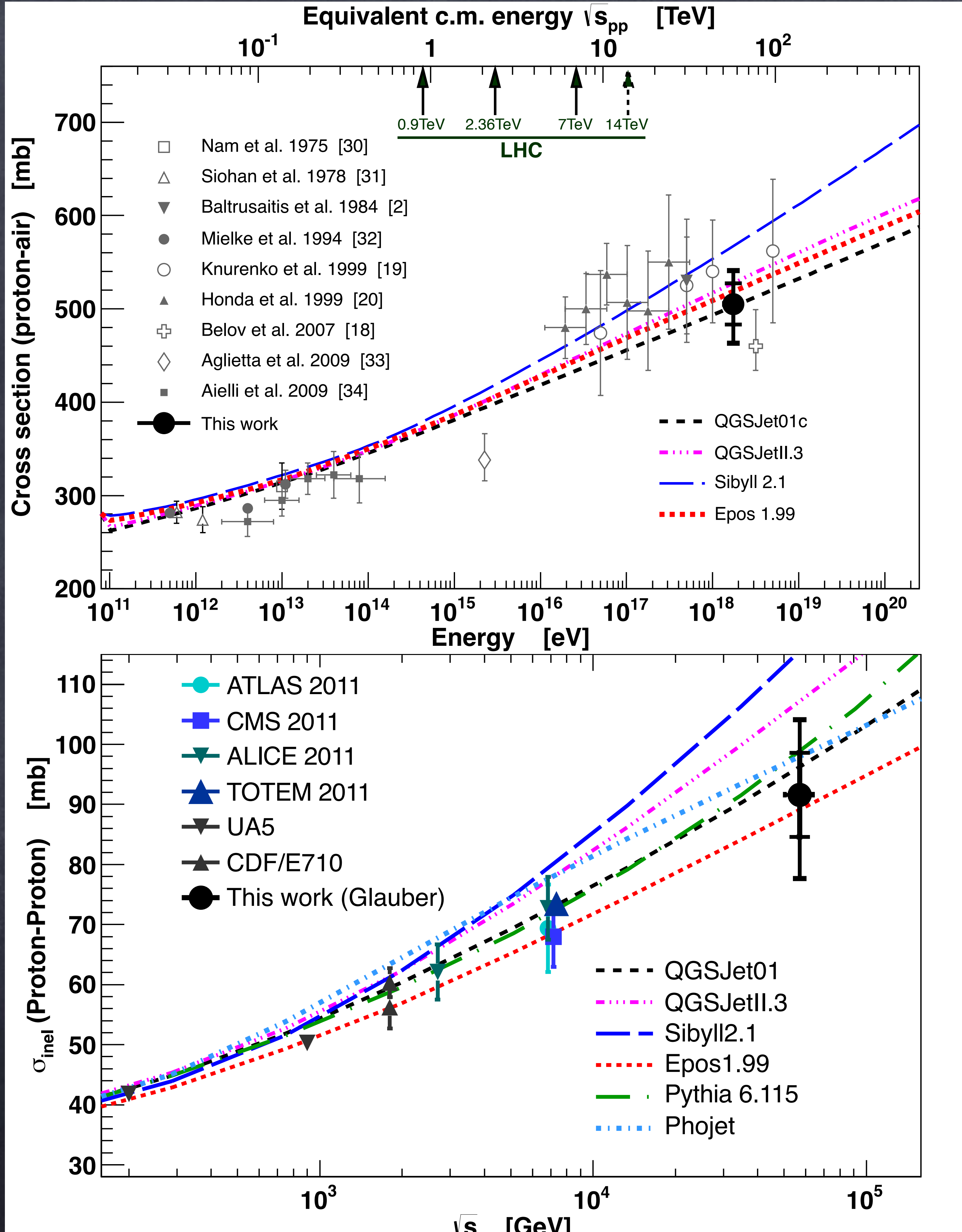

p-air cross section derived from exponential tail of depth of shower maxima

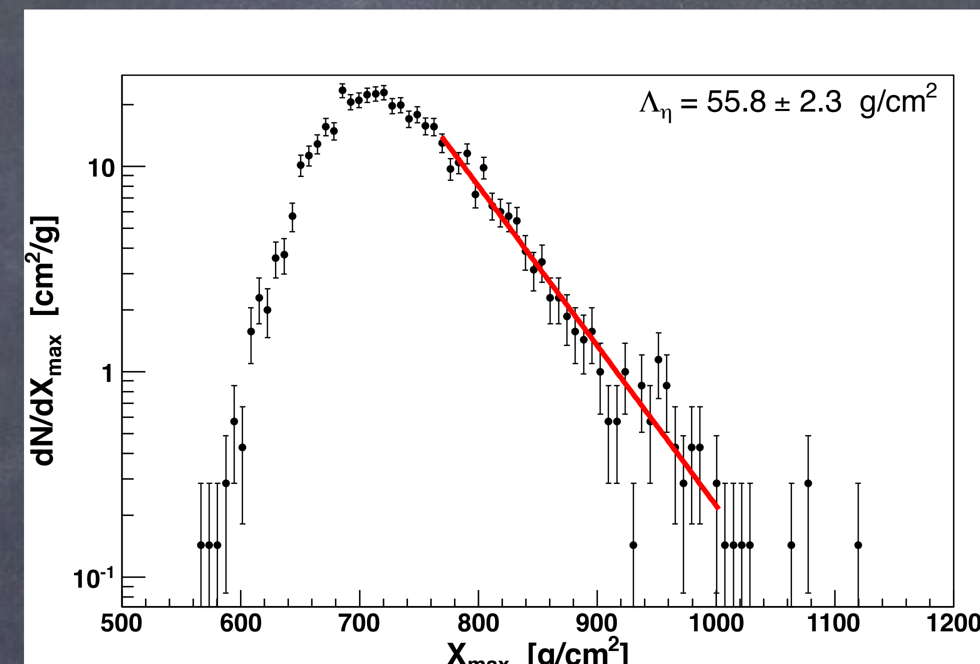

pp cross section derived from Glauber model

Pierre Auger Collaboration, PRL 109, 062002 (2012)

Very High High Energy Neutrinos

The „grand unified“ differential neutrino number spectrum

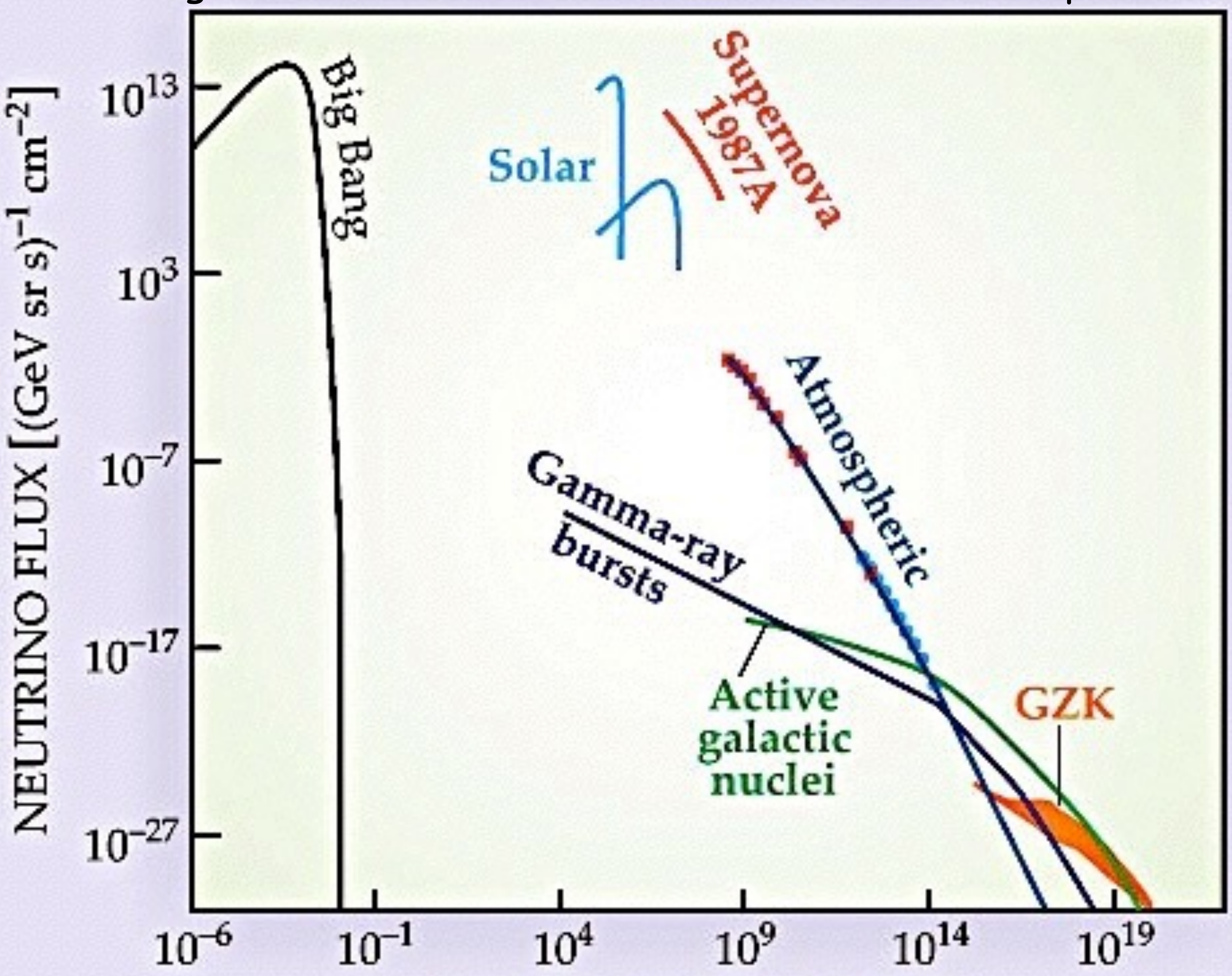

From Physics Today

Summary of neutrino production modes

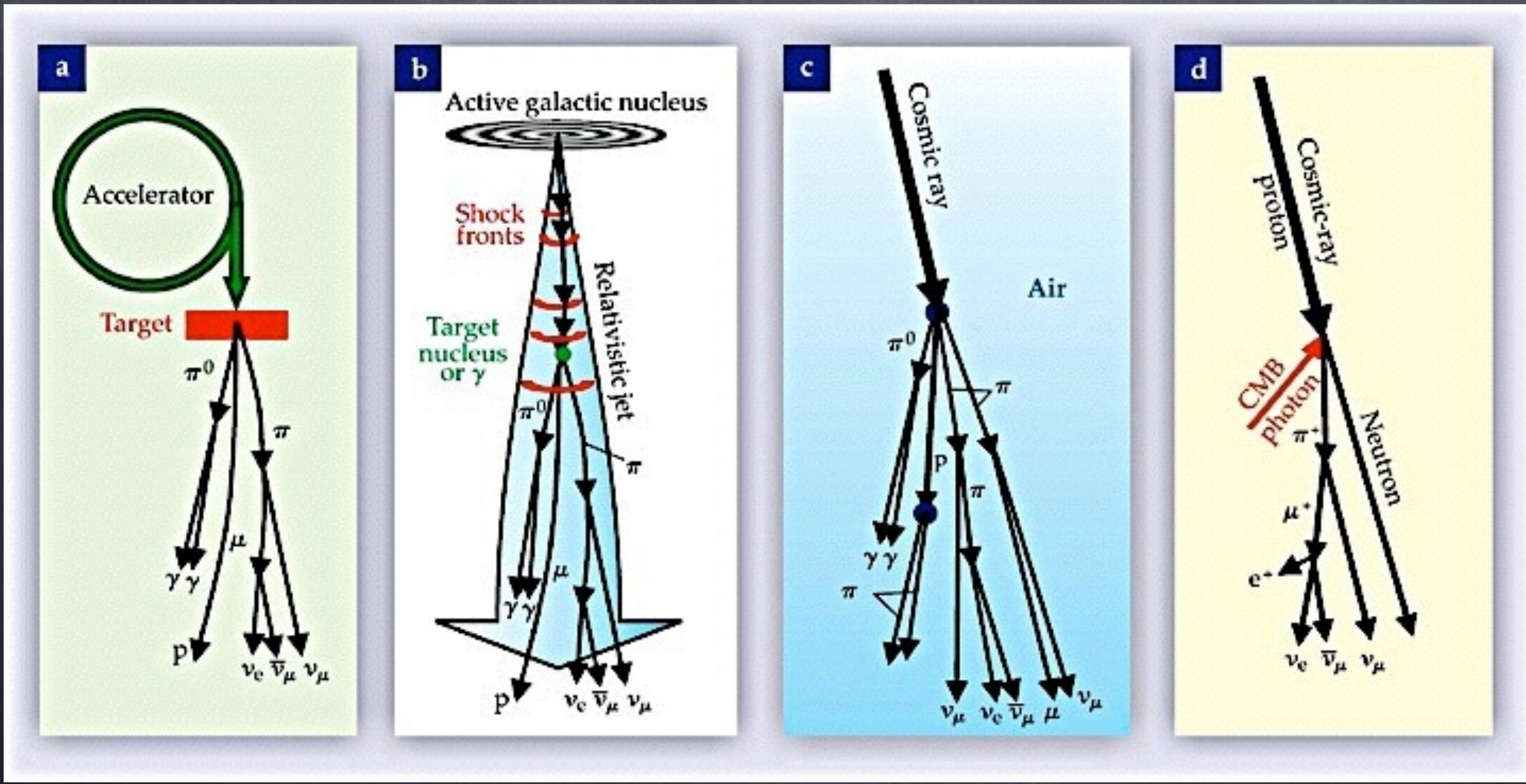

From Physics Today

IceCube observed 283 cascade and 105 track events from the Southern sky above 1 TeV deposited energy:

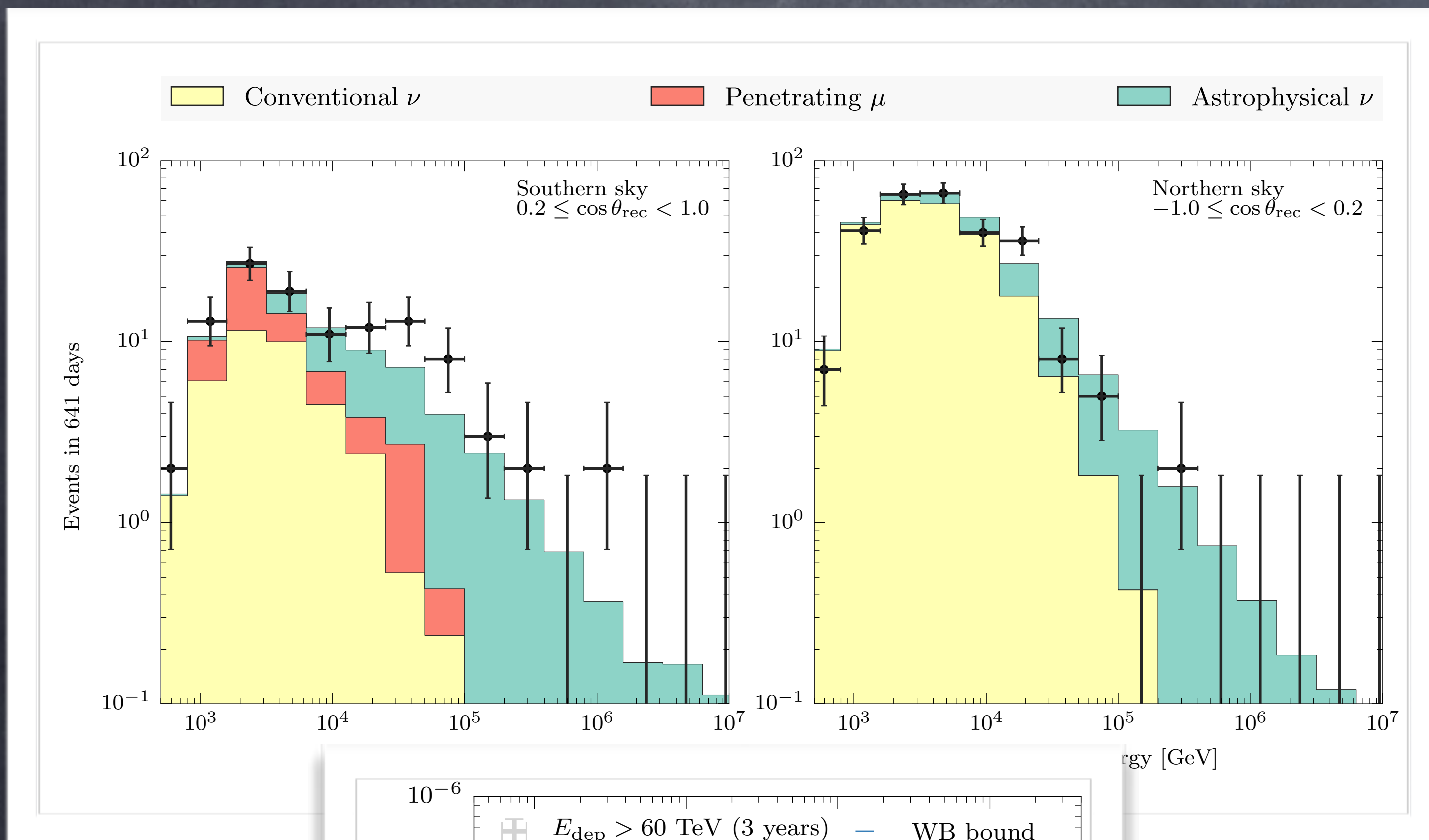

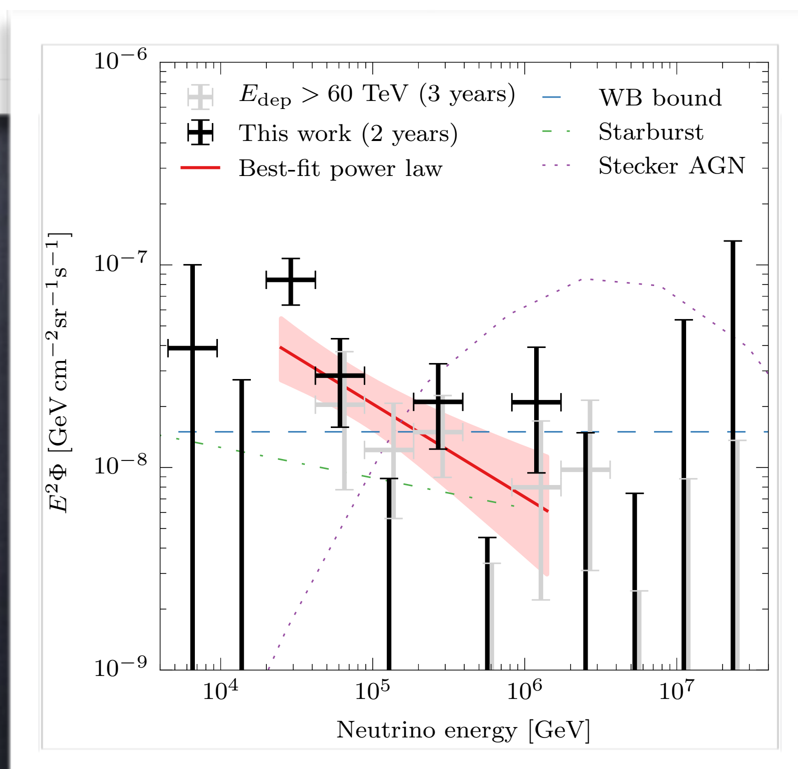

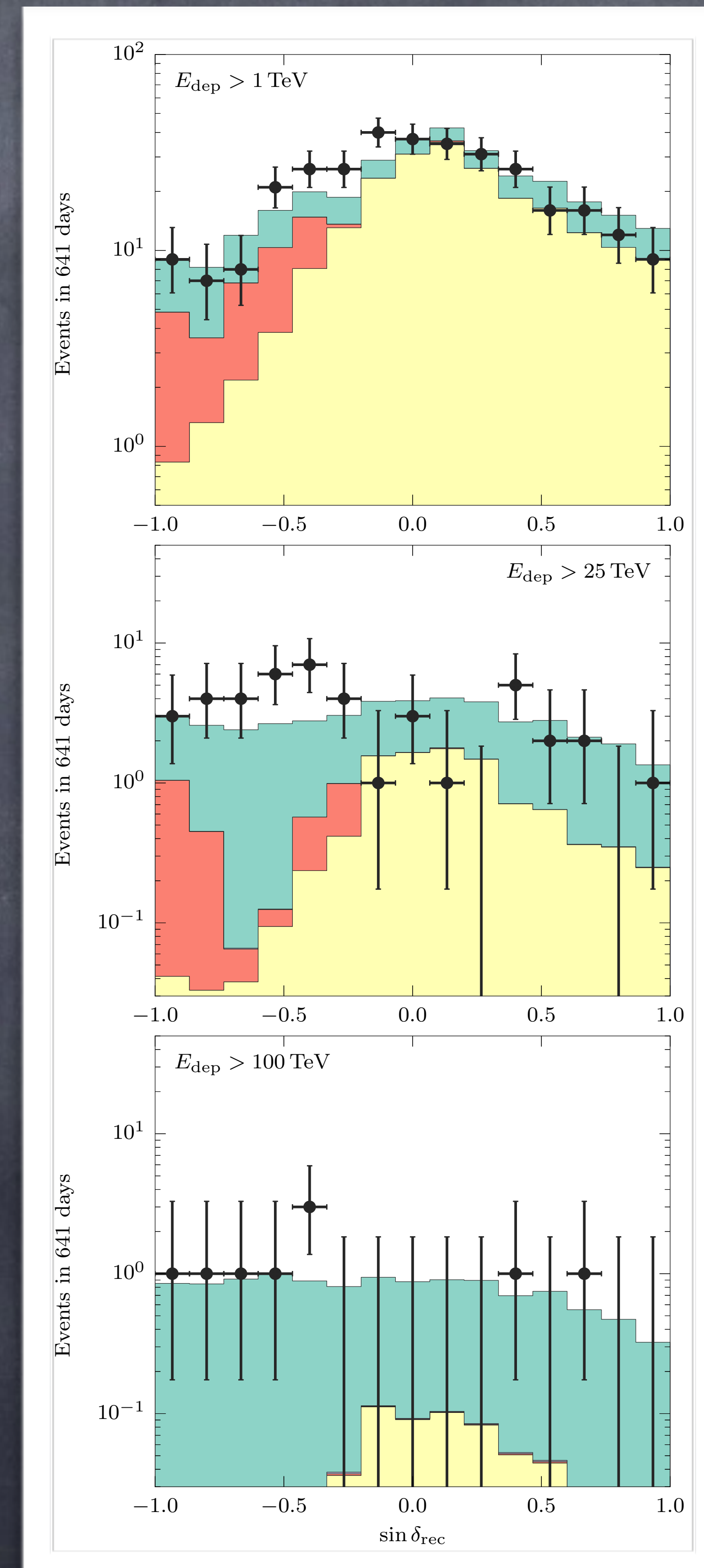

IceCube collaboration, Phys.Rev. D 91 (2015) 022001 [arXiv:1410.1749]

Sky distribution

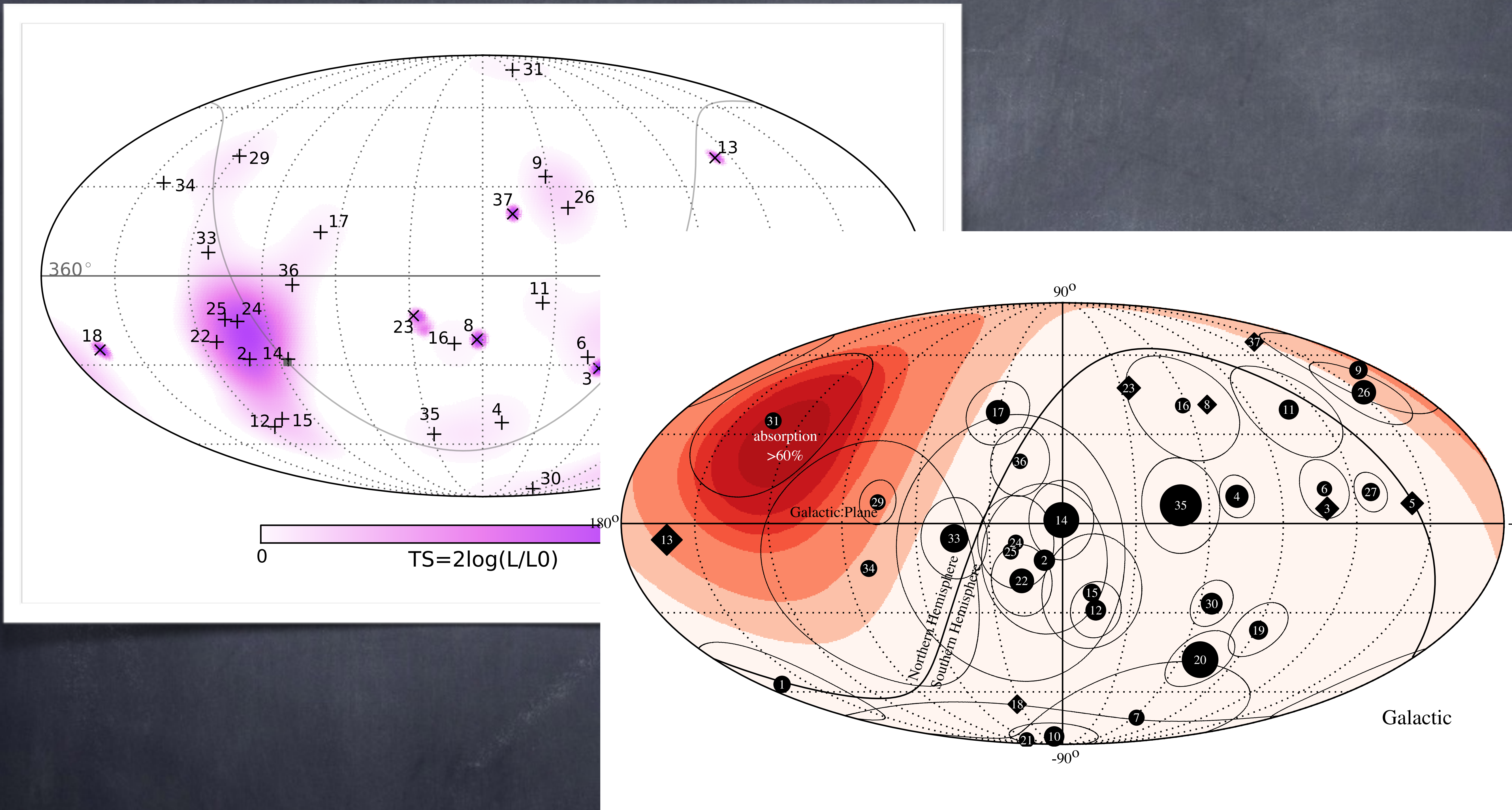

IceCube collaboration, Phys.Rev. Lett. 113 (2014) 101101 [arXiv:1405.5303]

A possible Correlation of IceCube Neutrinos with the Cosmic Ray Excess seen by Telescope Array ?

Telescope Array Collaboration, ApJ. Lett. 790 (2014) L21 [arXiv:1404.5890]

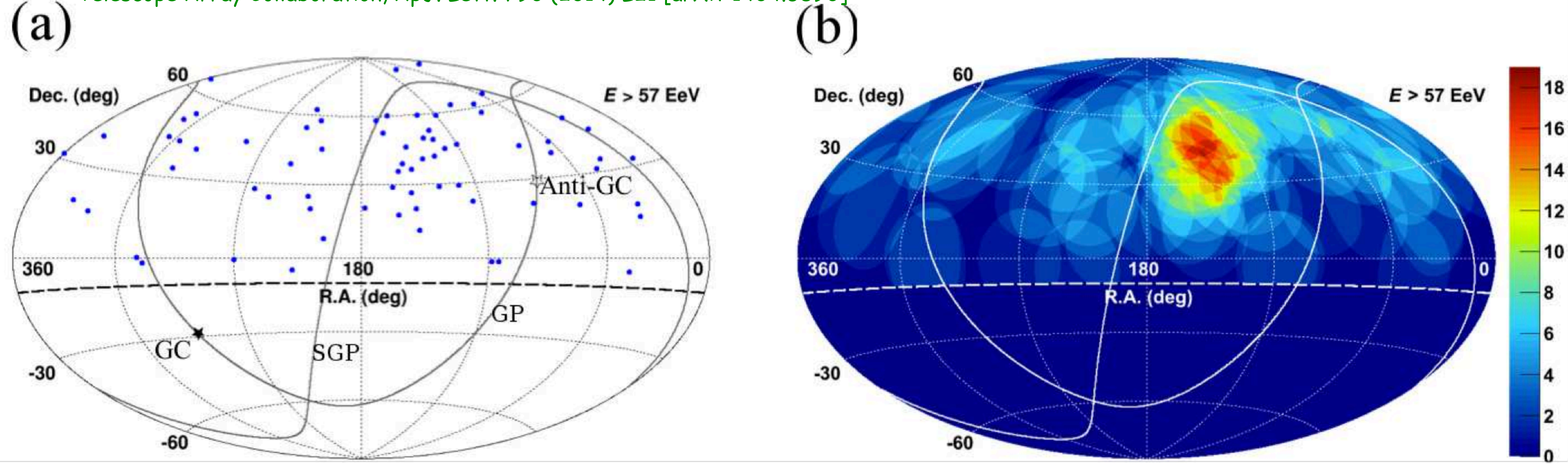

Fang, Olinto et al., arXiv:1404.6237

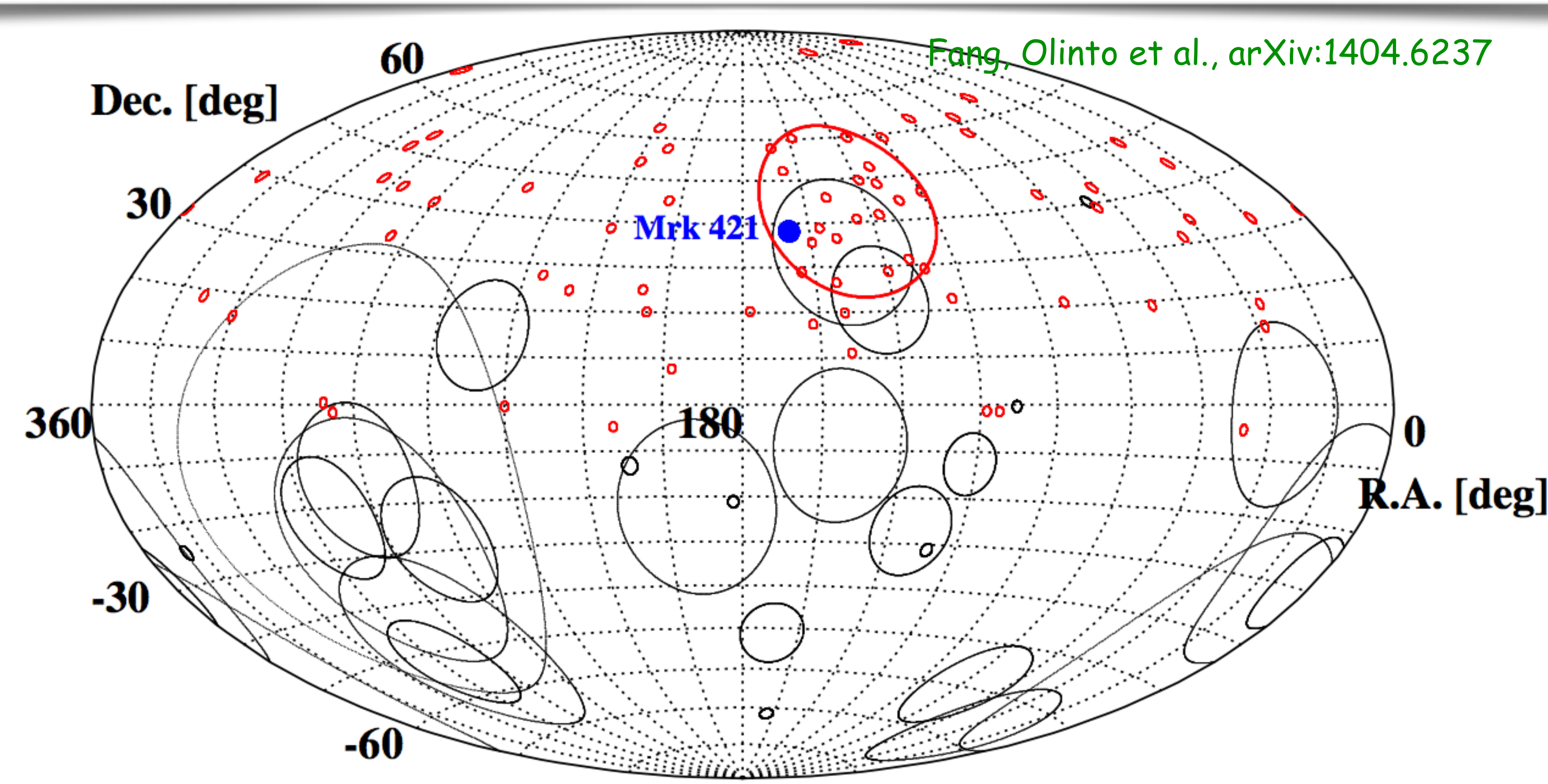

Cosmogenic Neutrinos: Maximal Fluxes for Pure Proton Injection insufficient to explain IceCube neutrinos

- Including secondary photons
- strong source evolution is here constrained by Fermi-LAT results

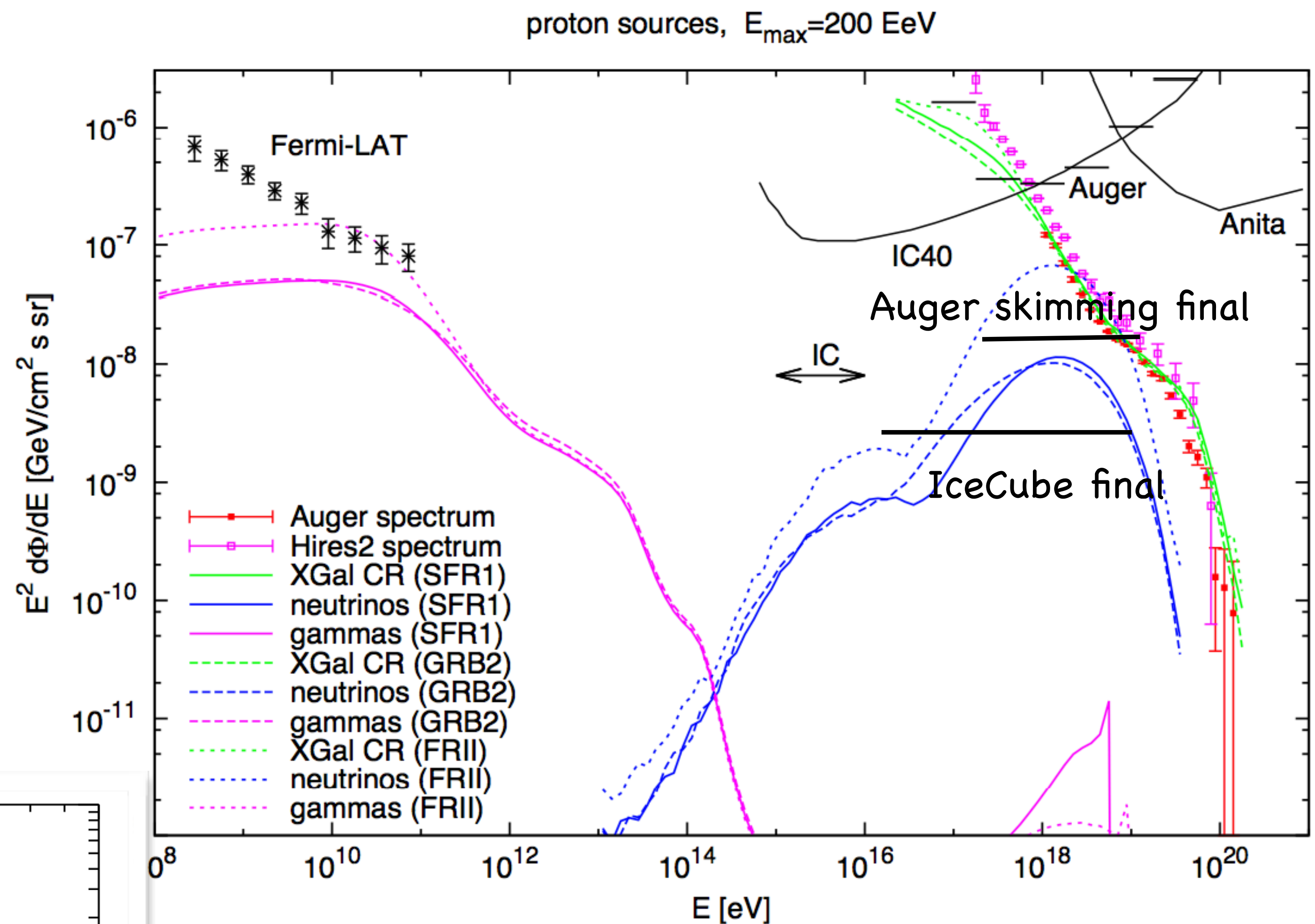

n scenario with $E_{\max} = 200\,\text{EeV}$ for different source evolution models (SFR1, GRB2 source spectral index is $\alpha = 2.4$ for the SFR1 and GRB2 models, while $\alpha = 2.2$ for Indicated are the propagated proton spectrum, the resulting (all flavor) neutrino luxes. The photon background measured by Fermi-LAT [10] is indicated, besides the ν bounds included in figure 1.

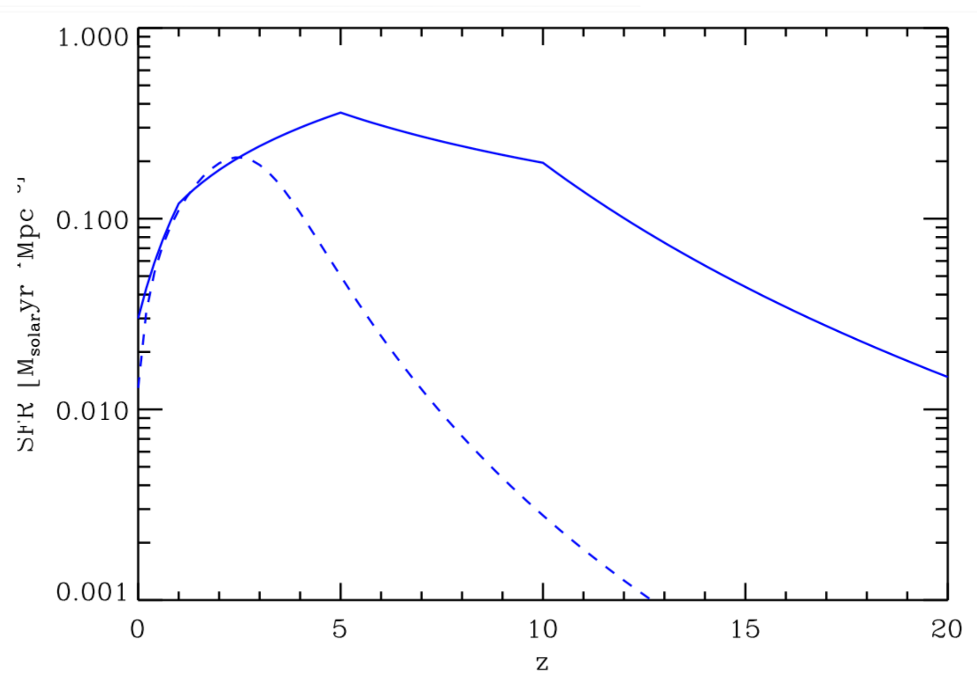

Roulet, Sigl, van Vliet, Mollerach, JCAP 1301, 028

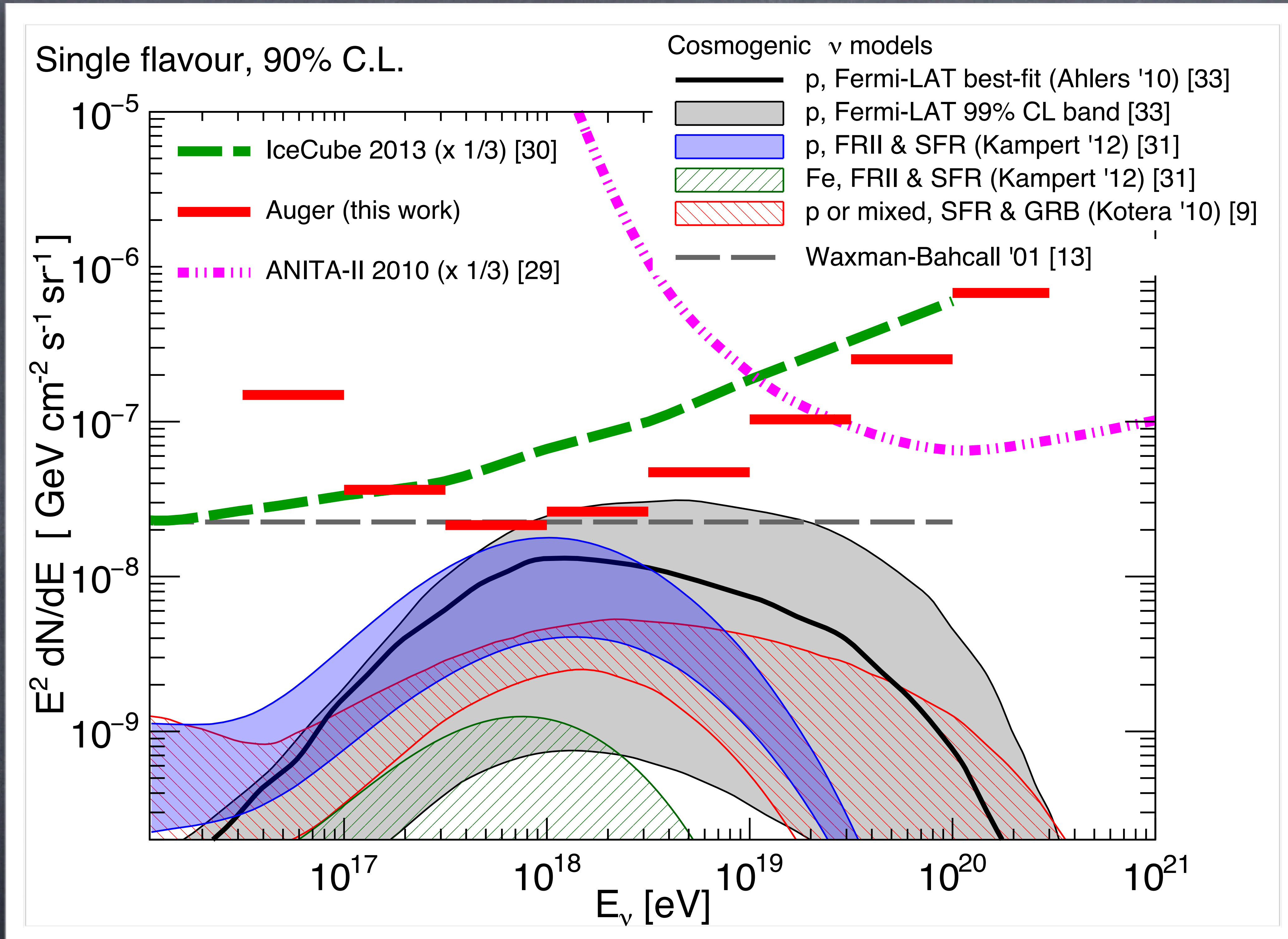

Pierre Auger Collaboration, arXiv:1504.05397

At the highest energies the neutrino flux limits start to constrain cosmogenic flux predictions

Discrete Extragalactic High Energy Neutrino Sources

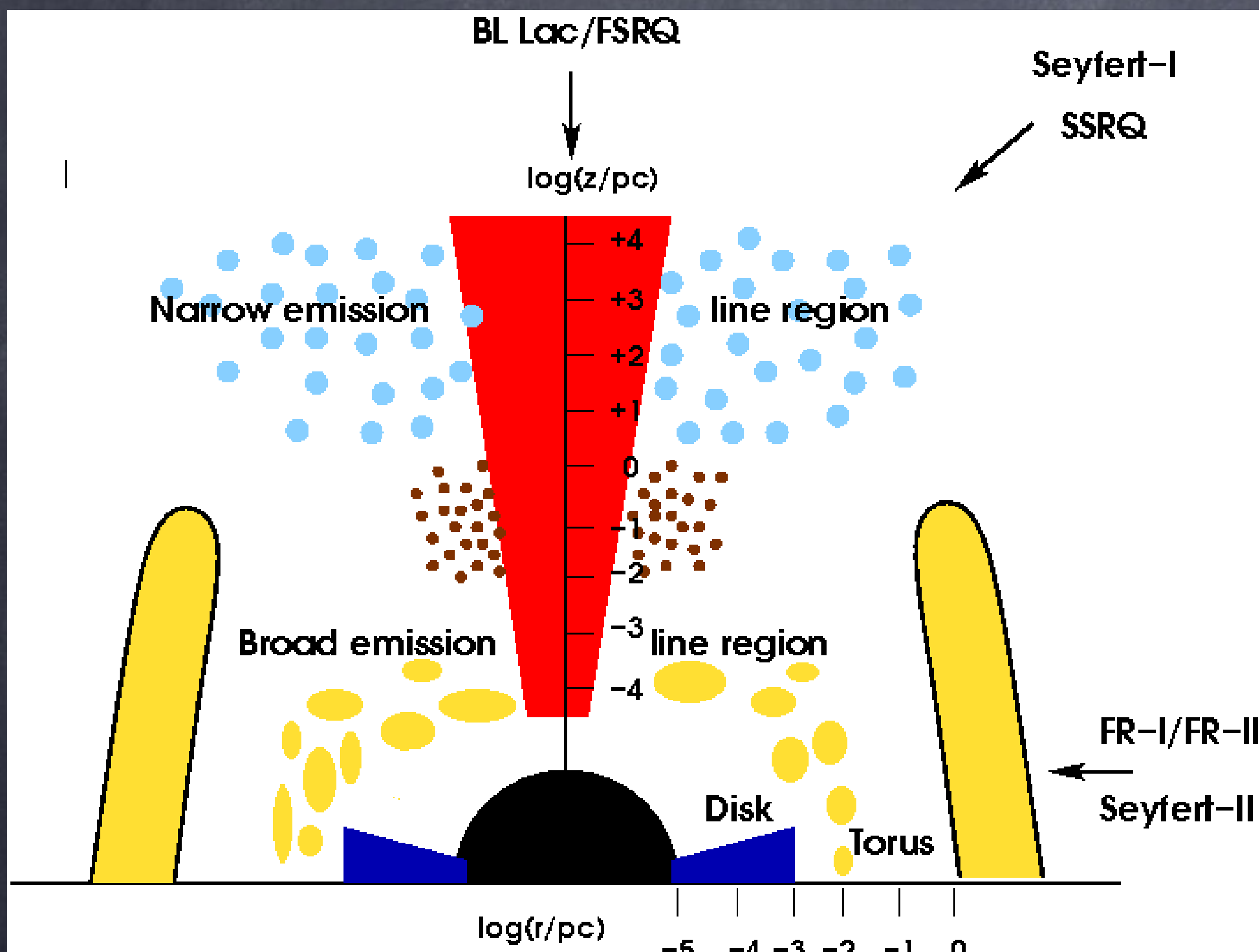

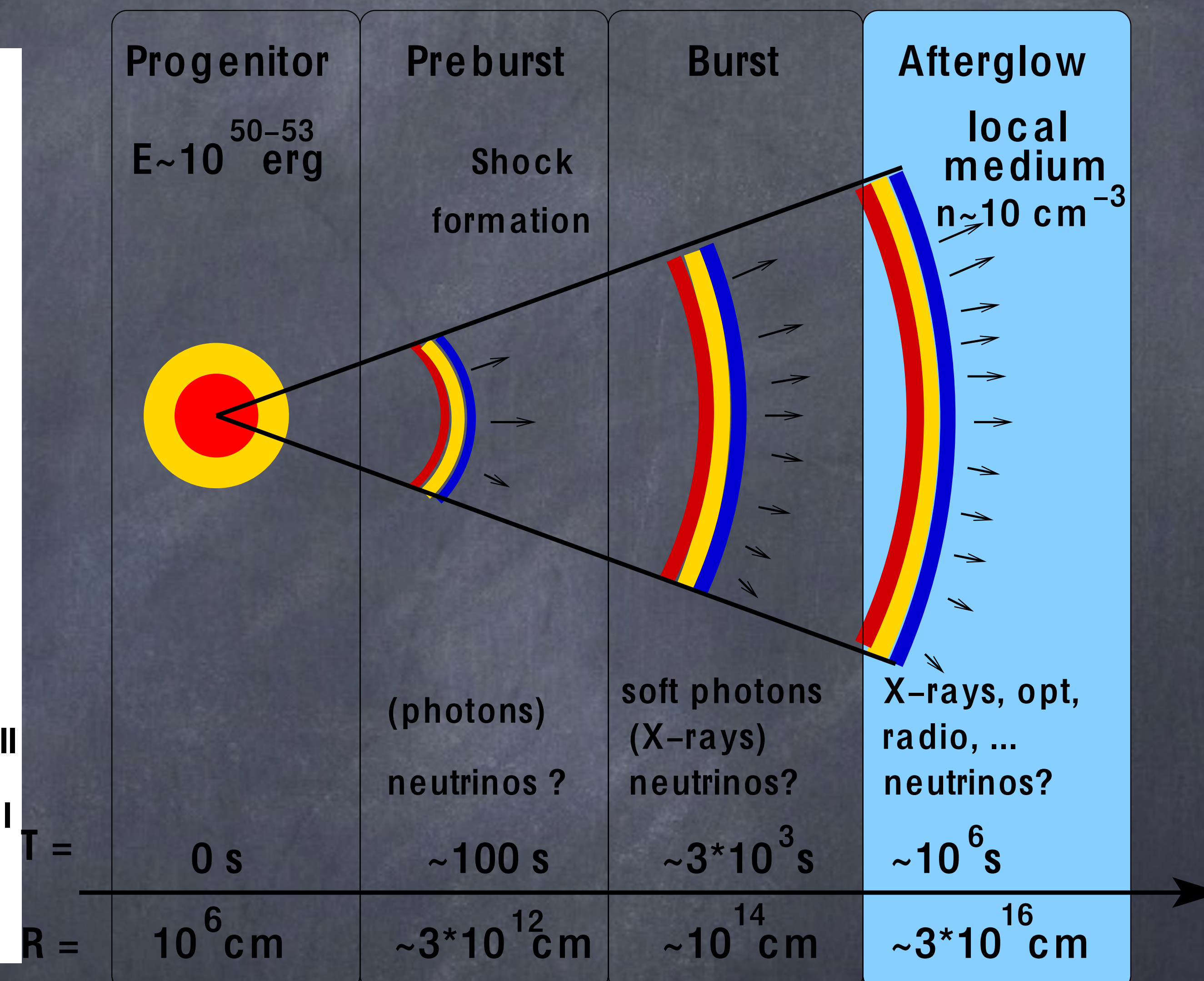

active galaxies **gamma ray bursts**

Figures from J. Becker-Tjus, Phys.Rep. 458 (2008) 173

Lorentz Symmetry Violation in the Electromagnetic Sector

The idea:

Experimental upper limits on UHE photon fraction

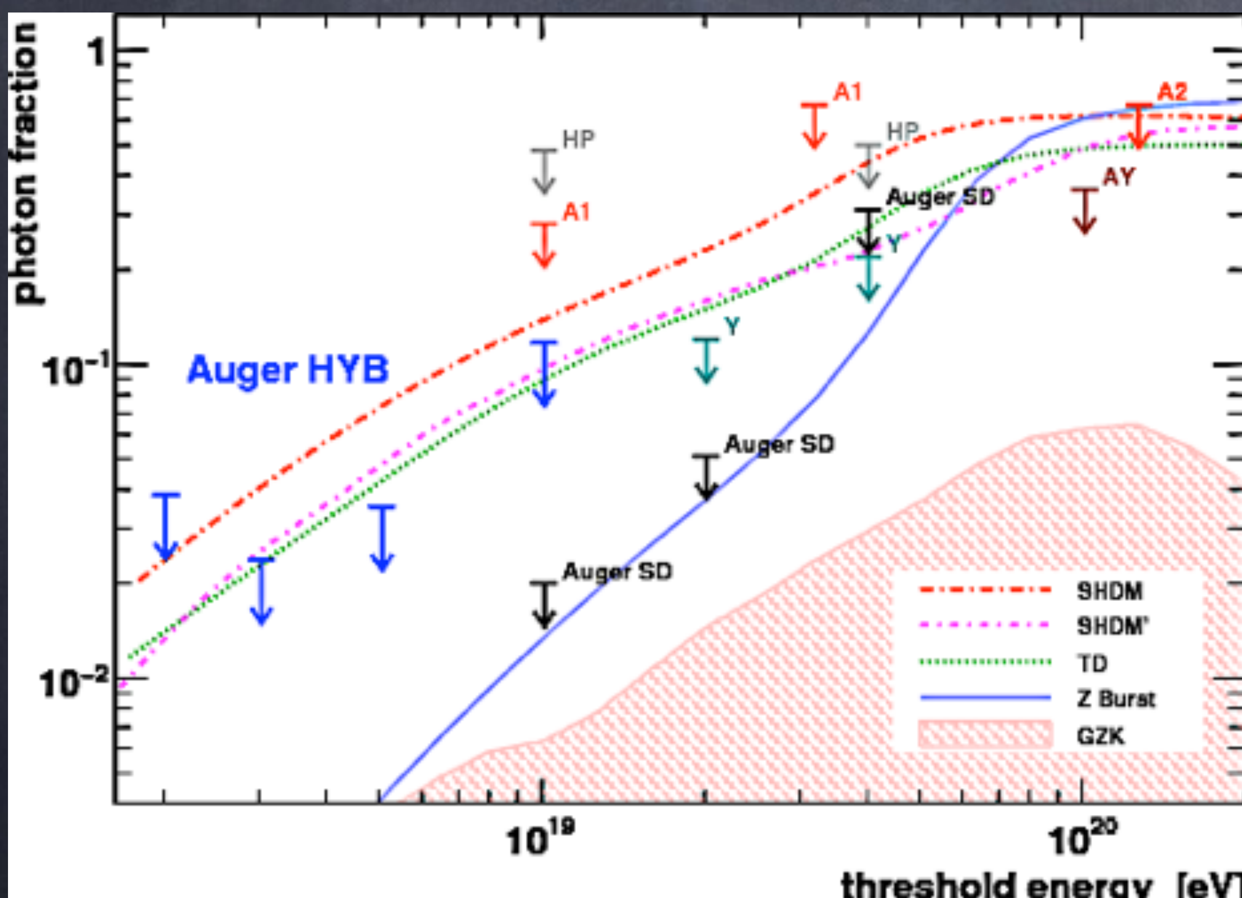

Pierre Auger Collaboration, Astropart. Phys. 31 (2009) 399

Contradict predictions if pair production is absent

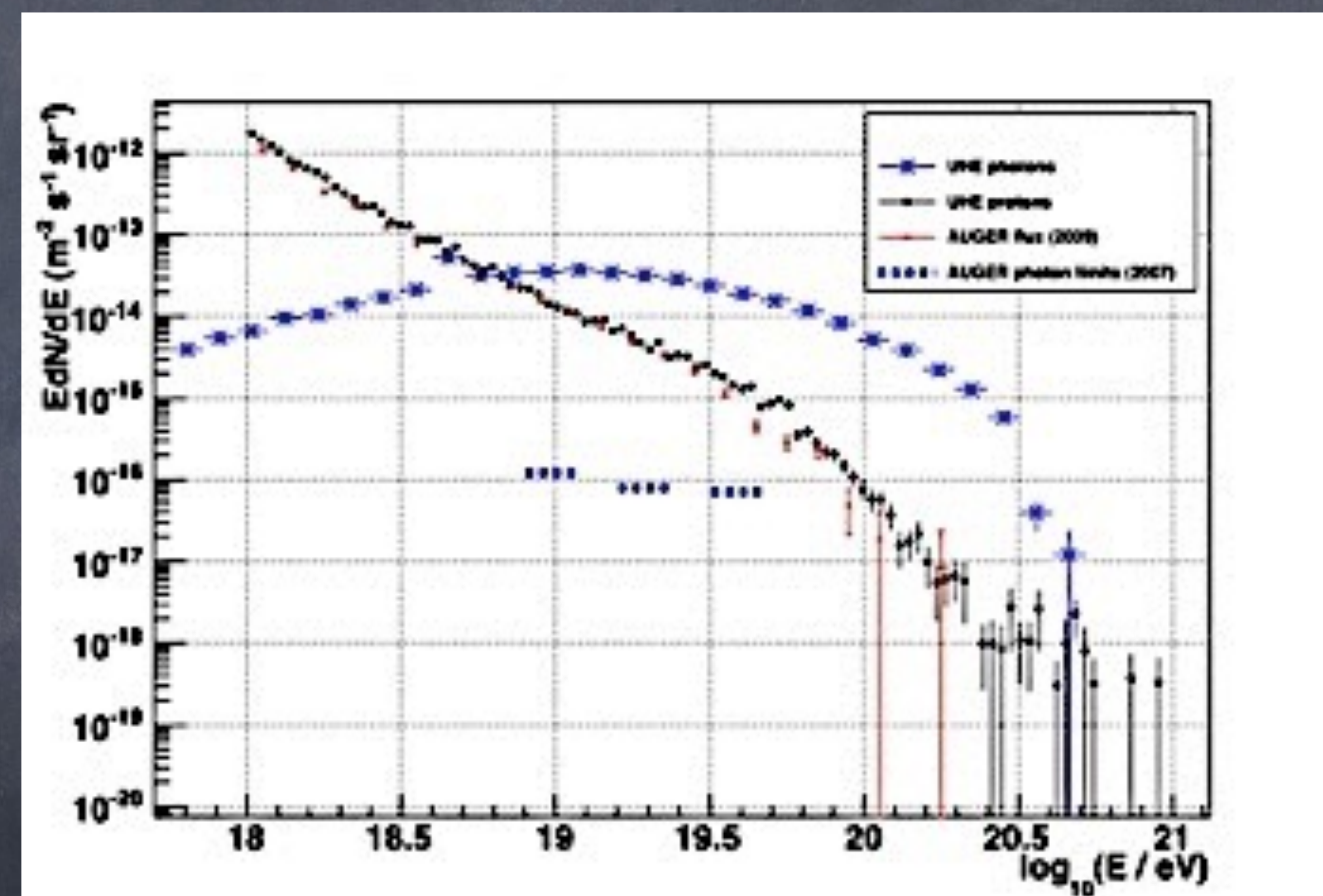

Maccione, Liberati, Sigl, PRL 105 (2010) 021101

Lorentz Symmetry Violation in the Photon Sector

For a photon dispersion relation

$$\omega_{\pm}^2 = k^2 + \xi_n^{\pm} k^2 \left(\frac{k}{M_{\rm Pl}} \right)^n , n \geq 1 ,$$

pair production may become inhibited, increasing GZK photon fluxes above observed upper limits: In the absence of LIV for electrons/positrons for n=1 (CPT-odd terms) this yields:

$$\xi_1 \leq 10^{-12}$$

Even for n=2 (CPT-even) one has sensitivity to $\xi_2 \sim 10^{-6}$

Such strong limits may indicate that Lorentz invariance violations are completely absent !

The modified dispersion relation also leads to energy dependent group velocity $V=\partial E/\partial p$ and thus to an energy-dependent time delay over a distance d:

$$\Delta t = -\xi\, d \frac{E}{M_{\rm Pl}} \simeq -\xi \left(\frac{d}{100\,{\rm Mpc}}\right)\left(\frac{E}{\rm TeV}\right)\,{\rm sec}$$

for linearly suppressed terms. GRB observations in TeV γ-rays can therefore probe quantum gravity and may explain that higher energy photons tend to arrive later (Ellis et al.).

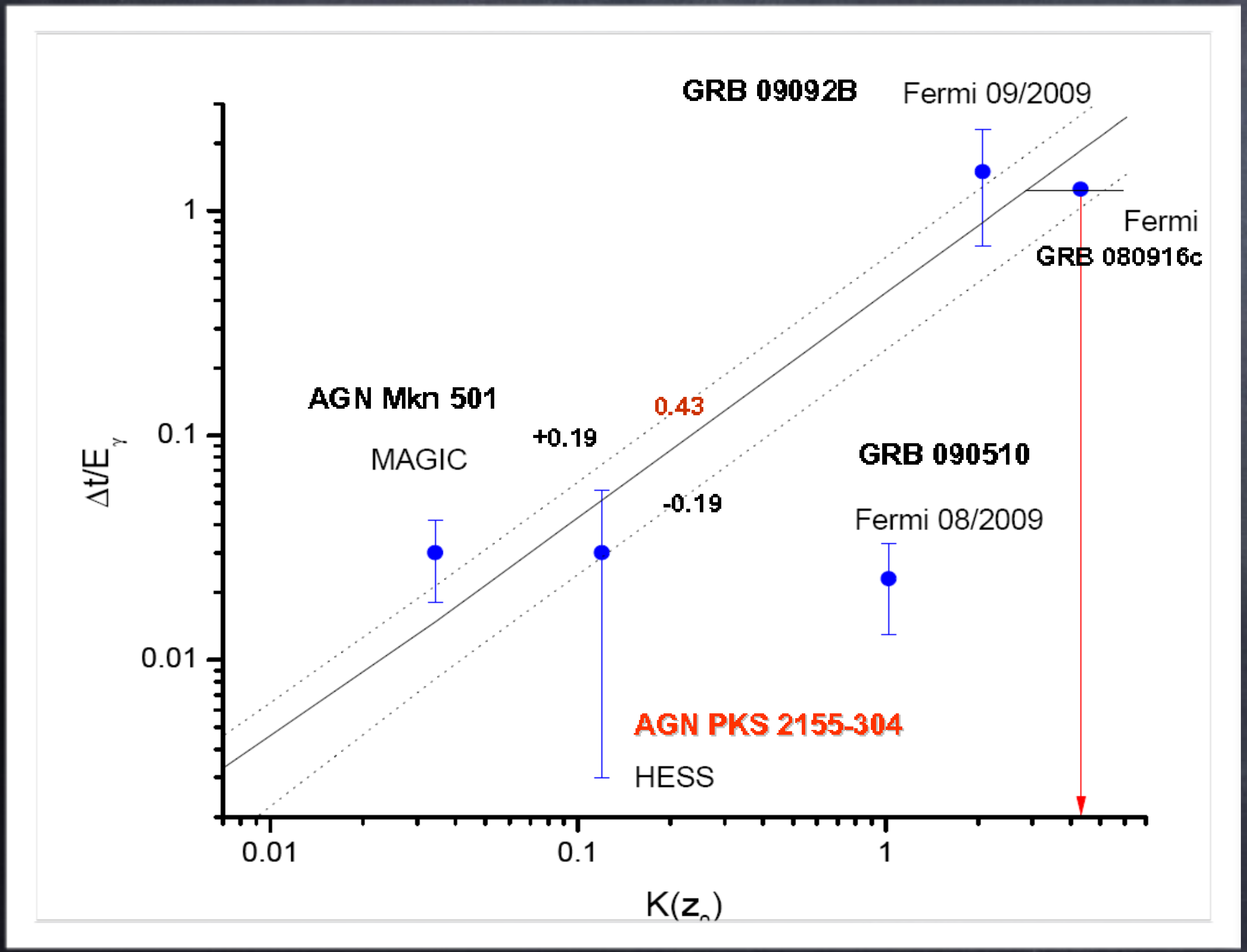

But the UHE photon limits are inconsistent with interpretations of time delays of high energy gamma-rays from GRBs within quantum gravity scenarios based on effective field theory

Maccione, Liberati, Sigl, PRL 105 (2010) 021101

Possible exception in space-time foam models,

Ellis, Mavromatos, Nanopoulos, arXiv:1004.4167

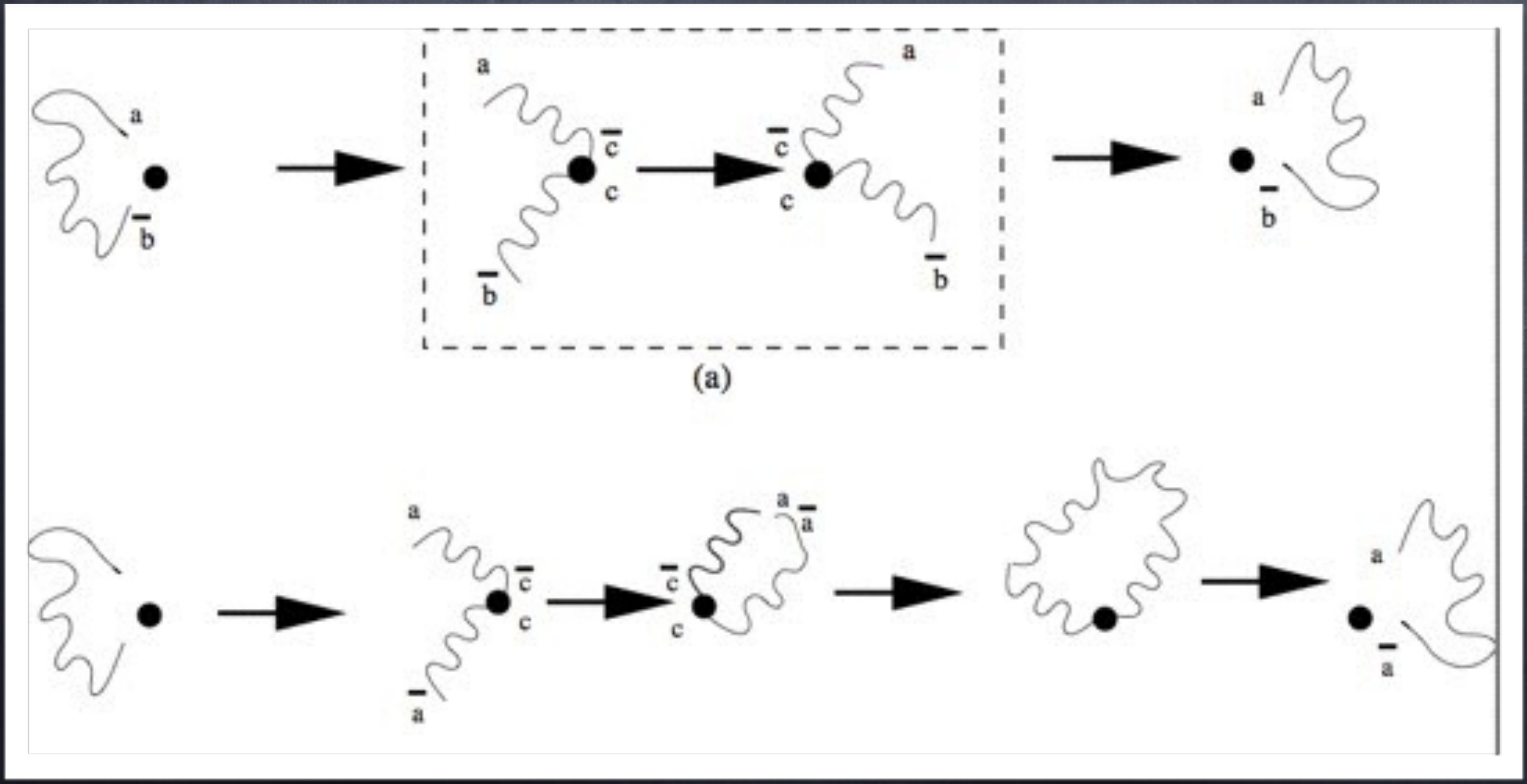

3-Dimensional Effects in Extragalactic Cosmic Ray Propagation

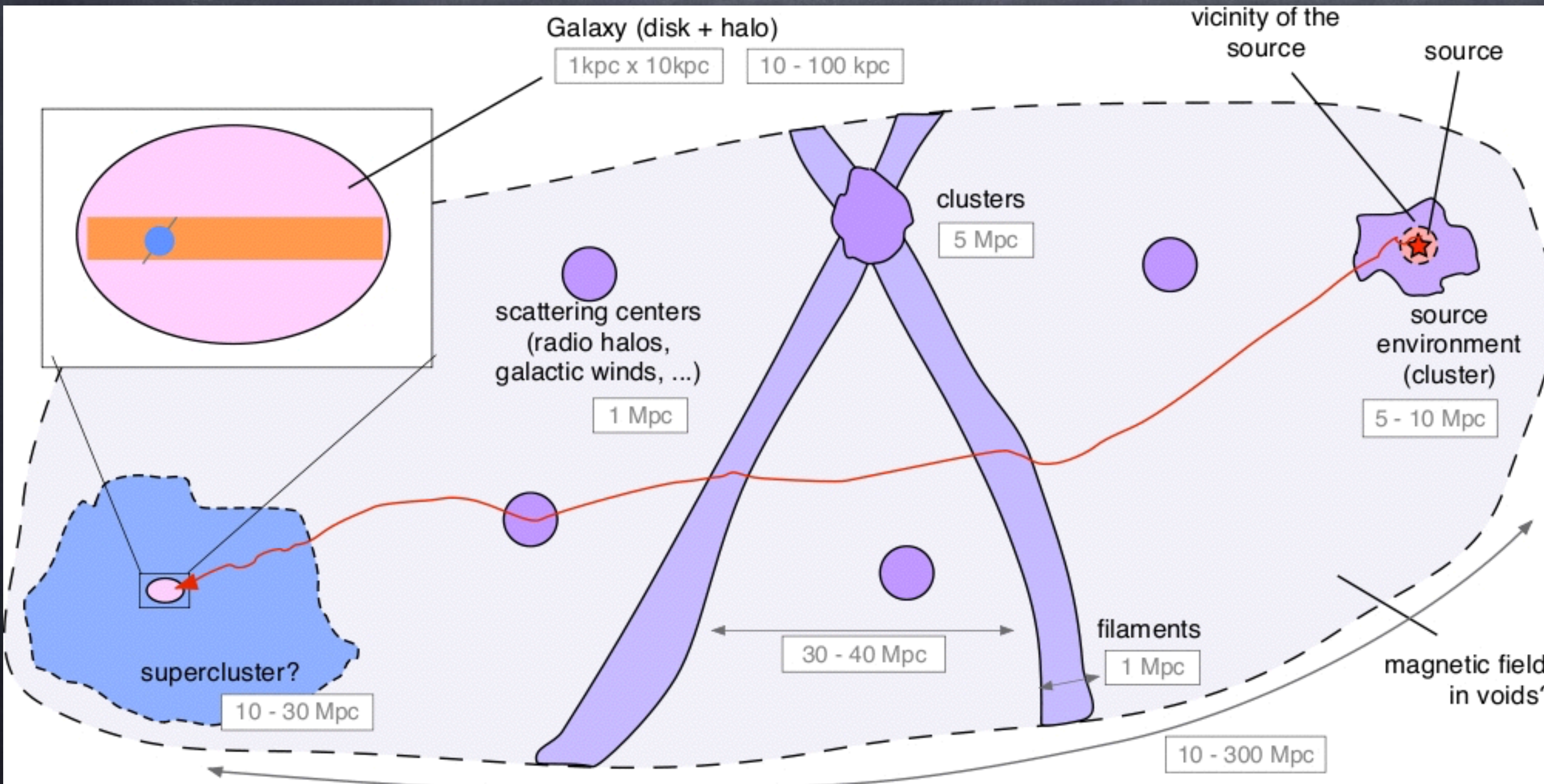

Kotera, Olinto, Ann.Rev.Astron.Astrophys. 49 (2011) 119

Structured Extragalactic Magnetic Fields

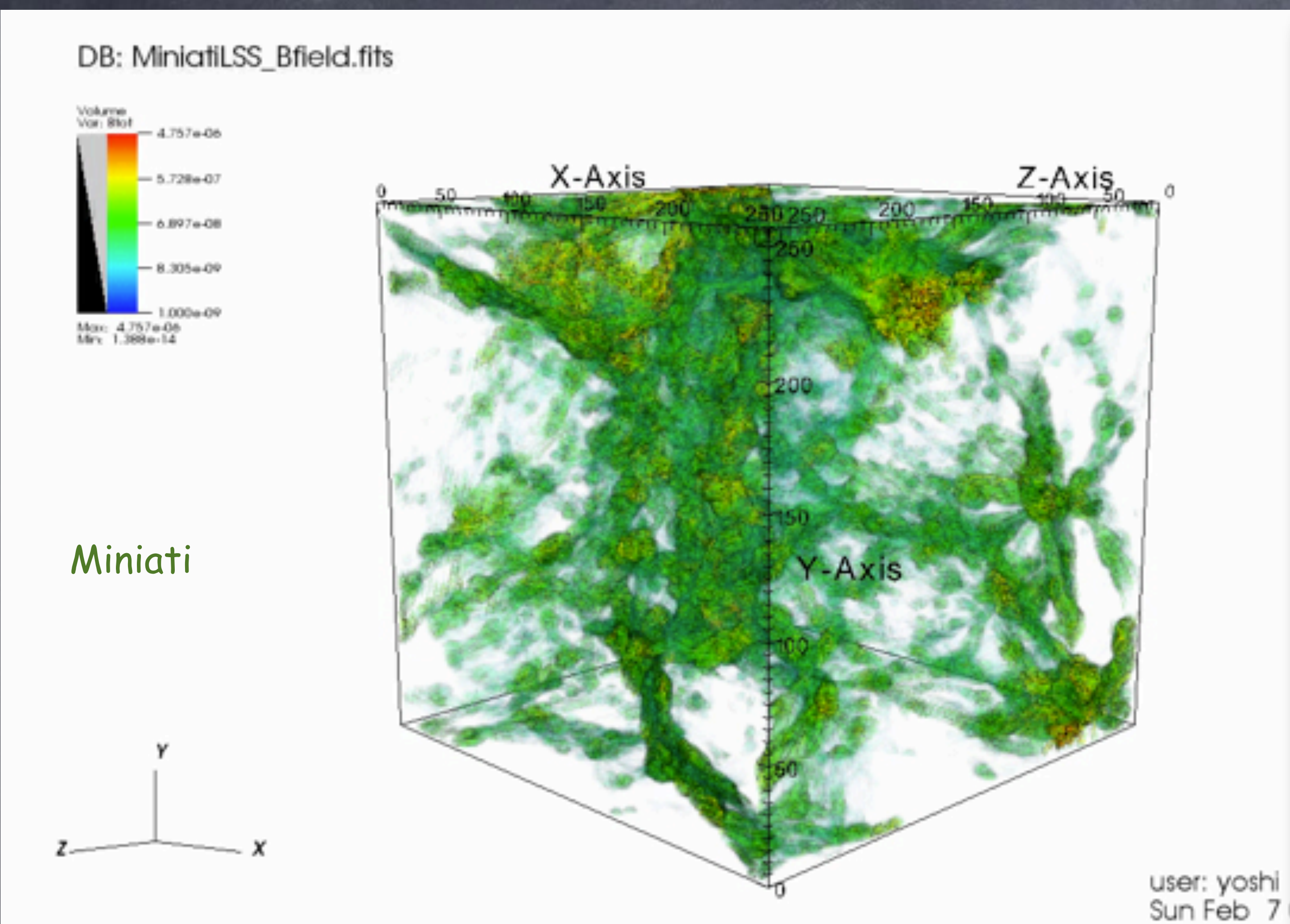

Miniati

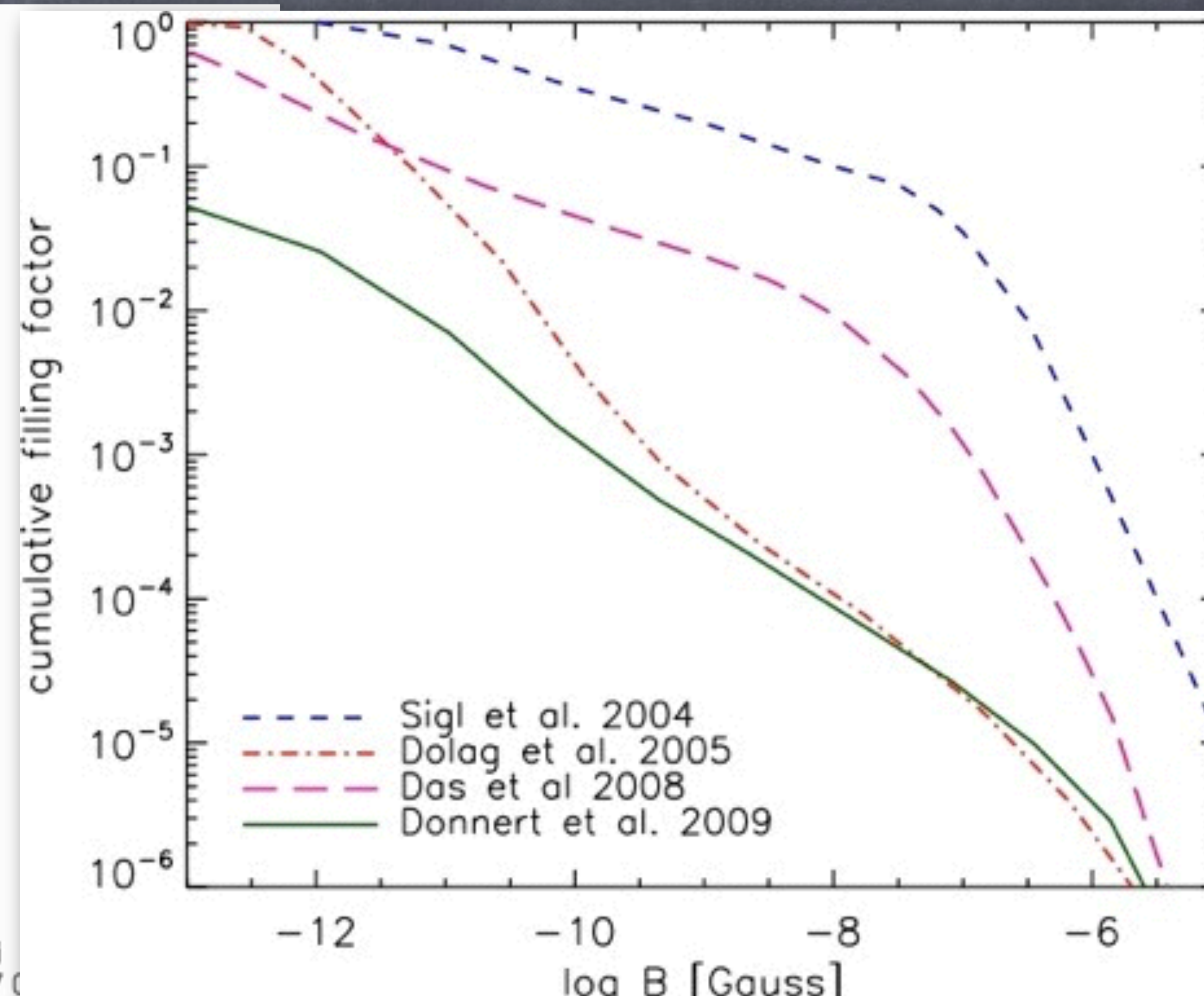

Kotera, Olinto, Ann.Rev.Astron.Astrophys. 49 (2011) 119

Filling factors of extragalactic magnetic fields are not well known and come out different in different large scale structure simulations

The Magnetic Universe: Understanding the origin and evolution of B fields

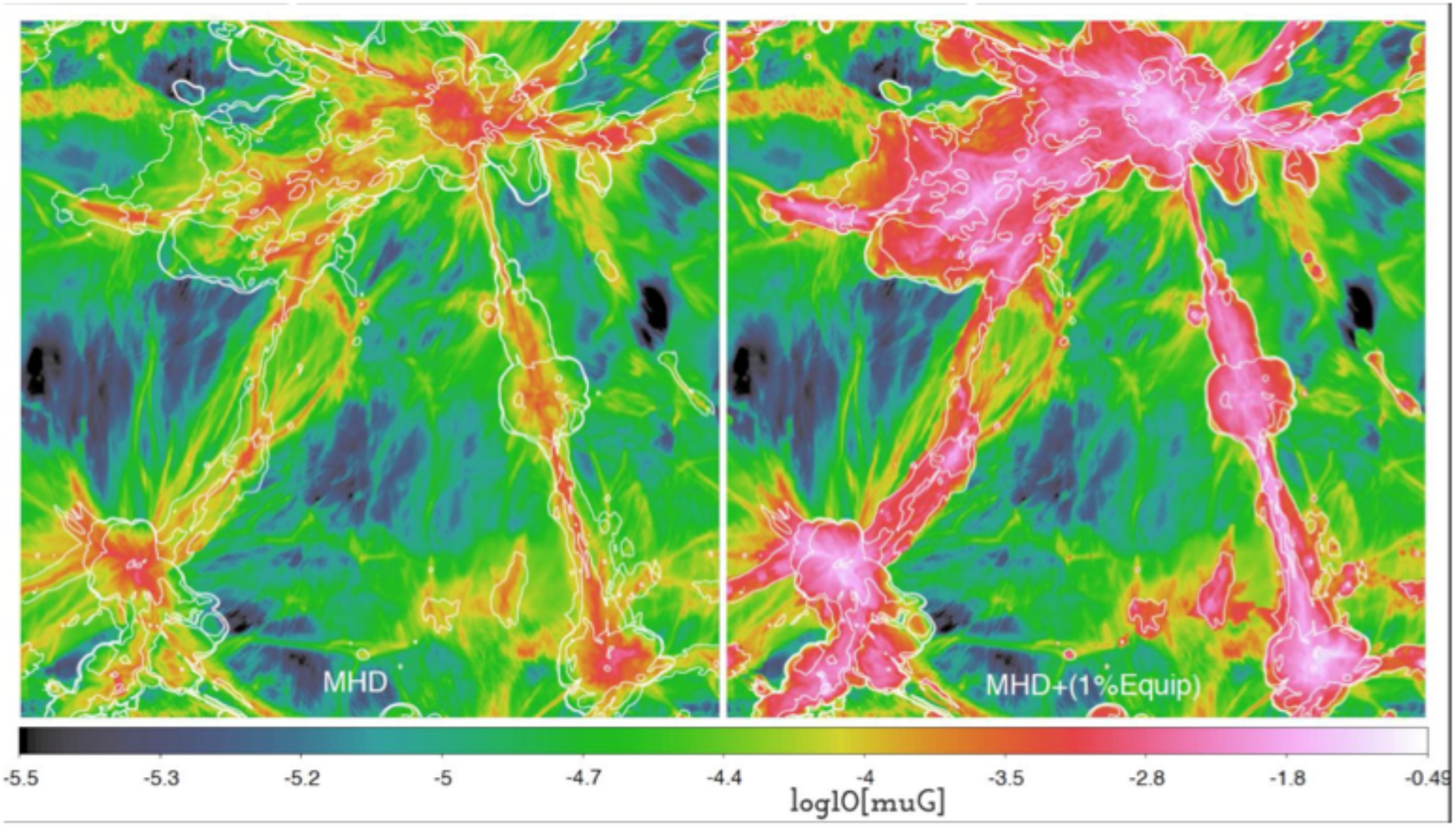

(Vazza et al. 2014)

- Determine the role of magnetism in regulating galaxy evolution
- Detection and characterization of the magnetic cosmic web
- Magnetic evolution of AGN over cosmic time

Observations and simulations of the non-thermal Universe

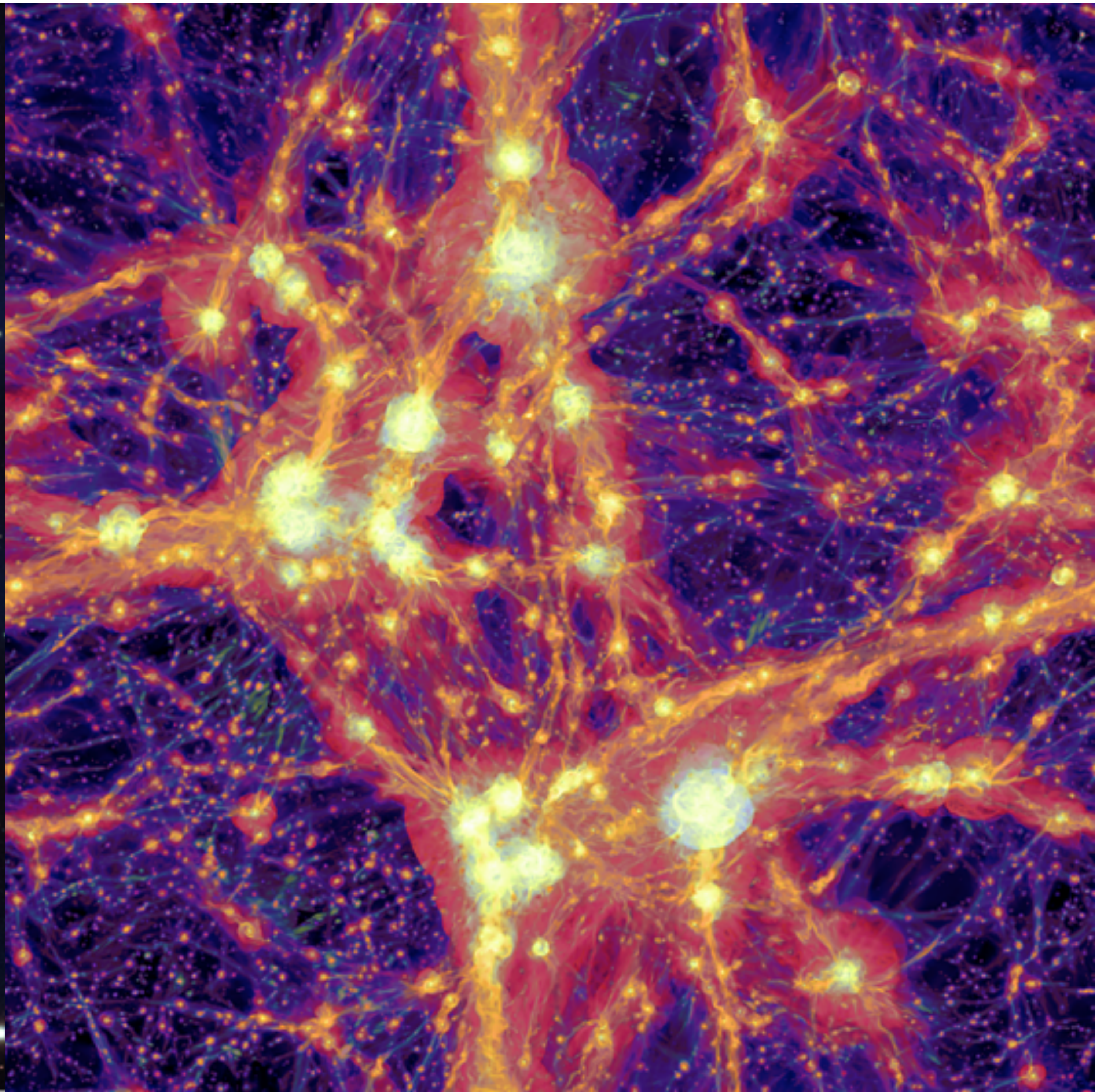

Observational Status of Extragalactic Magnetic Fields

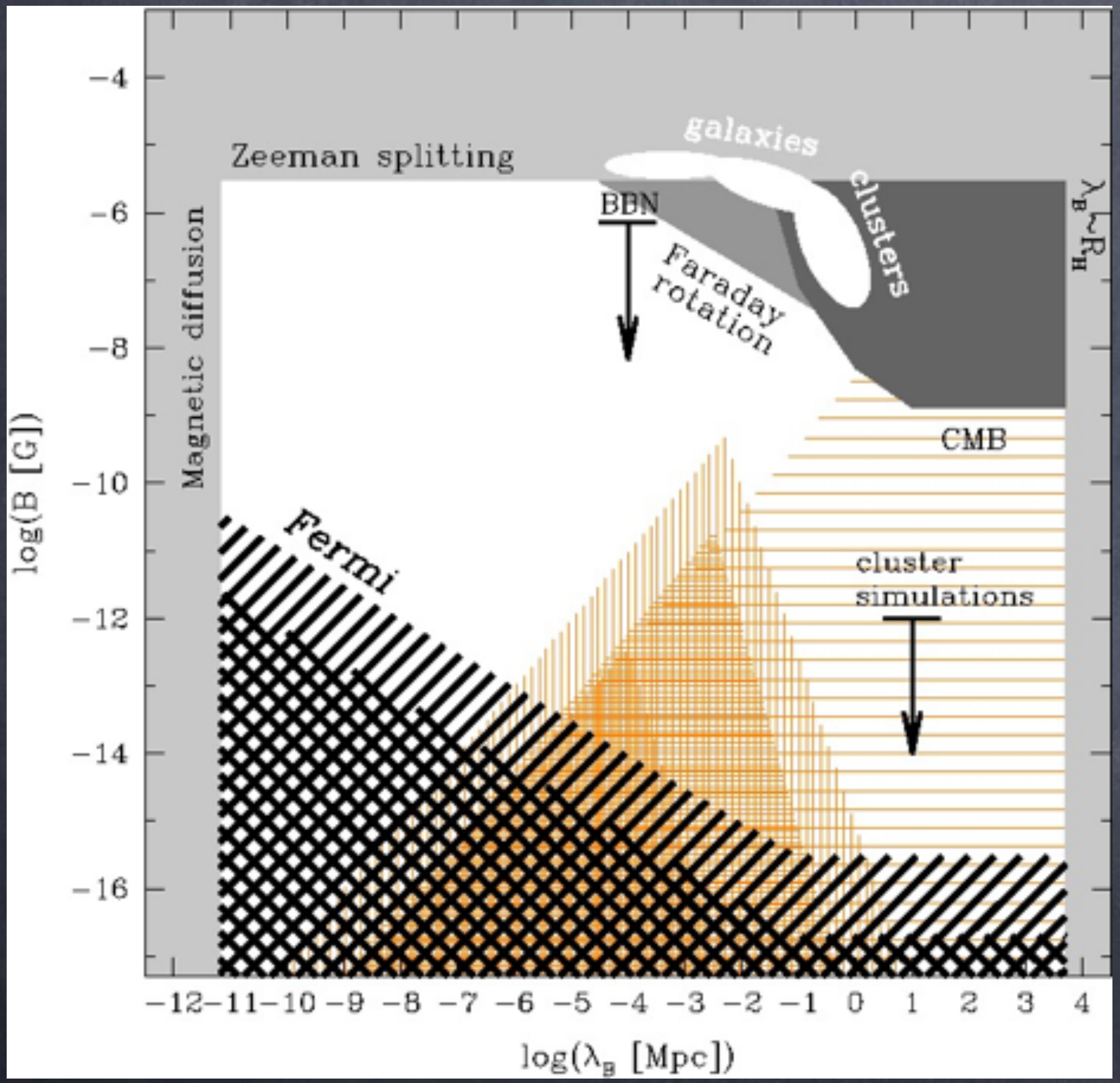

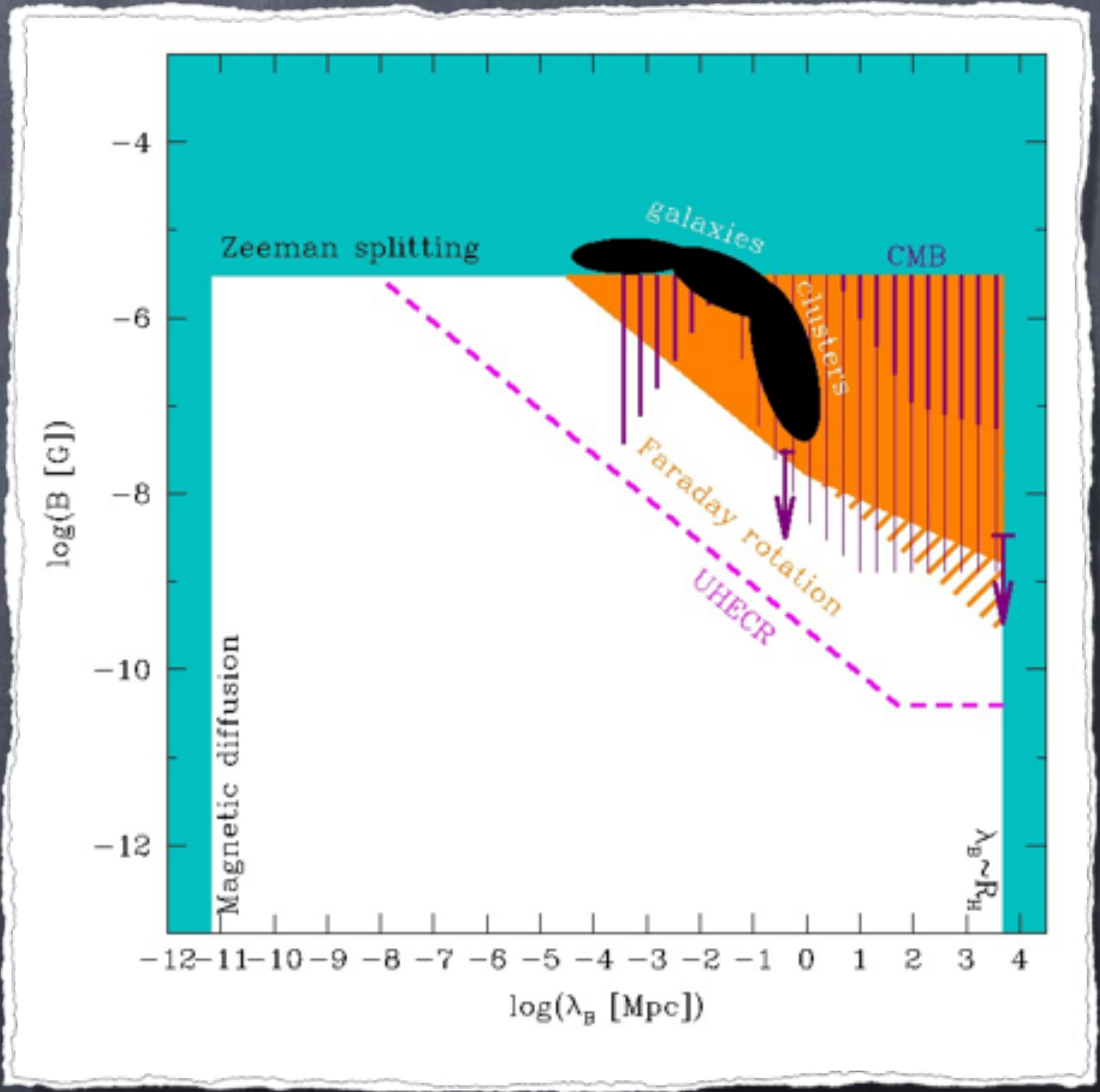

Neronov and Vovk, Science 328 (2010) 73

Neronov and Semikoz, PRD 80 (2009) 123012

Magnetic Field Influence on Charged Particle Propagation

$B \sim 10^{-14}$ G and a coherence scale $l_c \sim 1$ kpc are possible ranges for primordial fields from cosmological phase transitions (for significant magnetic helicity)

gyro-radius

$$r_g(p,B) \simeq \frac{p}{qB} \simeq 1 \left(\frac{p/Z}{100\,\mathrm{GeV}}\right)\left(\frac{B}{10^{-14}\mathrm{G}}\right)^{-1} \mathrm{pc}\,.$$

deflection angle

$$\theta(E,d) \simeq \frac{(2dl_c/9)^{1/2}}{r_g}$$

$$\simeq 3^\circ\, Z \left(\frac{E}{100\,\mathrm{GeV}}\right)^{-1}\left(\frac{d}{1\,\mathrm{kpc}}\right)^{1/2}\left(\frac{l_c}{1\,\mathrm{kpc}}\right)^{1/2}\left(\frac{B_{\mathrm{rms}}}{10^{-14}\,\mathrm{G}}\right),$$

time delay

$$\tau(E,d) \simeq d\theta(E,d)^2/4 \simeq$$

$$\simeq 1\, Z^2 \left(\frac{E}{100\,\mathrm{GeV}}\right)^{-2}\left(\frac{d}{1\,\mathrm{kpc}}\right)^{2}\left(\frac{l_c}{1\,\mathrm{kpc}}\right)\left(\frac{B_{\mathrm{rms}}}{10^{-14}\,\mathrm{G}}\right)^{2} \mathrm{y}\,,$$

Effects of Primordial Magnetic Fields on Electromagnetic Cascades

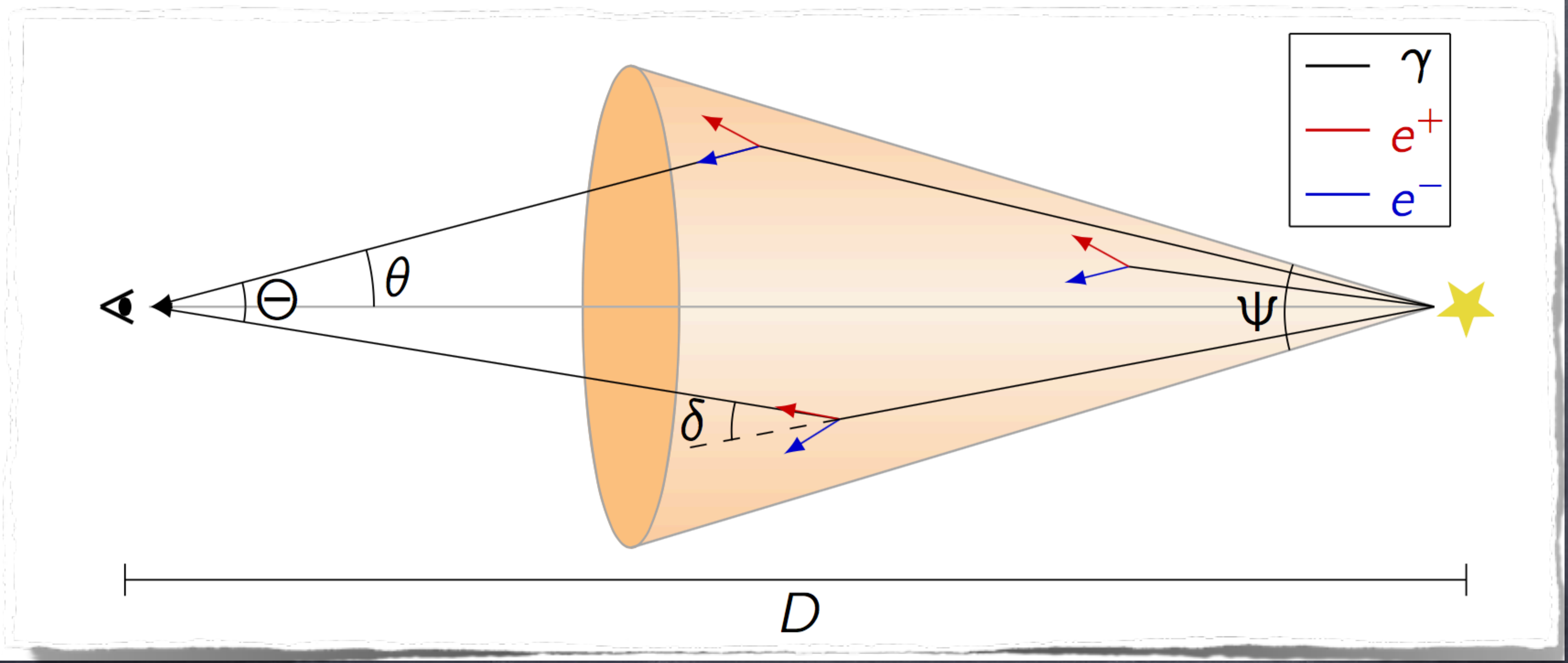

principle: deflection of electrons and positrons out of the beam can lead to a flux suppression of electromagnetic cascades if photon flux dominated by inverse Compton scattering, i.e. for hard injection spectra

Electromagnetic Cascades and TeV γ-Rays

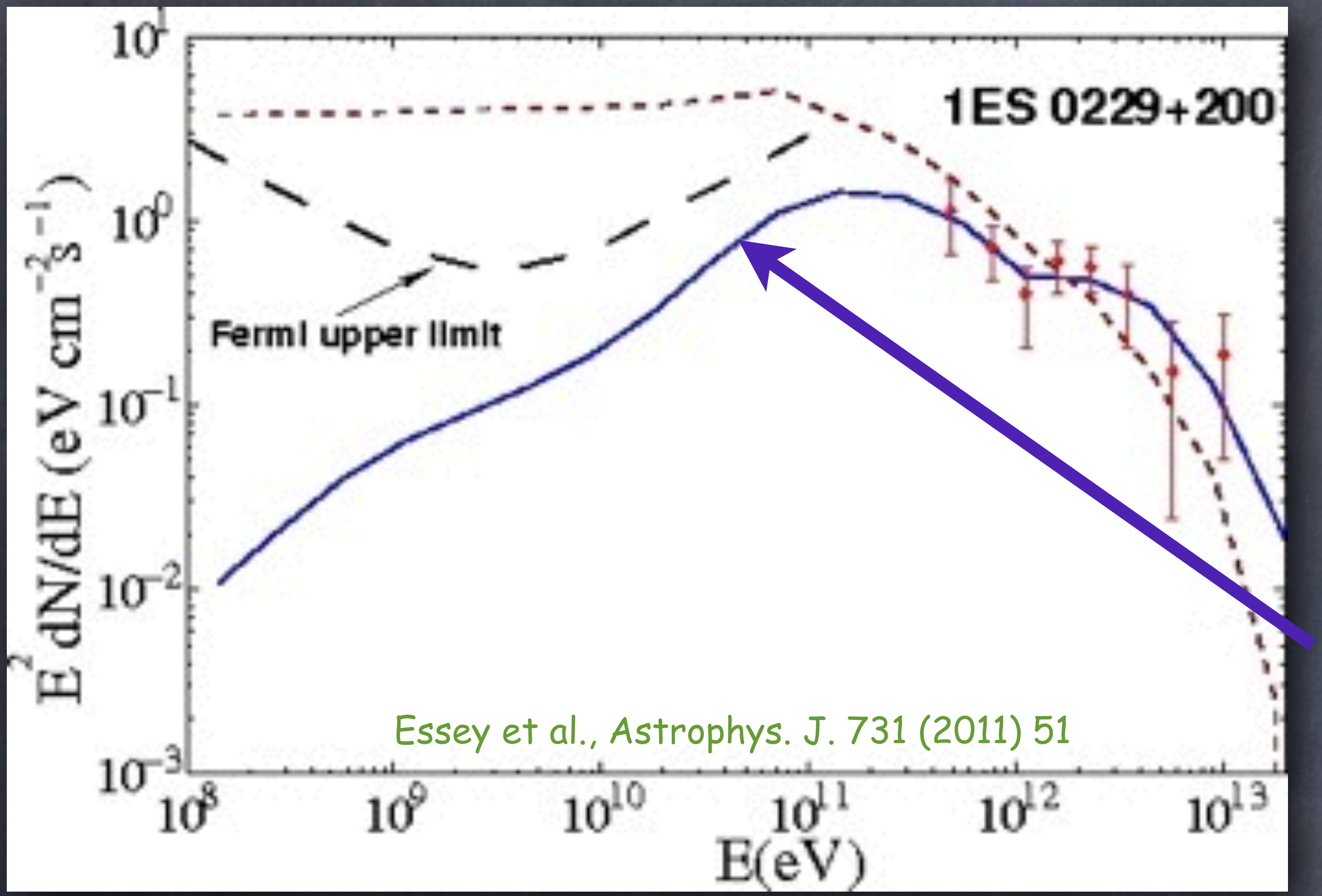

Pure γ-ray injection tends to underproduce "prompt" TeV γ-rays (observed by IACT) and overproduce GeV γ-ray cascades (not observed by Fermi LAT)

Solution 1:
magnetic fields > 10^{-17} G sufficiently disperse the GeV γ-ray cascades [Neronov et al.]

Solution 2:
cascade absorption by plasma beam instabilities [Broderick et al., Schlickeiser...]: conditions satisfied ?

Solution 3:
Primary cosmic rays produce TeV γ-rays continuously during propagation [Essey et al.]: variability ?

Solution 4:
γ-ray mixing with new light states (ALPS, hidden photons)
[Roncadelli, Montanino. De Angelis, Hooper, Serpico, Mirizzi ...]

Solution 5:
Lorentz invariance violation [Mavromatos...]:
stronger constraints from UHE γ-rays

Sensitivities from γ-Ray Observations versus Theory

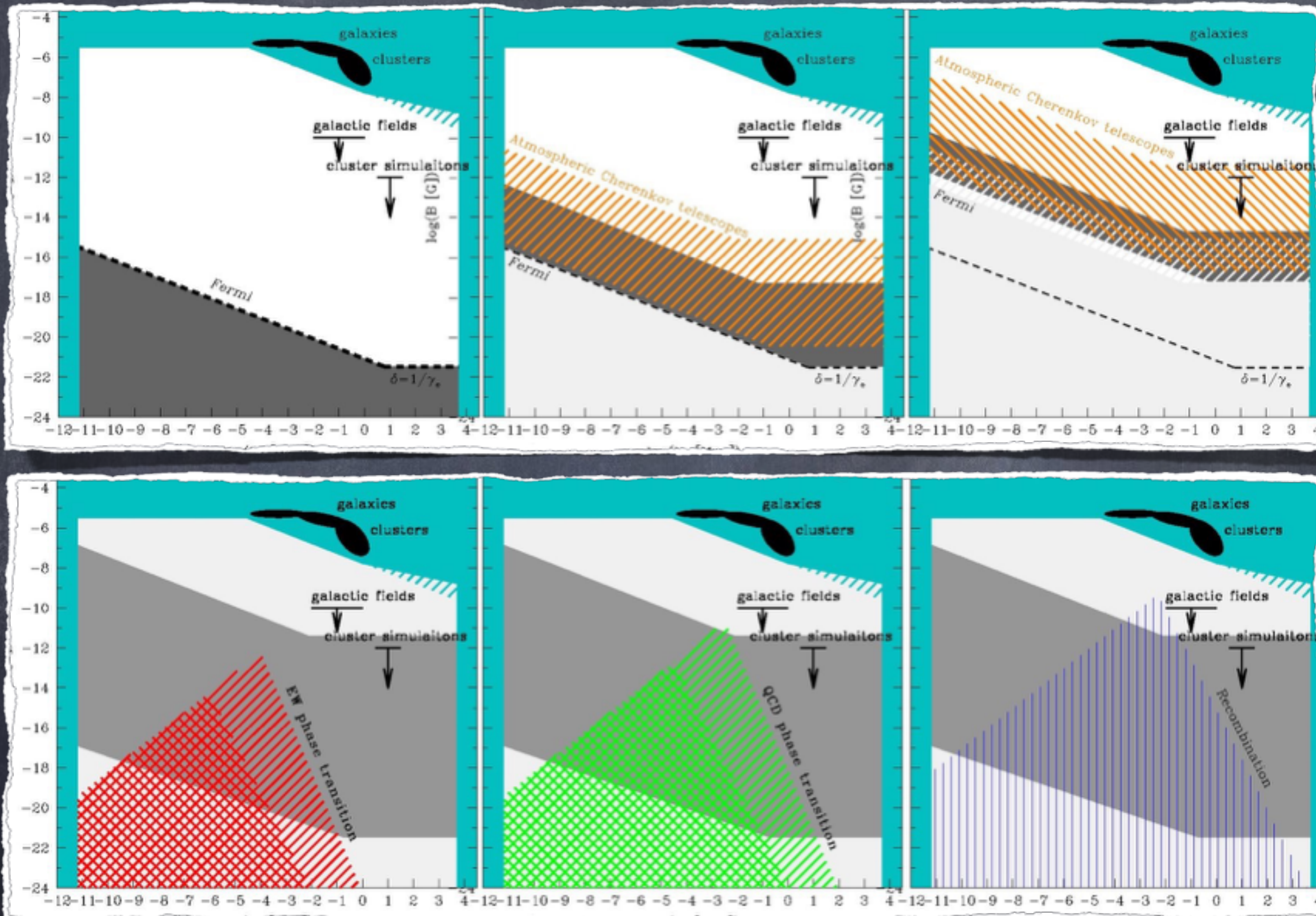

Neronov and Semikoz, PRD 80 (2009) 123012

EGMF - Origin

The origin of EGMF is still uncertain - mainly two different seed mechanisms:

- Astrophysical scenario: Seed magnetic fields are generated during structure formation (e.g. by a Biermann Battery [Biermann, 1950]) and are then amplified by the dynamo effect [Zeldovich et al., 1980]
- Cosmological scenario: Strong seed magnetic fields are generated in the Early Universe, e.g. at a phase transition (QCD, electroweak) [Sigl et al., 1997] or during inflation [Turner and Widrow, 1988], and some of the initial energy content is transfered to larger scales.

The latter are the so-called primordial magnetic fields and will be focused on in the following.

- Basics for the time evolution: Homogeneous and isotropic magnetohydrodynamics in an expanding Universe.

Primordial Magnetic fields - Simple Estimates

The main problem is that the comoving horizon at the temperature T_g of creation is very small,

$$l_{H,0} \sim \frac{T_g}{T_0}\frac{1}{H(T_g)} \simeq 0.2 \left(\frac{100\,\mathrm{MeV}}{T_g}\right)\,\mathrm{pc}\,,$$

so that length scales of interest today are far in the tail.
A magnetic field in equipartition with radiation corresponds to $B \simeq 3 \times 10^{-6}\,$G.

Primordial Magnetic fields - Basic MHD

Magnetohydrodynamics (MHD)

- Maxwell's equations:
  $\nabla \cdot \mathbf{B} = 0, \ \nabla \times \mathbf{E} = -\partial_t \mathbf{B}, \ \nabla \times \mathbf{B} = 4\pi \mathbf{j}$
- Continuity equation for mass density ρ: $\partial_t \rho + \nabla(\rho \mathbf{v}) = 0$
- Navier-Stokes equations:
  $\rho \left(\partial_t \mathbf{v} + (\mathbf{v}\nabla)\,\mathbf{v}\right) = -\nabla p + \mu \Delta \mathbf{v} + (\lambda + \mu)\nabla\left(\nabla \mathbf{v}\right) + \mathbf{f}$

For the magnetic field and the turbulent fluid it follows therefore

$$\partial_t \mathbf{B} = \frac{1}{4\pi\sigma}\Delta \mathbf{B} + \nabla \times (\mathbf{v} \times \mathbf{B})$$

$$\partial_t \mathbf{v} = -\left(\mathbf{v}\nabla\right)\mathbf{v} + \frac{(\nabla \times \mathbf{B}) \times \mathbf{B}}{4\pi\rho} + \mathbf{f}_v .$$

Primordial Magnetic fields - Basic MHD

- Switch to Fourier (k-)space: $B(\mathbf{x}) \to \hat{B}(\mathbf{q})$, $v(\mathbf{x}) \to \hat{v}(\mathbf{q})$

$$\partial_t \hat{\mathbf{B}}(\mathbf{q}) = -\frac{1}{4\pi\sigma} q^2 \hat{\mathbf{B}}(\mathbf{q}) + \frac{iV^{\frac{1}{2}}}{(2\pi)^{\frac{3}{2}}} \mathbf{q} \times \left[\int \mathrm{d}^3 k \left(\hat{\mathbf{v}}(\mathbf{q}-\mathbf{k}) \times \hat{\mathbf{B}}(\mathbf{k}) \right) \right]$$

$$\partial_t \hat{\mathbf{v}}(\mathbf{q}) = -\frac{iV^{\frac{1}{2}}}{(2\pi)^{\frac{3}{2}}} \int \mathrm{d}^3 k \left[\left(\hat{\mathbf{v}}(\mathbf{q}-\mathbf{k}) \cdot \mathbf{k} \right) \hat{\mathbf{v}}(\mathbf{k}) \right]$$
$$+ \frac{iV^{\frac{1}{2}}}{(2\pi)^{\frac{3}{2}}} \frac{1}{4\pi\rho} \int d^3 k \left[\left(\mathbf{k} \times \hat{\mathbf{B}}(\mathbf{k}) \right) \times \hat{\mathbf{B}}(\mathbf{q}-\mathbf{k}) \right] . \quad (1)$$

Terms of the type $\hat{\mathbf{v}}(\mathbf{q}-\mathbf{k}) \times \hat{\mathbf{B}}(\mathbf{k})$ describe mode-mode coupling such that power from small length scales $1/k$ can be transported to large length scales $1/q$.

Primordial Magnetic Fields - Correlation Function

Aim: Computation of the correlation function for B and v

- Homogeneity: The correlation function cannot depend on the position in space
- Isotropy: The correlation function only depends on the magnitude of the spatial separation

In Fourier space this means that the most general Ansatz is [de Kármán and Howarth, 1938]

$$\langle \hat{B}(\mathbf{k})\hat{B}(\mathbf{k}')\rangle \sim \delta(\mathbf{k}-\mathbf{k}')[(\delta_{lm} - \frac{k_l k_m}{k^2})\frac{M_k}{k^2} + i\epsilon_{lmj}\frac{k_j}{k}H_k^m]$$

$$\langle \hat{v}(\mathbf{k})\hat{v}(\mathbf{k}')\rangle \sim \delta(\mathbf{k}-\mathbf{k}')[(\delta_{lm} - \frac{k_l k_m}{k^2})\frac{U_k}{k^2} + i\epsilon_{lmj}\frac{k_j}{k}H_k^v]$$

Master Equations for the Power Spectra

In the absence of helicity, $H_k^m = H_k^v = 0$, the master equation for the magnetic field power spectrum then reads

$$\langle \partial_t M_q \rangle = \int_0^\infty \mathrm{d}k \Bigg\{ \Delta t \int_0^\pi \mathrm{d}\theta \Bigg[-\frac{1}{2}\frac{q^2 k^4}{k_1^4} \sin^3\theta \langle M_q \rangle \langle U_{k_1} \rangle + \frac{1}{2}\frac{q^4}{k_1^4}\left(q^2 + k^2 - qk\cos\theta\right)\sin^3\theta \langle M_k \rangle \langle U_{k_1} \rangle - \frac{1}{4} q^2 \left(3 - \cos^2\theta\right) \sin\theta \langle M_k \rangle \langle M_q \rangle \Bigg] \Bigg\},$$

where θ is the angle between $\mathbf{q}$ and $\mathbf{k}$.

Primordial Magnetic Fields: Full-Blown Numerical MHD Simulations versus semi-analytical methods based on transport equations

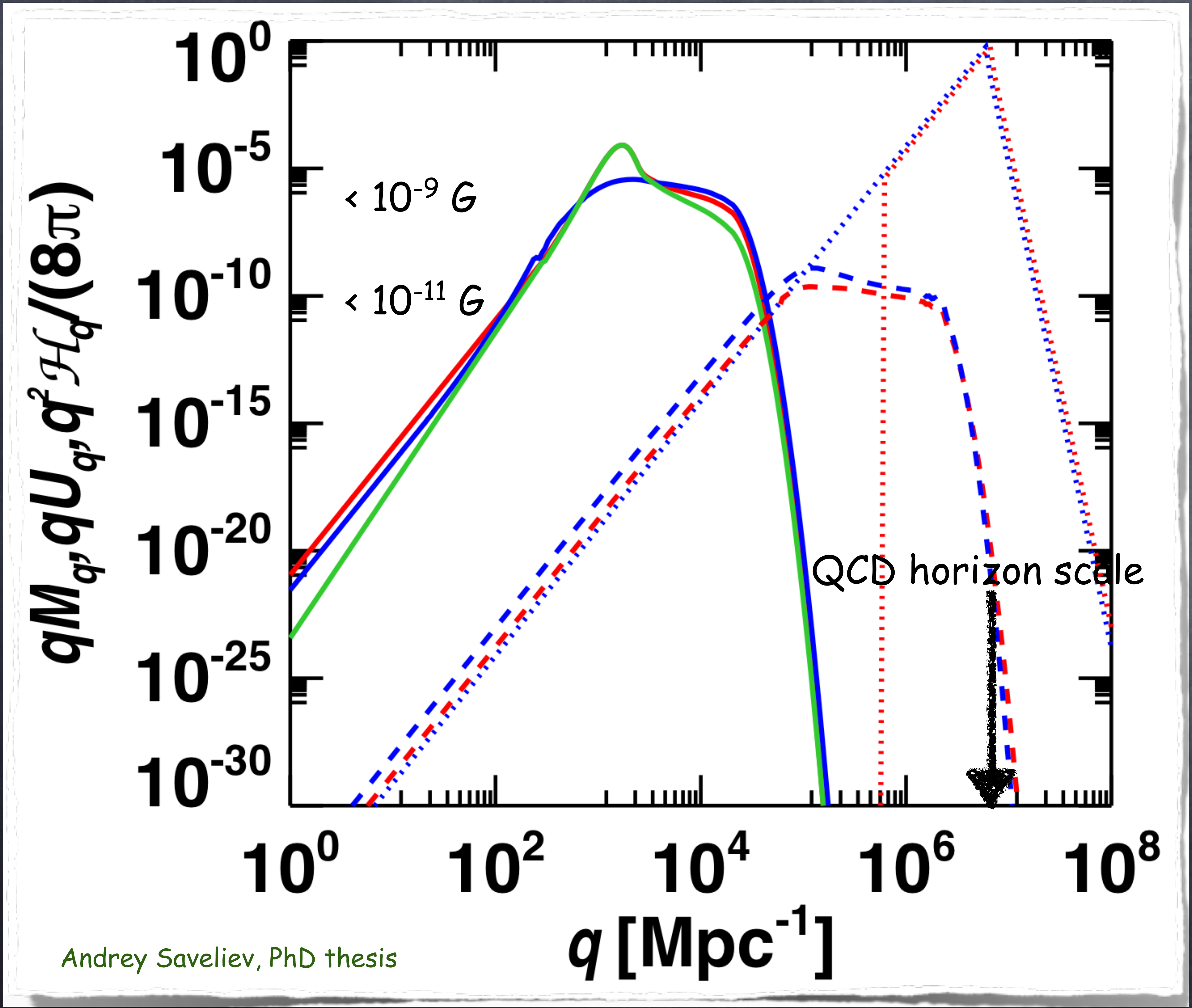

normalized to turbulence energy, < 10^{-6} G

magnetic fields

turbulent velocity

magnetic helicity

dotted = initial condition

dashed = final state without helicity

solid = final state with maximal helicity

Extragalactic iron propagation produces nuclear cascades in structured magnetic fields:

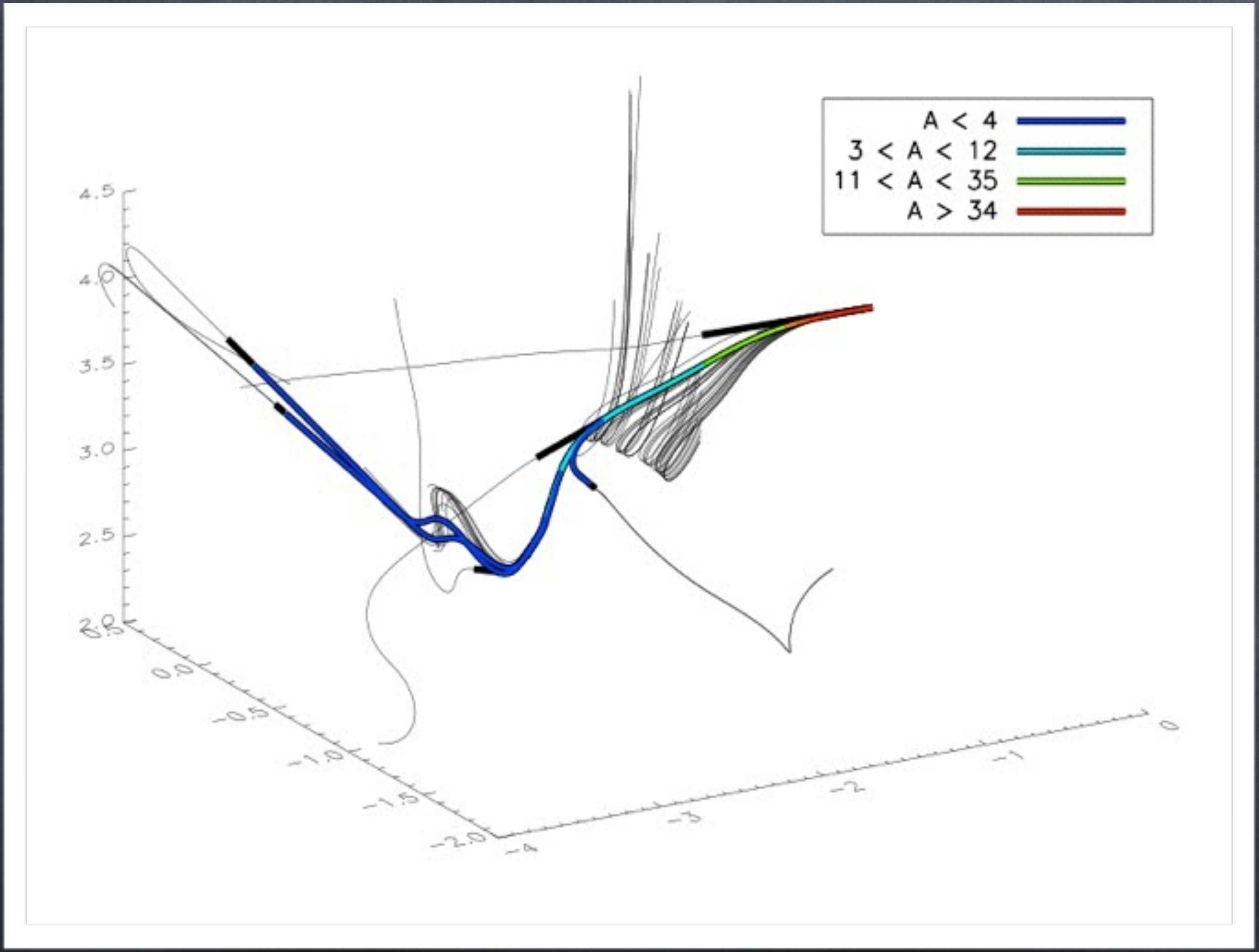

Initial energy 1.2 x 10^{21} eV, magnetic field range 10^{-15} to 10^{-6} G. Color-coded is the mass number of secondary nuclei

CRPropa 2.0/3.0

CRPropa is a public code for UHE cosmic rays, neutrinos and γ-rays being extended to heavy nuclei and hadronic interactions

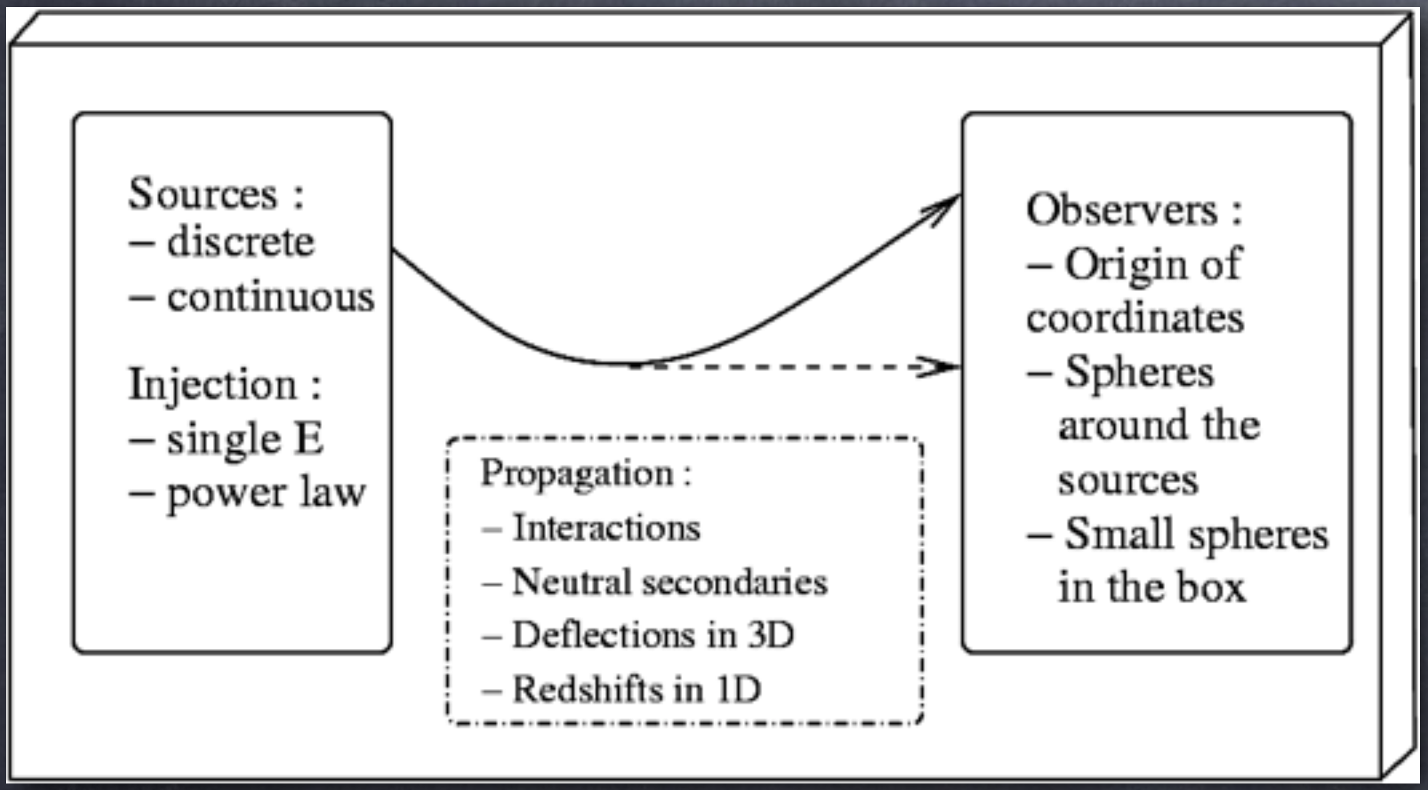

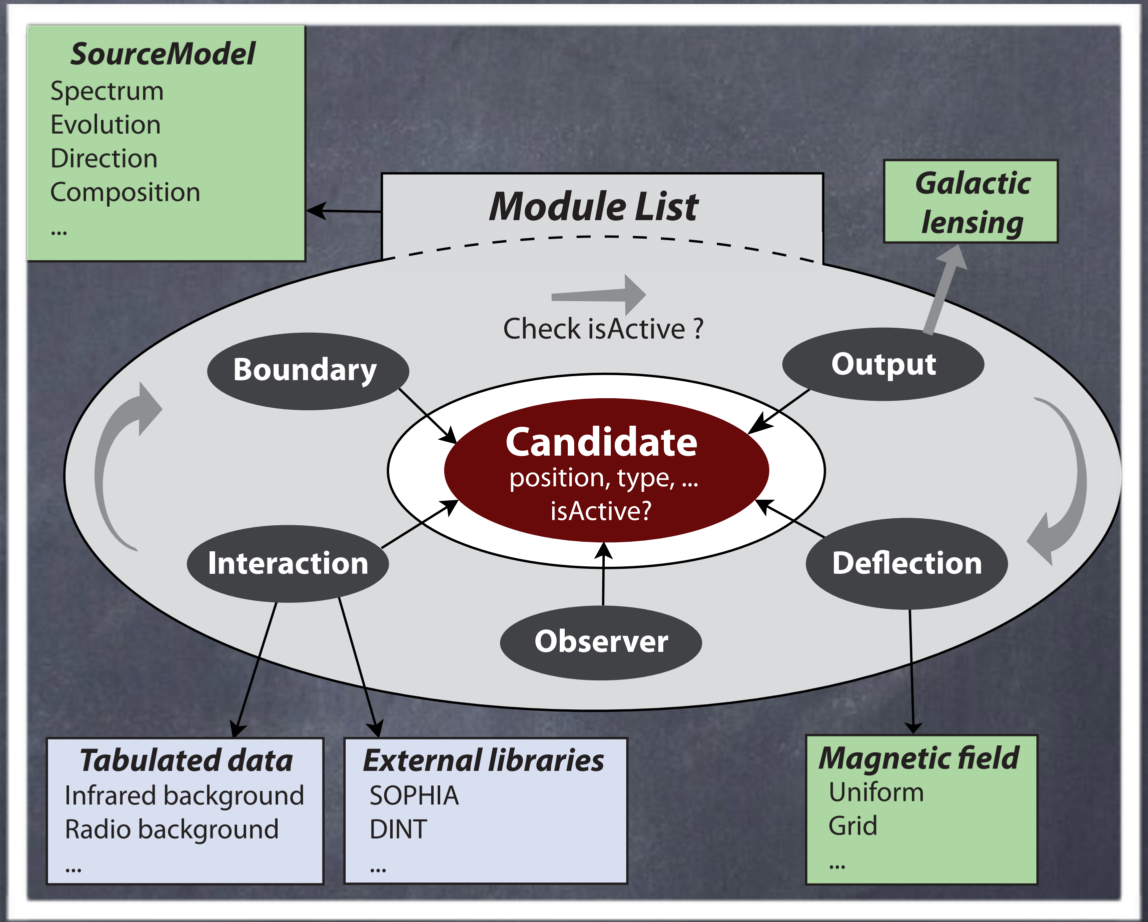

Version 1.4: Eric Armengaud, Tristan Beau, Günter Sigl, Francesco Miniati, Astropart.Phys.28 (2007) 463.

Version 2.0 at https://crpropa.desy.de/Main_Page

Version 3.0: Luca Maccione, Rafael Alves Batista, David Walz, Gero Müller, Nils Nierstenhoefer, Karl-Heinz Kampert, Peter Schiffer, Arjen van Vliet Astroparticle Physics 42 (2013) 41

Model Predictions for Spectrum, Composition and Anisotropy versus the Data

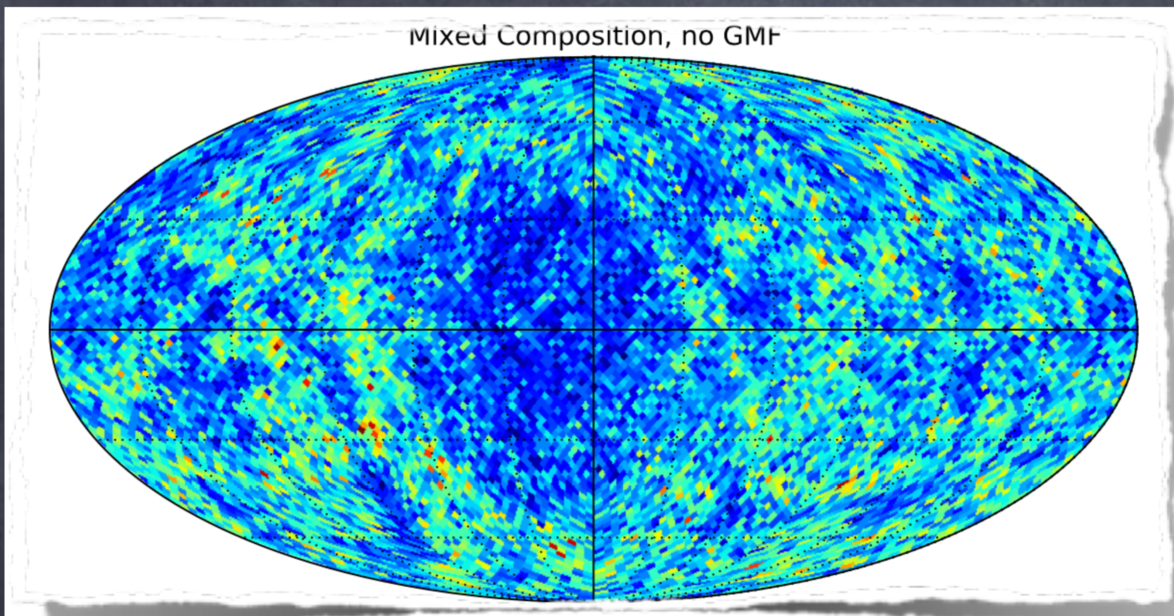

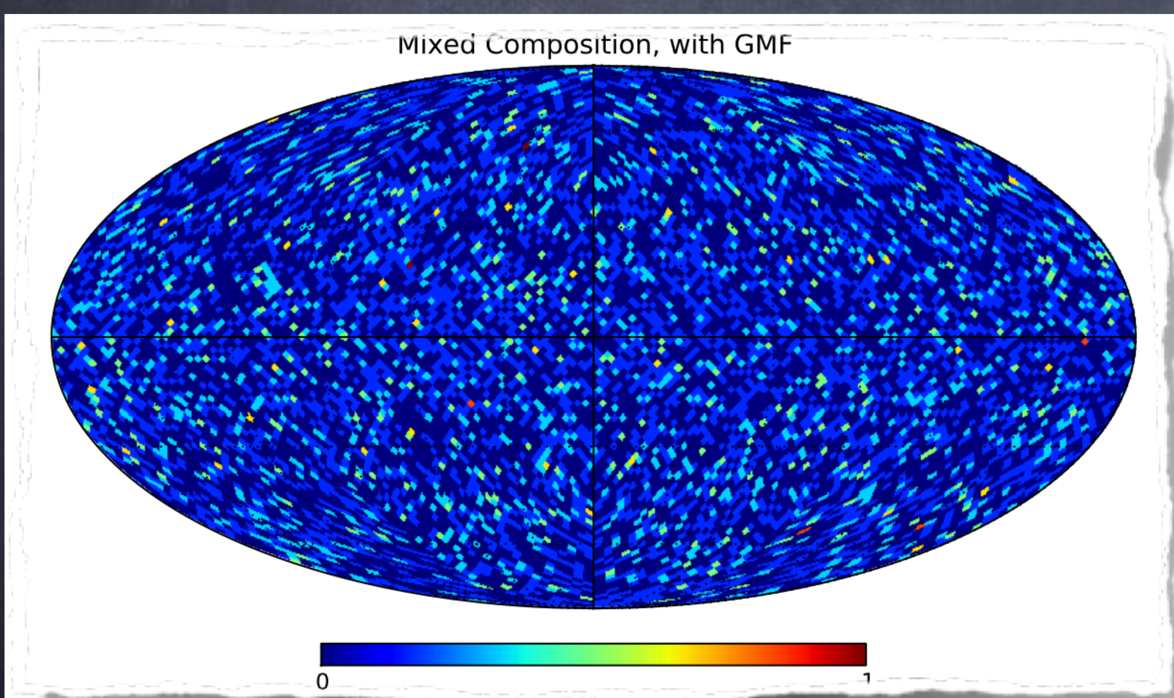

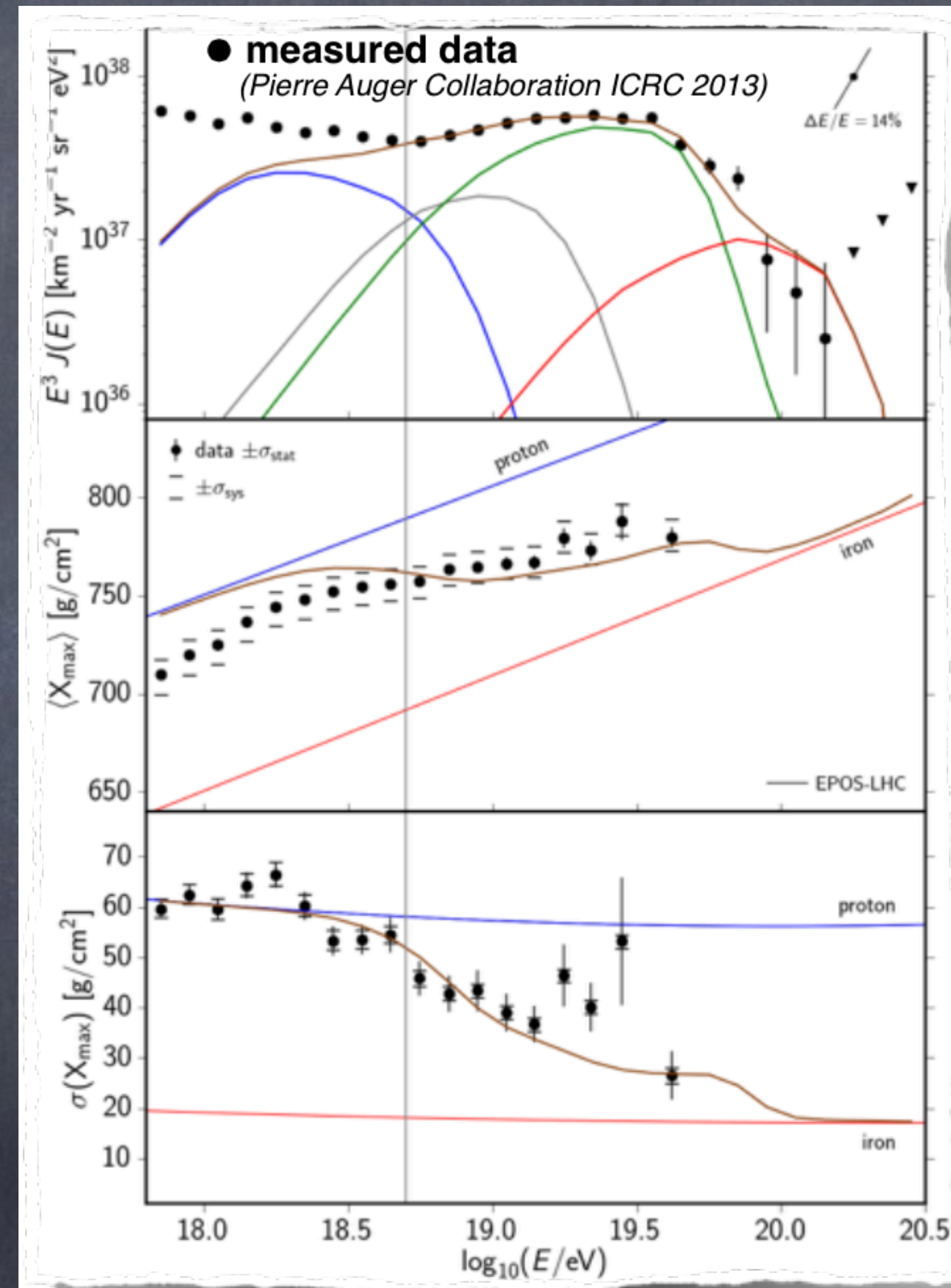

combining spectral and composition information with anisotropy can considerably strengthen constraints on source characteristics, distributions and magnetization

Conclusions

1.) The sources of ultra-high energy cosmic rays are still not identified due to rather small anisotropies; composition seems to become heavier at the highest energies which appears economic in terms of shock acceleration power

2.) The observed X_{max} distribution of air showers provides potential constraints on hadronic interaction models: Some models are in tension even when “optimizing” unknown mass composition; however, systematic uncertainties are still high.

Conclusions

3.) Highest Energy Cosmic Rays, Gamma-rays, and Neutrinos give the strongest constraints on violations of Lorentz symmetry => terms suppressed to first and second order in the Planck mass would have to be unnaturally small

4.) Cosmic Rays and electromagnetic cascades probe extragalactic and primordial magnetic fields through deflection and time delay